NTNU

Norwegian University of
Science and Technology

Experimental Study of Direct Tensile Strength in Sedimentary Rocks

Stina Stokmo Jensen

Petroleum Geoscience and Engineering
Submission date: July 2016
Supervisor: Rune Martin Holt, IPT
Co-supervisor: Anna Stroisz, SINTEF

Norwegian University of Science and Technology
Department of Petroleum Engineering and Applied Geophysics

Abstract

Tensile strength is an important parameter in rock mechanics, and is amongst other things used as a criterion for initiation and propagation of fractures in hydraulic fracture modeling. The tensile strengths are determined for three sedimentary rock types using the standard test method for direct tensile strength from American Society of the international association for Testing and Materials (ASTM).

The tensile strength testing was done on Castlegate sandstone, Mancos shale and Mons chalk. For Castlegate sandstone and Mons chalk two different specimen sizes, 1.5 inches and 2 inches in diameter, were used to study the size effect on the tensile strength results. Both rock types showed a clear size effect, however, while the tensile strength of Castlegate sandstone decreased for increasing specimen size, the tensile strength of Mons chalk increased with increasing specimen size. Mancos shale specimens were tested with different inclination angles relative to the bedding plane to study the anisotropy effect. The tensile strengths for shale varied greatly with the inclination angle and the largest tensile strengths were seen for samples with a 45° inclination angle relative to the bedding.

Resulting tensile strengths for all rock types was compared to existing tensile strengths calculated from the Brazilian tensile strength method. The comparison showed that the direct tensile strength test yields lower, and more correct, values than the Brazilian strength test.

The tensile strengths were also compared to known correlations between the tensile strength and fracture toughness. Some of the correlations showed a better match than the others.

Sammendrag

Strekkstyrke er en viktig parameter innenfor bergmekanikk, og er blant annet benyttet som et kriterium for begynnelse og forplantning av sprekker innen modellering av hydrauliske frakturer. Strekkstyrke er beregnet for tre sedimentære bergarter ved hjelp av en standard testmetode for direkte strekkstyrke fra ASTM (American Society of International Association for Testing and Materials).

Testene for strekkstyrker ble gjort for Castlegate sandstein, Mancos skifer og Mons kritt. For Castlegate sandstein og Mons kritt er to forskjellige prøvestørrelser, 1.5 tommers og 2 tommers diameter, benyttet for å studere størrelseseffekten på den resulterende strekkstyrken. Begge bergartene viste en klar størrelseseffekt, mens strekkstyrken til Castlegate sandstein minket med økende prøvestørrelse, økte strekkstyrken til Mons kritt med økende prøvestørrelse. Mancos skifer prøver ble testet med forskjellig helningsvinkel i forhold til lagdelingene for å studere effekten av anisotropi. Strekkstyrkene for skifer varierte mye med helningsvinkel, og den største strekkstyrken ble observert for prøver med en 45 graders helningsvinkel i forhold til lagdelingen.

Den resulterende strekkstyrken for alle bergartene ble sammenlignet med eksisterende verdier for strekkstyrke beregnet fra den brasilianske strekkstyrketesten. Sammenligningen viste at den direkte strekkstyrketesten gir lavere, og mer korrekte, verdier enn den brasilianske testen.

Verdiene for strekkstyrke ble også sammenlignet med kjente korrelasjoner mellom strekkstyrke og bruddstyrke. Noen av korrelasjonene viste en bedre overensstemmelse enn andre.

Acknowledgements

This master thesis study has been made possible by the financial and technical contributions from The Norwegian University of Science and Technology and SINTEF Petroleum Research.

I would firstly like to thank my supervisor Rune M. Holt for suggesting this interesting topic and providing valuable guidance and advice. A deep gratitude goes to my co-supervisor Anna Stroisz at SINTEF for her time and technical expertise throughout the project period.

I would also like to thank Lars Erik Walle for lending help with the software and experimental setup, and Jørn Stenebråten and Eivind Sønstebø for providing useful solutions and a deeper insight into rock mechanics. In addition I would like to thank Hans Lund for his help with sample preparation.

Last but not least, a special thank you to all my friends and family for all the support and encouragement throughout these years at NTNU.

Table of Contents

List of Figures

List of Tables

1 Introduction

In petroleum engineering, Hydraulic Fracturing (HF) serves many purposes. Most common is the stimulation of low permeability formations like tight sands, carbonates and gas/oil shales. In addition, fracturing often occurs during water injection and plays an important role in waste storage. Hydraulic Fracturing is also the most reliable way of determining in-situ stresses through extended leak off tests (XLOT).

In hydraulic fracturing modeling, the tensile strength of the rock is a highly important parameter that dictates the minimum borehole pressure required to induce fractures. When using the HF simulation software MDEM (Modified Discrete Element Method), a tensile failure criterion is used to initiate and propagate the fractures.

Tensile strength can be determined from several different tests in the laboratory. While the Brazilian strength test is the most popular one, the direct tensile strength test gives the most accurate values.

The main purpose of this thesis is therefore to carry out direct tensile strength tests in the Formation Physics Lab at SINTEF Petroleum. Three types of rocks are selected for testing: Castlegate sandstone, Mancos shale and Mons chalk. These rocks are selected because they are analogous to reservoirs encountered in the field. Chalk and sandstone is tested for two different specimen sizes to investigate a possible size effect, while shale is tested for different inclination angles to investigate the possible effect of anisotropy. In addition, a literature review will be carried out to get an overview of previous laboratory experiments measuring tensile strength in rocks, focusing on size effect and anisotropy effects. The literature survey will also include any published relationships between tensile strength and fracture toughness.

2 Theory

2.1 Tensile Strength

The tensile strength, T_0, is the maximum amount of tensile stress that can be applied before the rock fails, and is a characteristic property of the rock. Anisotropic strength characteristics are very common for rocks that have pronounced directional features such as flow structure, foliation and lamination. The tensile strength parallel to the bedding is usually higher than the tensile strength perpendicular to the bedding. There is however no guarantee that the tensile strength at an angle to the bedding has a value that is between the strength parallel and perpendicular to the bedding. Ultimate tension strengths are important for fracture studies because all fractures across the bedding planes are caused by tension.

Tensile strength of rock is an important parameter used in the design and stability analysis of underground structures. Rock tensile strength dictates the maximum roof span of underground openings, the stability of boreholes, and the minimum borehole pressures for hydraulic fracturing process (Klanphumeesri, 2010).

2.2 Determination of Tensile Strength

There are different tests for measuring or deriving the tensile strength in the laboratory, such as “direct tensile strength measurements”, “Brazilian tests”, and “point load tests”. The tensile strength tests are important in rock mechanics, because they give input parameters for planning of hydraulic fracturing. The values of tensile strength depend strongly on the test method.

Direct tensile strengths of rocks have rarely been determined as it is difficult to induce tensile fracture by pulling the intact rock core apart. As a result, indirect methods have been widely used to determine the rock tensile strength, which include Brazilian tension test and ring tension test. A common disadvantage of these methods is that their results usually over-estimate the actual tensile strengths of the rocks. This is primarily due to the effects of the stress gradient along the incipient failure plane, and the presence of the compressive stress normal to the induced tensile stress at the fracture initiation point (Klanphumeesri, 2010).

The different testing methods will be further described in Chapter 3.1.

2.3 Fracture Toughness

Fracture toughness describes the rock's resistance to fracturing and is therefore an important parameter when estimating the failure of rock and rock structures using rock fracture mechanics principles. A crack will start to grow if the stress intensity factor exceeds the fracture toughness, which is the critical limit, at the crack tip. In fracture mechanics a crack is defined as any opening in the rock that has one or two dimensions much smaller than the third, and the width to length ratio, termed crack aspect ratio is typically 10^{-3} to 10^{-5} (Backers, 2004).

There are three basic modes of fracturing that the crack tips can experience, as shown in Figure 2-1, and the modes are divided based on the crack surface displacement. Mode I is also called the opening mode, or tensile mode, and here the crack tip is subjected to displacements perpendicular to the crack plane. Mode I is in many situations the dominating mode. Tensile fractures can be generated within a rock mass in both tensile and compressive stress fields and are therefore very common fractures. Mode II is also called sliding mode because the two faces will slide against each other parallel with the direction of the crack due to in-plane shear stress acting on the crack tip. In Mode III, tearing mode, shear displacement is acting parallel to the front in the crack plane. Any combination of the three basic fracturing modes is referred to as a mixed mode, and could be a mix of any two or all three.

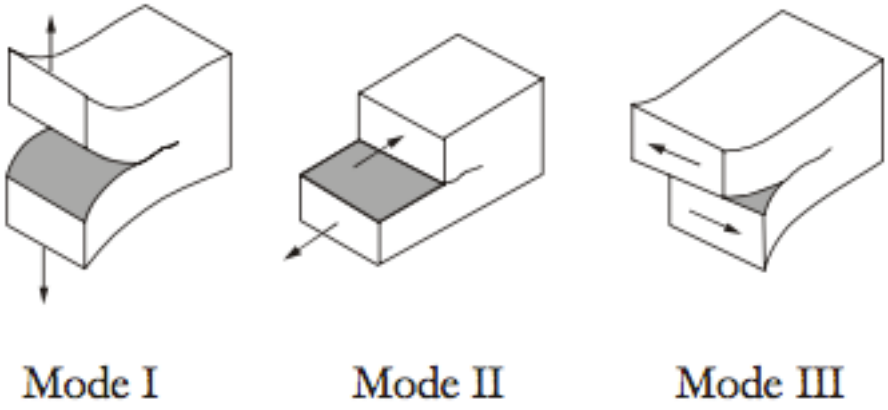

Figure 2-1: The three basic modes of fracturing (Backers, 2004)

The fracture toughness can be linked to tensile strength through the Griffith theory by the equation:

$$T_0 = \frac{K_{IC}}{\beta_c \sqrt{\pi \alpha}} \tag{2.1}$$

Where α is crack radius for the crack that is most likely to develop in the failure process, β_c is the crack shape factor, and K_{IC} is the fracture toughness. This also suggests that, provided that the same crack initiates fracture growth and tensile failure, there should be a relationship between fracture toughness and tensile strength. Tensile strength and fracture toughness can also be linked through equation 2.2 where w_s is the surface energy of the crack and E is Young's modulus.

$$T_0 = \sqrt{\frac{2 w_s E}{\pi a}} \tag{2.2}$$

2.4 Hydraulic Fracturing

The tensile strength of the rock is a necessary parameter during a hydraulic fracturing process, as it dictates the minimum borehole pressure that is required to induce fractures. Hydraulic fracturing is a very important process in the petroleum industry, because it helps improve the oil recovery from a reservoir. The hydraulic fracturing process is a way to improve flow towards the production well, which will increase the drainage efficiency and therefore increase the recovery factor of the reservoir. A key parameter when modeling hydraulic fracture propagation is the fracture toughness, which can describe radius, shape and length of the induced fractures.

2.5 Rock Properties

There are three different petroleum related rock types used during the laboratory experiments carried out for this thesis; Mancos shale, Castlegate sandstone and Mons chalk. Most rock types are proven to be weaker in tension than compression, and all fractures across the bedding planes are caused by tension. It is therefore interesting to compare the results from the tests performed in this thesis to other tensile strength tests conducted on the same rock types. This will be further examined in Chapter 5.4.

2.5.1 Mancos Shale

From the rock mechanical viewpoint, it is natural to define a shale as a rock in which clay minerals constitute a load-bearing framework. In practice this means that clay content needs to be higher than about 40% (Fjaer, 2008). Because of the large abundance of clay minerals, pore sizes in shale are very small; typically between 5 and 25 nm. The nanometer size pores lead to laboratory-measured permeabilities in the nano-Darcy range. North Sea shales typically display porosities of 30-55% (Fjaer, 2008).

In the last few years the petroleum industry has experienced a significant boom in production of shale gas, which has caused a higher demand of new technology in order to produce shale gas in an economically viable way. The shale may have a large volume of initial gas in place, however, to produce this gas economically artificial stimulation treatment such as horizontal drilling or hydraulic fracturing, or both, is necessary. In gas shale, the shale can be the reservoir, the source rock and also the trap for natural gas all at once.

Mancos shale is an anisotropic rock, that can be used as an analogue to gas shale, and the Mancos shale is dominantly gray marine shale located in the Uinta Basin in Colorado and Wyoming, USA. Mancos shale consists of 40-45% quartz, around 20-25% clay, about 20% carbonates and some organic material (slightly in excess of 1 weight %), and the porosity is about 6-8%. The Young's modulus for Mancos shale varies with the inclination angle. Figure 2-2 summarizes some main results from CID (consolidated isotropically drained) and UCS (uniaxial compressive strength) tests in terms of estimated uniaxial compressive strength (C0) and Young's modulus (E) as function of inclination. Note that Young's modulus is deduced from an unloading-reloading cycle from the UCS tests, thus being more representative of an elastic modulus (Fjaer and Nes, 2013).

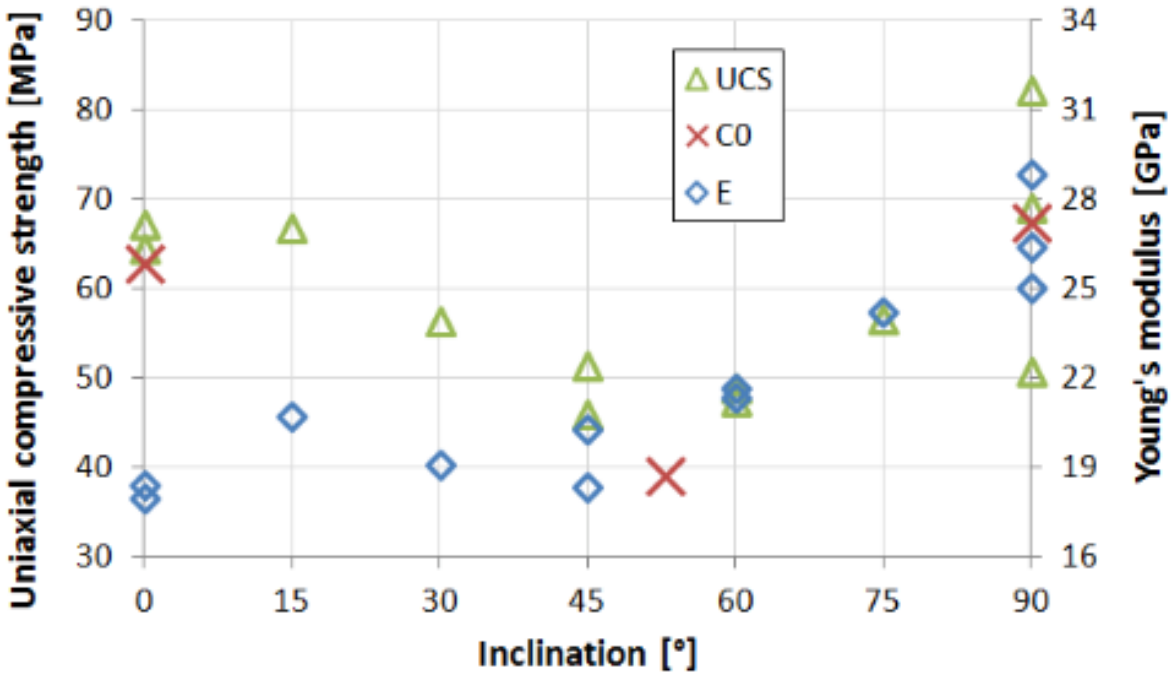

Figure 2-2: Uniaxial compressive strength and Young's modulus vs. inclination angle (Fjaer and Nes, 2013)

2.5.2 Castlegate Sandstone

Castlegate sandstone is an isotropic rock that can be used as an analogue to sandstone reservoir rock. The dominant grain sizes of sandstone are typically 0.01-1 mm. Pore sizes are the same order of magnitude, but slightly smaller. This gives permeabilities ranging from microDarcy to several Darcies. The predominant matrix material is quartz (Fjaer, 2008). Castlegate sandstone consists of 70% quartz, and 30% feldspar and rock fragments. The porosity is about 28.5% and the Young's modulus is about 3.4 GPa.

2.5.3 Mons Chalk

Chalk particles originate as skeletons of algae that are called coccospheres, with a typical initial size of 30 μm. During burial the coccospheres are crushed, and most particles (and pores) of present chalk are in the range of a few (1-10) μm, with associated matrix permeabilities between micro- and milliDarcy (Fjaer, 2008).

Chalk porosity may be as high as 70 percent. In normally pressured areas, chalk porosity is typically less than 10% at depths greater than 2000m. In North Sea reservoirs however, chalk porosities of 15-50% are found at depths of 2500-3500m because of overpressure. These

reservoirs are also naturally fractured, leading to high reservoir scale permeabilities in the 100-milliDarcy range (Fjaer, 2008).

Mons chalk is an isotropic rock that can be used as an analogue to chalk reservoir rock. The chalk is from a 6km long stretch of chalk cliffs located at the eastern coast of the Danish island Møn in the Baltic Sea. This chalk is a pure chalk and has a weight percent of calcite that is approximately 99.8. In addition to calcite minerals the chalk can also contain silica and clay minerals. Mons chalk has a porosity of about 40-44% and a permeability of 2 milliDarcy. There is no measured value for Young's modulus, but a calculated guess is that the value is around 5 GPa.

3 Literature Review

A literature review is carried out to study the previous research on different tensile strength tests, the relationship between the tensile strength derived from the different tests and the relationship between tensile strength and fracture toughness.

3.1 Different Tensile Strength Tests

There are a number of different laboratory tests designed to find the tensile strength of rocks. Since the early years of rock mechanics the technology has continuously evolved and along the way new methods of finding tensile strength have been developed. The literary review identifies some of the most important and used methods, including direct tensile strength test, Brazilian strength test, point load strength test and ring tension test.

3.1.1 Direct Tensile Strength Test

The direct tensile strength test is the most basic test for determining the tensile strength of rock, and a standard test method has been established by ASTM and published as "Standard Test Method for Direct Tensile Strength of Intact Rock Core Specimens" (ASTM, 2008a).

To measure the direct tensile strength of a rock, a cylindrical shaped rock specimen is glued into metal end cups at both ends. The metal end cups are attached to a MTS (Material Test Systems Inc.) loading frame so the specimen can be loaded in tension until it fails; the tensile stress applied at this point is then the tensile strength of the rock. This method is used in the experiments carried out as a part of this thesis and is further described in Chapter 4.

The equation used to calculate the tensile strength from this test method is equation 3.1.

$$T_0 = \frac{F}{A'} \tag{3.1}$$

Where T_0 is the tensile strength, F is the maximum load carried by the specimen during the test, and A' is the cross-sectional area of the specimen.

3.1.2 Brazilian Strength Test

The standard method for the Brazilian strength test is established in "Standard Test Method for Splitting Tensile Strength of Intact Rock Core Specimens" (ASTM, 2008b) and is an indirect way of determining tensile strength. This method is used more often than the direct

tensile strength test due to easier and less time consuming sample preparation and experimental procedure. Compared to the point load strength measurements the Brazilian test tends to give more reproducible results.

For the Brazilian strength test, the test specimens are circular disks with a thickness-to-diameter ratio between 0.2 and 0.75. The diameter has to be at least ten times greater than the largest mineral grain constituent, a diameter of 54 mm usually satisfy the criterion. One example of the test setup is shown in Figure 3-1, where the test specimen is located between two platens that diametrically compress the specimen to failure.

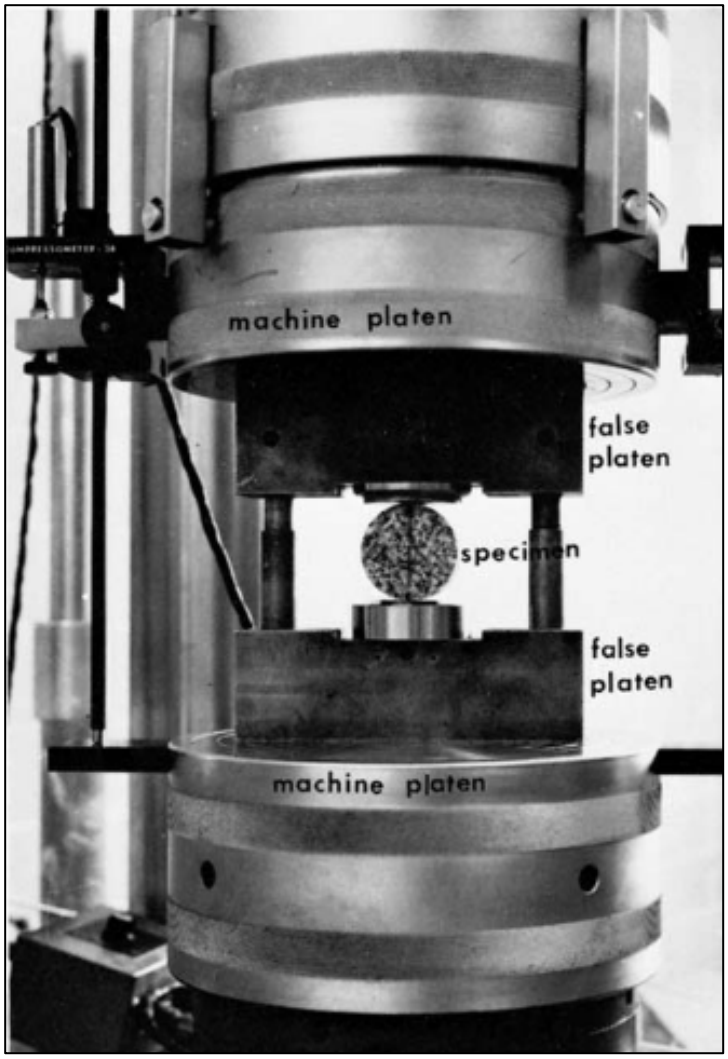

Figure 3-1: Setup for Brazilian strength test (ASTM, 2008b)

The splitting tensile strength, σ_t, is then calculated by equation 3.2.

$$\sigma_t = \frac{2F}{\pi D t} \tag{3.2}$$

Where F is the load at failure, D is the diameter of the specimen and t is the thickness at the center of the specimen.

Figure 3-2 shows the definitions of inclination angle in regards to bedding, for the Brazilian strength test (BTS) and the direct tensile strength test (TS). The angle θ is defined as the angle between the x-axis and the bedding plane, whereas β is defined as the angle between the y-axis and the bedding plane. The Brazilian test is an indirect method for determining tensile strength of a material. Due to the disc geometry, the tensile stresses are applied perpendicular to the applied load. BTS values measured at β° are designed to be analogous to direct TS values measured at θ°. This setup has β=θ=30° (Simpson, 2013).

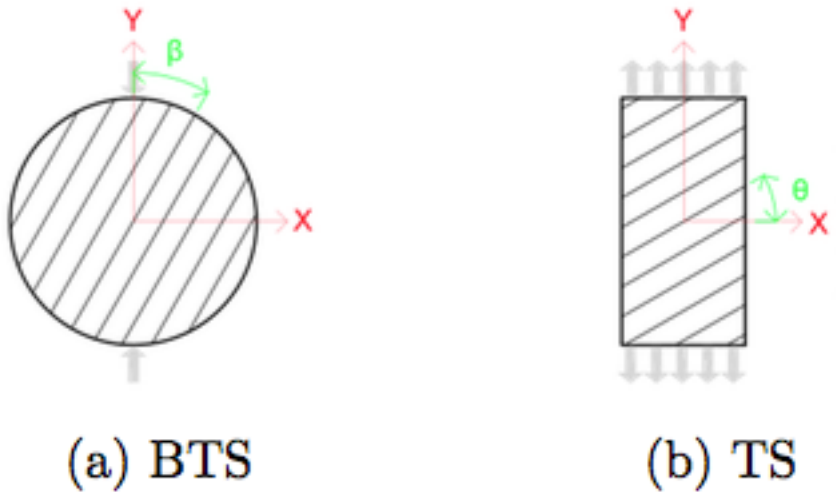

Figure 3-2: Inclination angle (to bedding) for (a) Brazilian Tensile Strength and (b) direct Tensile Strength (Simpson, 2013)

Simpson (2013) conducted a study on Brazilian tensile strength on the same rock types as investigated in this thesis, Castlegate sandstone, Mons chalk and Mancos shale. The results from those tests will be used for a comparison between the direct and Brazilian tensile strengths in Chapter 5.4. The calculated tensile strength of Castlegate sandstone and Mons chalk was not presented in the thesis paper, however, since the experiments were conducted in

collaboration with SINTEF Petroleum, unpublished results were made available by SINTEF Petroleum. The following tables show the results that will be used for the comparison.

Table 3-1: Brazilian tensile strength results for Castlegate sandstone and Mons chalk

Rock Type	Number of Samples Tested	Average Diameter [mm]	Average Thickness [mm]	Average Brazilian Strength [MPa]	Standard Deviation
Castlegate Sandstone	7	47.83	24.45	1.072	±0.095
Mons Chalk	8	47.72	24.82	0.867	±0.368

Table 3-2: Brazilian tensile strength results for Mancos shale

Inclination Angle θ [°]	Number of samples tested	Average Diameter [mm]	Average Thickness [mm]	Average Tensile Strength [MPa]	Standard Deviation
0	4	47.88	24.82	3.066	±0.607
15	4	47.93	24.72	3.030	±0.437
30	4	47.96	24.78	3.217	±0.365
45	4	47.94	24.63	2.759	±0.338
60	4	47.81	24.71	3.165	±0.677
75	4	48.01	24.68	2.630	±0.345
90	4	47.87	24.71	2.979	±0.810

3.1.3 Point Load Strength

The point load strength index can be found by subjecting a rock specimen to an increasingly concentrated load until the specimen fail by splitting, the failure load is then used to calculate the index. The concentrated load is applied by spherically truncated, conical platens of a standard geometry, as seen in Figure 3-3.

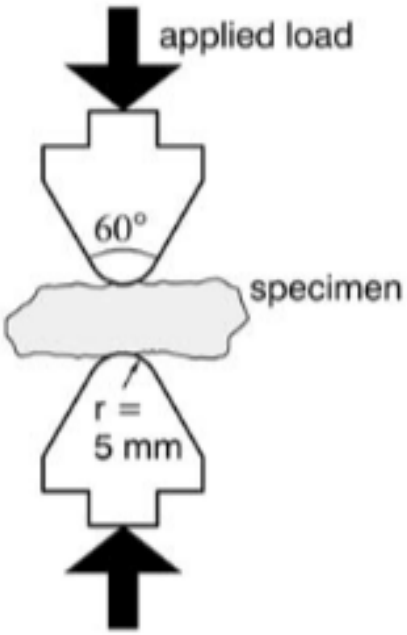

Figure 3-3: Simple sketch of point load strength test apparatus (Fjaer, 2008)

No extensive sample preparation is required because the specimen can be in the form of a core, a cut block or an irregular lump. From the point load strength test the point load strength index can be calculated by equation 3.3.

$$I_s = \frac{F_c}{D_e^2} \tag{3.3}$$

Where I_s is the point load strength index, F_c is the failure load and D_e is the equivalent core diameter. The equivalent core diameter is equal to the thickness in a diametrical test, and equal to $4A/\pi^{1/2}$ for specimens in the shape of blocks or lumps. To find the uniaxial tensile strength, T_0, equation 3.4 shows the correlation between the point load strength index and the uniaxial tensile strength.

$$I_s = 0.80T_0 \tag{3.4}$$

3.1.4 Ring Tension Test

In the ring tension tests, rock disks are diametrically compressed until failure. The rock disks usually have a thickness to diameter ratio of about one to four. A standard method stating a standard disk size was not discovered through the literature study. Figure 3-4 shows the setup for the ring tension test in a compression load machine.

Figure 3-4: Setup for ring tension test (Klanphumeesri, 2010)

Klanphumeesri (2010) performed ring tensile strength tests on three rock types, where the specimen were 50mm long, with a nominal outer diameter of 100mm and the nominal inner diameter 30mm. In addition Klanphumeesri also performed direct and Brazilian tensile strength tests on the same rock types to compare the strength results. The ring tension test yielded the highest strength values and it was concluded that this was due to the high stress gradient along the incipient crack plane.

Fuenkajorn and Daemen (1986) performed a series of ring tension tests to measure tensile strengths. The tensile strength was measured at the center hole boundary, within the damaged zone, of the rock disk. Tests were carried out on rock disks with a diameter of nine inches with five different sized center holes. Figure 3-5 shows some of the failed specimens from the

ring tension tests, all specimens here have failed along the loaded diameter. The tensile strength from the ring tension test decreases with increasing center hole size.

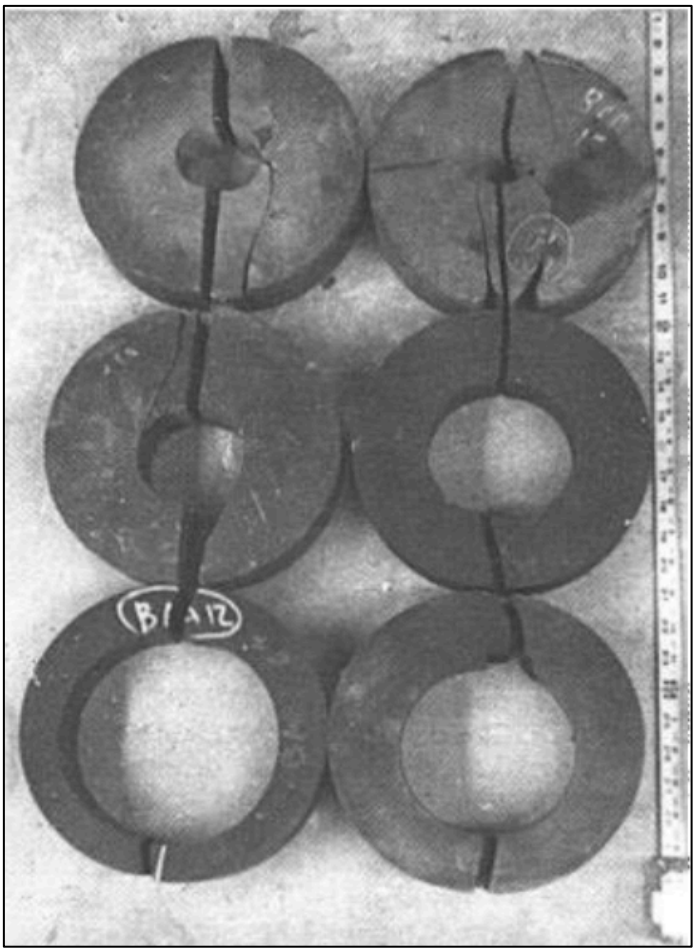

Figure 3-5: Rock disks of Pomona basalt after the ring tension tests (Fuenkajorn and Daemen, 1986)

The ring tensile strength, σ_R, can be calculated using equation 3.5, where P_f is the applied load, K_f is the stress concentration factor at the center hole boundary, D is the disk diameter and t is the thickness.

$$\sigma_R = \frac{2P_f K_f}{\pi D t} \tag{3.5}$$

An approximate value for the stress concentration factor can be found using equation 3.6, where r is the relative hole radius (hole radius divided by disk radius).

$$K_f = 6 + 38r^2$$
$$for\ 1.0 > r > 0.1 \tag{3.6}$$

The advantage of using a ring specimen is that the point of failure initiation is at the inner surface of the ring along the loaded diameter. The stress configuration at this point is simplified by the absence of the compressive strength component present in the Brazilian test (Fuenkajorn and Daemen, 1986).

3.2 Brazilian versus Direct Tensile Strength

While the process of determining the tensile strength from the Brazilian tension test is based on the assumptions of linear elasticity and Griffith criterion, the behavior of many rocks may not exactly satisfy these assumptions. Therefore, depending on the characteristics of each rock, the values of tensile strength obtained from the direct and Brazilian tension tests might be slightly different (Rafiei and Martin, 2014).

At the time of failure the stress intensity factors for both tests reach the mode I fracture toughness of the material (K_{IC}). The ratio of the Brazilian tensile strength to the direct tensile strength is given in equation 3.7 (Rafiei and Martin, 2014).

$$\frac{\sigma_{t,D}}{\sigma_{t,B}} = \frac{\left[1 + 0.600\left(\frac{a}{D}\right) - 0.704\left(\frac{a}{D}\right)^2 + 17.208\left(\frac{a}{D}\right)^3\right]}{\frac{\left[1 - \frac{a}{2b} + 0.326\left(\frac{a}{b}\right)^2\right]}{\left[\sqrt{1 - \frac{a}{b}}\right]}} \tag{3.7}$$

Here $\sigma_{t,D}$ is the direct tensile strength, $\sigma_{t,B}$ is the Brazilian tensile strength, a is the half-length of crack, b is the half-width of the plate and D is the diameter of the plate. The definition of a and b in the two different tests are shown in Figure 3-6.

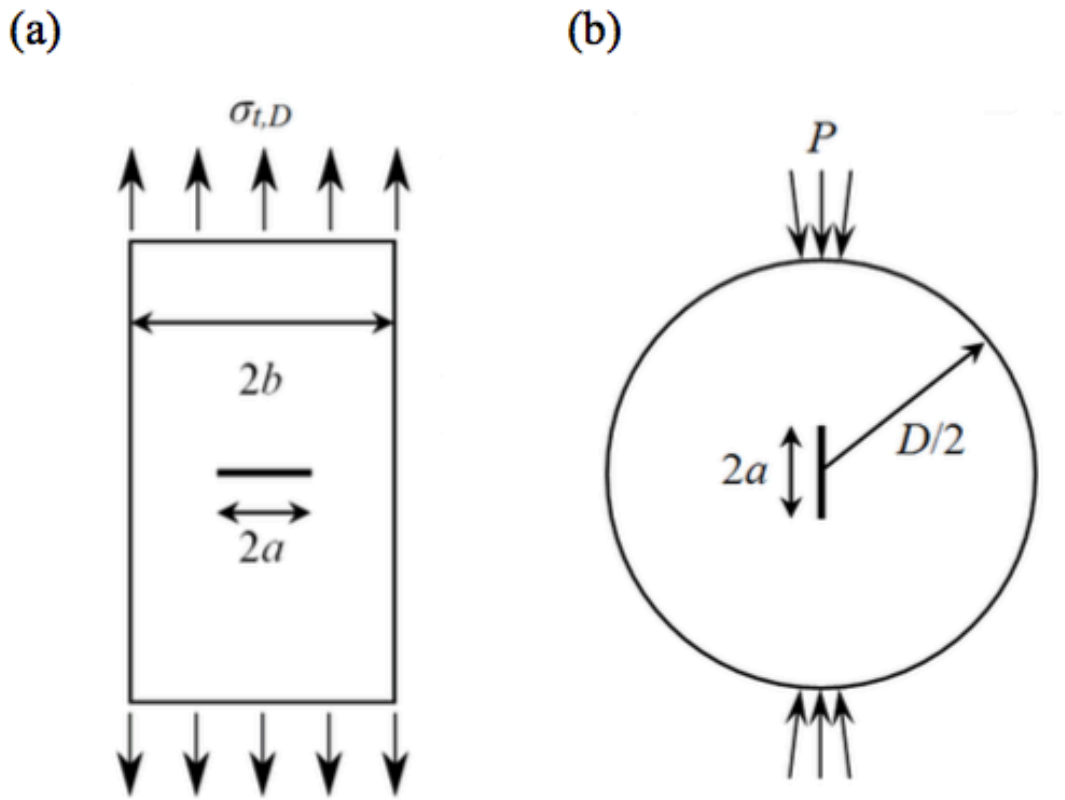

Figure 3-6: Geometry of test samples in (a) direct tension test, and (b) Brazilian tension test (Rafiei and Martin, 2014).

This particular equation is not used in this thesis, as the samples are torn apart and the a-value becomes equal to the b-value. The equation could be used if acoustic emission had been used to find the length of the initial crack.

According to Klanphumeesri (2010) the rock tensile strength decreases with increasing specimen size, and a direct comparison between the direct tensile strength and the Brazilian tensile strength is not valid due to the difference in specimen size. Klanphumeesri performed Brazilian and direct tensile strength tests on Phu Phan (PP) sandstone, Saraburi (SB) marble and Saraburi (SB) limestone and made a qualitative comparison between the strength results stating that the direct tensile strengths for these three rock types are lower than the Brazilian tensile strengths. This probably holds true for other rocks with comparable physical properties.

Considering the size effect, the test results can be postulated that if both tests used the same specimen size, the tensile strength obtained from the direct tension test would be even lower than those obtained from the Brazilian test. To obtain a direct tension test specimen with a

mid-section diameter of 54mm or larger, the total specimen length would however become impractical for preparation and testing (Klanphumeesri, 2010).

3.3 Tensile Strength and Fracture Toughness

The literature shows that some experimental studies have been carried out to express the relationship between tensile strength and mode I fracture toughness by equations. Three equations are found in "An empirical relation between mode I fracture toughness and the tensile strength of rock" (Zhang, 2002). The purpose of these experimental studies is to create a way to calculate fracture toughness from tensile strength because the current methods for measuring the fracture toughness are time-consuming and difficult.

Whittaker et al. expresses the relation between Mode I fracture toughness and tensile strength of various types of rock by

$$\sigma_t = 9.35K_{IC} - 2.53 \tag{3.8}$$

Where σ_t is the tensile strength and K_{IC} is the Mode I fracture toughness, with a coefficient of determination r^2=0.62. The tensile strengths used for this correlation comes from direct tensile strength tests and different Brazilian tests. This equation claims that a rock with zero tensile strength can resist crack propagation to some extent; however, this is not true for rock materials. When the tensile strength is zero, the fracture toughness should also be zero. Using this and some extra experimental data Zhang et al. made another equation for the relation between tensile strength and Mode I fracture toughness for several rock types, equation 3.9.

$$\sigma_t = 8.88K_{IC}^{0.62} \tag{3.9}$$

This equation has a coefficient of determination r^2=0.94, and builds on tensile strength results mainly from Brazilian tests.

Zhang (2002) uses several sources of experimental data and put them into the same plot, as seen in Figure 3-7 where the different data sources are shown by different shapes, to make a new equation, equation 3.10, correlating the tensile strength and Mode I fracture toughness of all rock types tested.

$$\sigma_t = 6.88K_{IC} \tag{3.10}$$

Here the coefficient of determination r^2=0.94. The experimental data used to create this equation is related to a number of different test methods for both tensile strength and fracture

toughness, and many different types of rock were tested. The test method used to find the tensile strength used for this equation is mainly Brazilian strength.

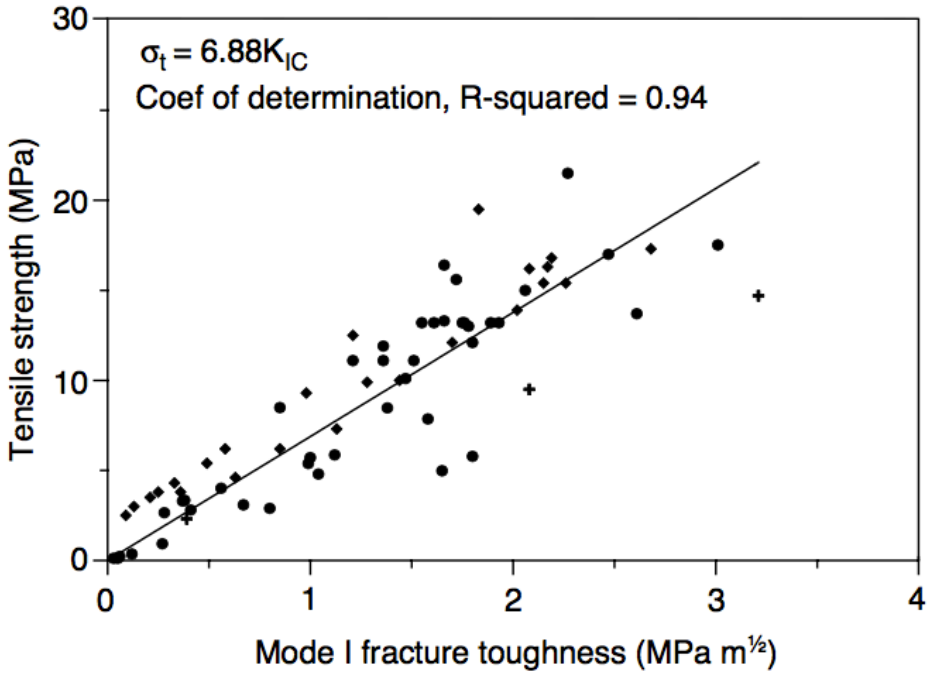

Figure 3-7: Empirical relation between fracture toughness and tensile strength of rocks (Zhang, 2002)

Backers (2004) studied the fracture toughness under Mode I and Mode II loading and after reviewing the work of Zhang (2002) he came up with a new equation describing the relationship between fracture toughness and tensile strength, equation 3.11 (Backers, 2004). This equation builds on tensile strength results for the Brazilian tensile strength test.

$$\sigma_t = 4K_{IC} \tag{3.11}$$

4 Laboratory Experiments

For this thesis, a series of direct tensile strength tests was carried out in the laboratory on three different rock types, Castlegate sandstone, Mancos shale and Mons chalk.

4.1 Experimental Setup

The direct tensile strength test is done in a MTS loading frame, a servo-controlled loading frame, where the rock sample is attached as shown in Figure 4-1. The attachments used include two cabin hooks and three chain links between the specimen and the loading frame at both ends to satisfy the required degrees of freedom. ASTM requires that the linkage at both ends shall be at least two times larger than the diameter of the metal end caps, and this setup satisfy this requirement. For this thesis the tests were done on two loading frames with different capacity, 10kN and 50kN, based on which of the frames was available at the time of testing.

Figure 4-1: Experimental setup for the direct tensile strength test

4.2 Experimental Procedure

The experimental procedure has been adapted from the standard test method of ASTM International (ASTM, 2008a). The MTS loading frames are computer-controlled, and the TestWorks-4 System Software was used to conduct the tests. The load cell measured the load and displacement.

4.2.1 Sample Preparation

All tested rock types are from big blocks purchased from TerraTek Inc., Salt Lake City. The blocks of Castlegate sandstone and Mons chalk are stored in ambient conditions. While the Mancos shale was sealed when received, and it was subsequently stored in inert oil after removal of the seal to avoid desiccation effects.

Cylindrical cores with diameters of 1.5” and 2” are drilled from the blocks of Castlegate sandstone and Mons chalk, and cut in lengths twice the size of the diameter. The rock samples are then measured to get an exact diameter and length, and numbered to easily identify them later. The samples are dried in a sample oven (set to 60° Celsius) for more than 48 hours. Afterwards the samples are weighed and glued to the end cups with two-component epoxy (Loctite EA3430), and then they are put in airtight containers for about two days to let the glue harden before testing.

The shale cores are drilled with a diameter of 1.5” at different angles to the bedding plane (θ), and cut to lengths of 3”. The samples are drilled in seven different angles regarding the bedding plane, which is shown in Figure 4-2, to investigate the effect of anisotropy on the results.

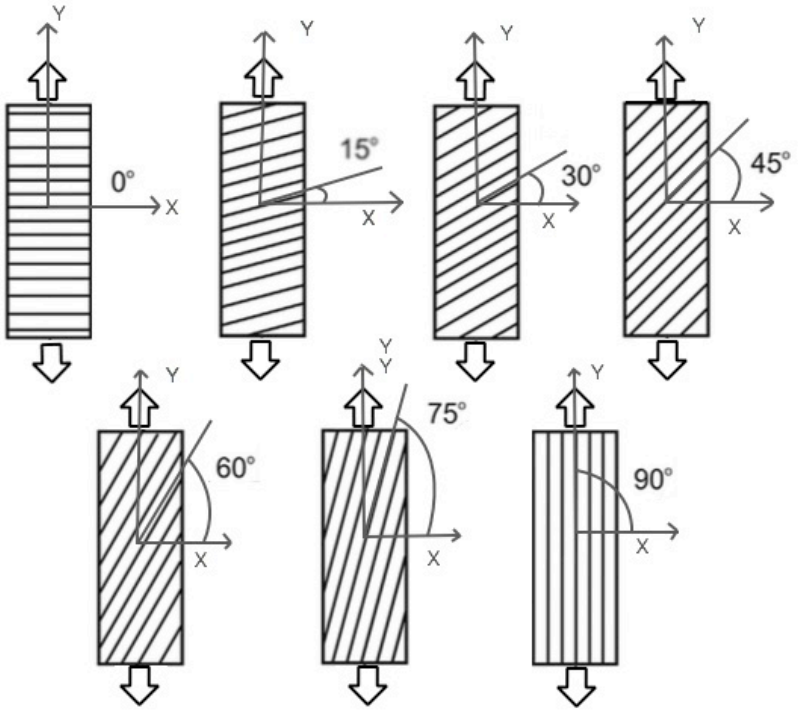

Figure 4-2: Different inclination angles, θ, for shale samples (modified from (Yilmaz, 2014))

After drilling the samples are stored in inert oil to prevent desiccation effects, and are only taken out of the oil when they are measured and glued to the end cups. To successfully attach the end cups to the samples, the sample is taken out of oil and the ends are wiped "dry" and lightly polished with sandpaper before the ends are wiped with isopropanol to remove most of the oil before gluing them to the end cups with two-component epoxy. The samples are left out of oil for about 15-20 minutes to let the epoxy settle before they are put back in oil for two days before testing.

4.2.2 The Direct Tensile Strength Test

The TestWorks-4 System Software allows the design of a specific program, where the test samples are first preloaded to -50N at a loading rate of -0.50 mm/s. Then the test samples are loaded up to failure with an unchanged loading rate. The loading rate for all sandstone and shale samples was mainly -0.10 mm/s, and -0.15 mm/s for all chalk samples. The loading rate is the movement of the crosshead, and since this test is a tension test all loads and loading rates are negative. All individual loading rates can be found in the tables in Appendix B

5 Results

The computer program, TestWorks4, used to run the tests in the loading frame gives three sets of values; time, load and crosshead position. All data is then interpreted in Excel, where the time is positive values while load and crosshead position are negative values. This is because the direct tensile strength test is a tension test and not a compression test, and therefore the values of the calculated tensile strengths are negative.

5.1 Direct Tensile Strength Results for Mancos Shale

In Table 5-1 the results from the tests performed on Mancos shale are listed as an average for each inclination angle. One of the samples with an inclination angle of 15 degrees failed at a much lower load than the other two and is therefore excluded from the table. The sample, MS5, failed at -207.3 Newton while the other two failed at -1006 and -1084.6 Newton, so it is assumed that MS5 had a weakness that was not discovered before testing. A full summary of the results for Mancos shale can be found in Appendix B.1 , and the individual loading rates are also specified there.

Table 5-1: Results from tests on Mancos shale

Inclination angle θ [°]	Number of samples tested	Average diameter [mm]	Average Length [mm]	Average Tensile Strength [MPa]	Standard Deviation
0	4	38.15	77.04	-0.314	±0.102
15	3	38.28	74.67	-0.908	±0.048
30	4	38.28	76.94	-1.128	±0.409
45	3	38.27	77.01	-2.378	±0.514
60	3	38.27	77.48	-2.423	±0.235
75	2	38.30	74.85	-1.625	±0.489
90	3	38.28	77.02	-2.079	±0.374

The calculated tensile strengths for all inclination angles are plotted in Figure 5-1 along with the average values. By drawing a line between the average values, some kind of trend line is visible, and if the values for θ=45° and θ=60° had been lower the trend line would be almost

linear. The fact that the tensile strengths are changing with the inclination angle points to the presence of an anisotropy effect, further discussed in Chapter 6.4.

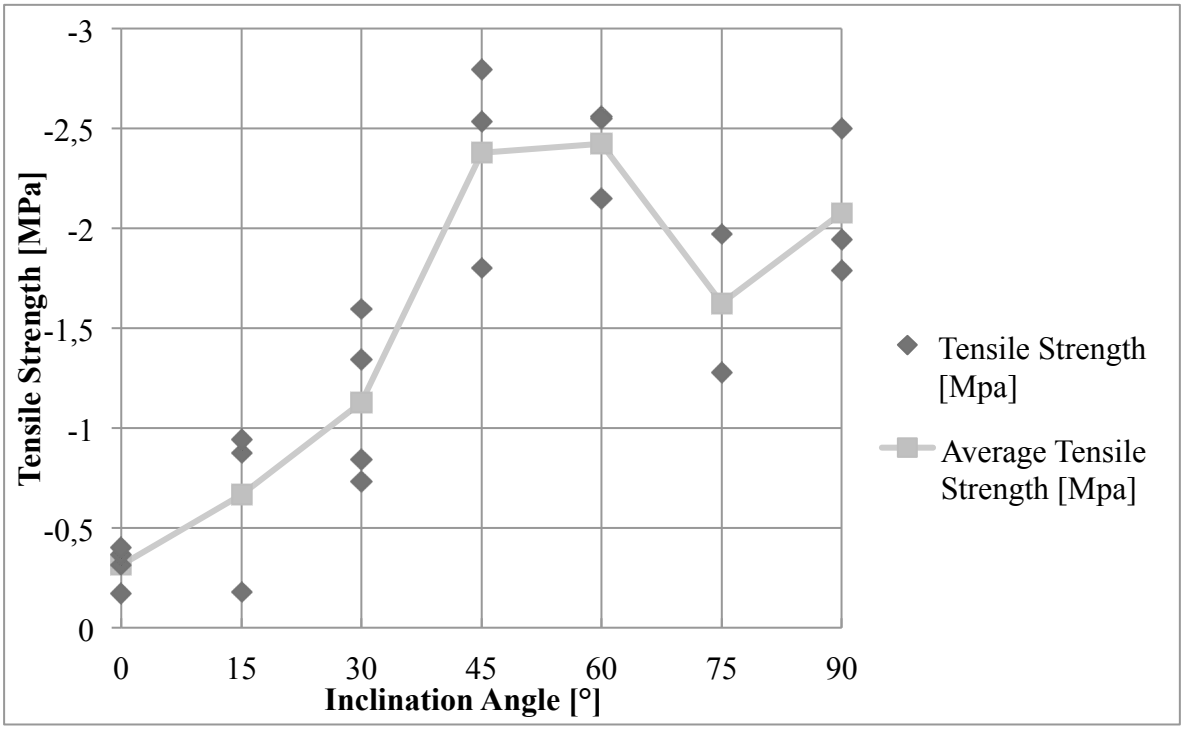

Figure 5-1: Tensile strength for all inclination angles of Mancos shale

Below is a picture of the Mancos shale samples with a 0° inclination angle after testing, and the red arrows are added where the failure plane may be difficult to locate. Pictures of all Mancos shale samples after testing are found in Appendix D.1 . From Figure 5-2 it is clear that the failure plane is oriented parallel to the bedding plane for specimens with an inclination angle of 0 degrees. Most of the shale specimens have a failure plane parallel to the bedding plane, as this is the way that requires the least amount of energy. For an inclination angle of 60 degrees, all specimens have failed close to on of the end cups and not parallel to the inclination angle. This might be caused by some undetected weakness in the rock, or the isopropanol used to wipe the oil before gluing may have moved into the specimen and caused a weakness zone. The tested specimens with a 75 degrees inclination show that the failure plane has moved parallel to the bedding plane for only a small distance, before crossing the bedding planes. This is due to the fact that this severity of inclination causes the energy required to follow the bedding plane to be higher than the energy required to cross the bedding planes.

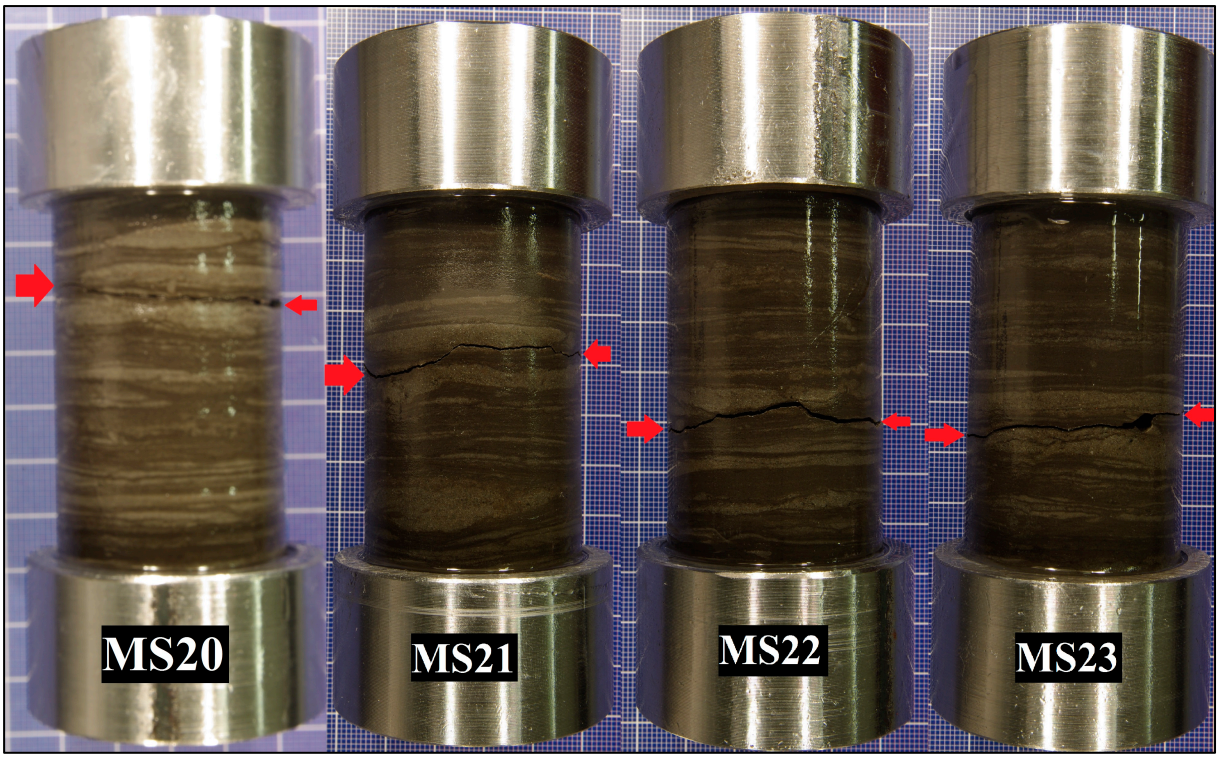

Figure 5-2: Samples of Mancos shale with a 0° inclination angle after testing

Stress and strain for all the tested samples are calculated and then presented in plots from Excel, the strain is set to zero at the point where the load is -50N, which is the end of the preload part of the tests. One stress versus strain curve is seen in Figure 5-3, and represents the typical result for Mancos shale samples. Some of the curves show an irregular shape, while most of them have an exponential shape. The curves for all Mancos shale samples can be found in Appendix C.1 . The reason for the discrepancies between the stress-strain curves will be further discussed in Chapter 6.1.

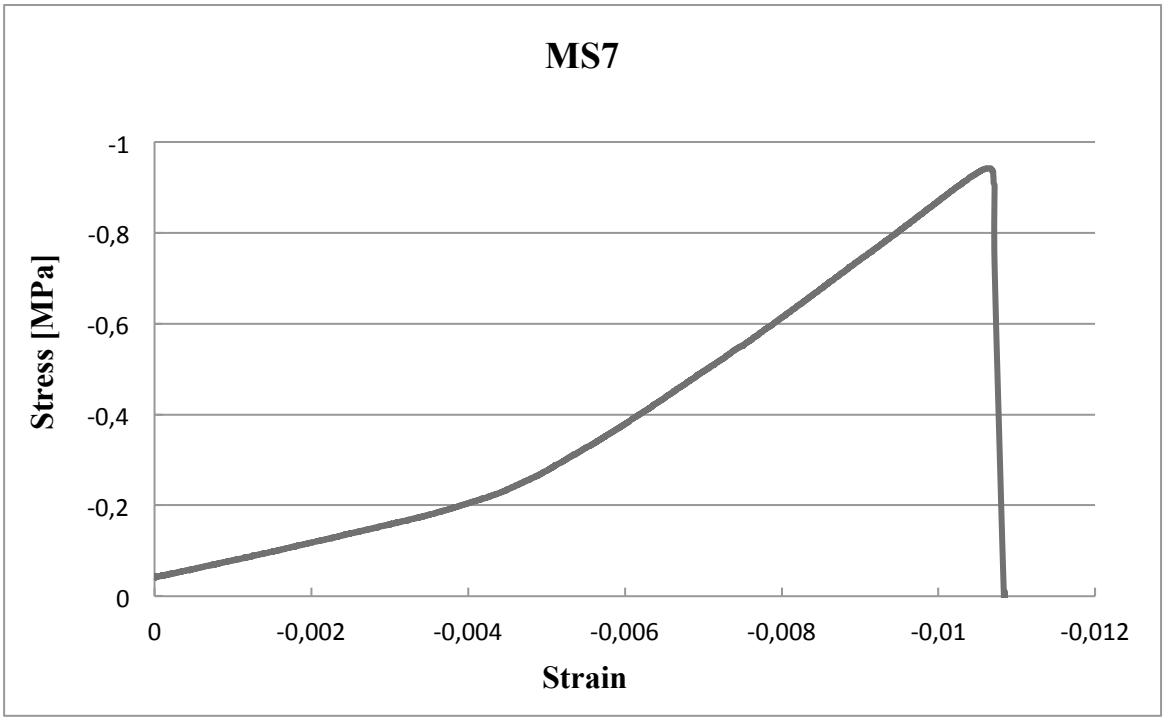

Figure 5-3: Stress-strain curve for Mancos shale sample 7

5.2 Direct Tensile Strength Results for Castlegate Sandstone

An unconfined test with a sandstone typically shows nonlinear stress-strain behavior during initial loading, with stiffening as the stress is increased. This nonlinearity can be attributed to pre-existing microcracks within the core, generated by stress release during coring (for cores from depth) or caused by weathering (for outcrop or near surface cores). For weak sandstones, where many grain contacts are not cemented, the grain contact itself is a nonlinear element (Fjaer, 2008).

The results from the direct tensile strength tests on Castlegate sandstone is shown in Table 5-2 as an average for each of the two specimen sizes tested. Castlegate sandstone was the first rock type to be tested for this thesis, the loading rates is therefore changing between the first few samples to find the best fit. A full summary of the data and results for all the specimens can be found in Appendix B.2 , the individual loading rates is also listed there. All the tensile strengths calculated for the Castlegate is shown in Figure 5-4, where tensile strength is plotted against the diameter of the specimen. The results show that the tensile strength increases with increasing sample size, which means there is some kind of size effect present.

Table 5-2: Results from tests on Castlegate sandstone

Number of samples tested	Average diameter [mm]	Average Length [mm]	Average Tensile Strength [MPa]	Standard Deviation
3	37.37	76.59	-0.461	±0.094
4	51.34	102.71	-0.589	±0.066

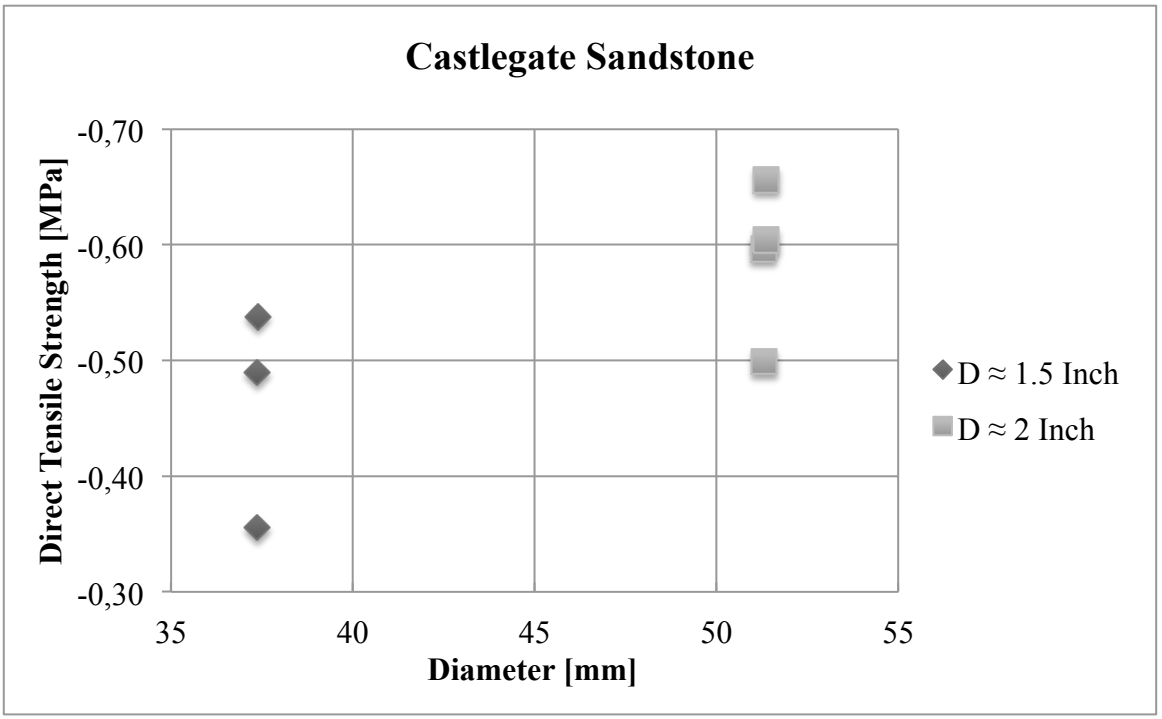

Figure 5-4: Direct tensile strength of Castlegate sandstone in relation to diameter

Figure 5-5 shows a typical stress versus strain curve for the sandstone samples, and the curves for all the sandstone samples is found in Appendix C.2 . Some of the samples have a curve that differs from the typical result, further discussed in Chapter 6.1.

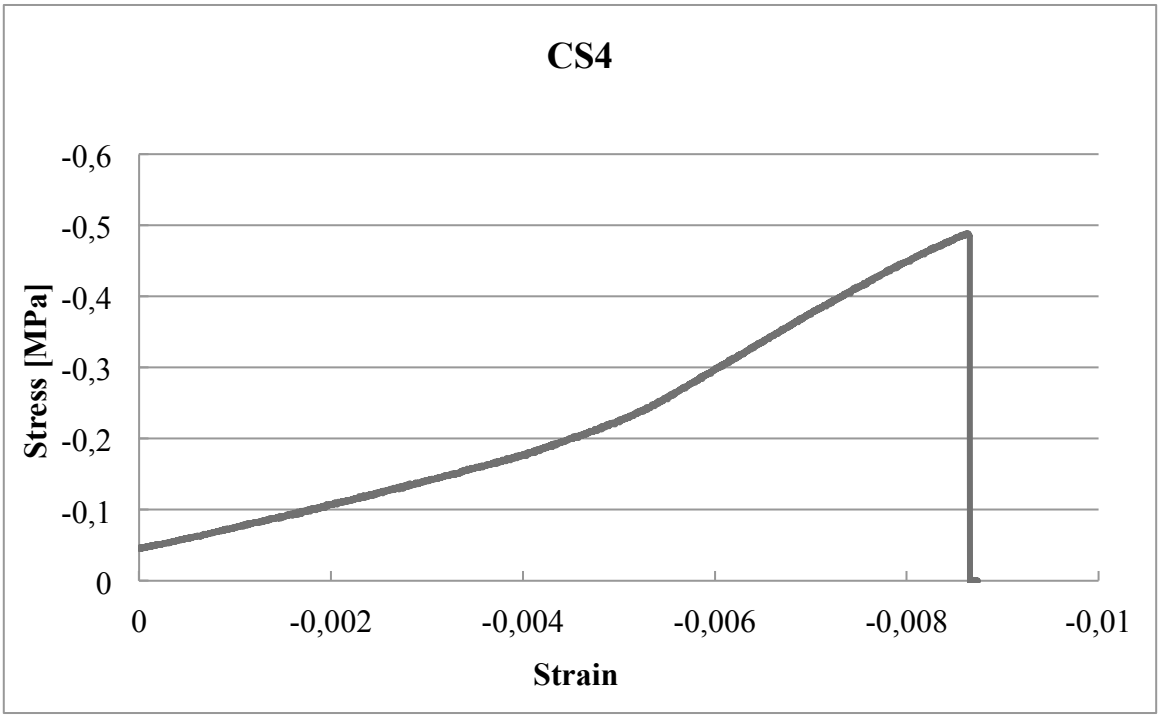

Figure 5-5: Stress-Strain curve for Castlegate sandstone sample 4

5.3 Direct Tensile Strength Results for Mons Chalk

In Table 5-3 the results from the direct tensile strength tests performed on Mons chalk is presented as an average for the two different specimen sizes tested. A full summary of the data and results for all the chalk specimens can be found in Appendix B.3 . The calculated tensile strengths for chalk are shown in Figure 5-6 with respect to the diameter of the specimens.

Table 5-3: Results from tests on Mons chalk

Number of samples tested	Average diameter [mm]	Average Length [mm]	Average Tensile Strength [MPa]	Standard Deviation
9	38.20	77.52	-1.907	±0.253
6	50.30	101.98	-1.583	±0.286

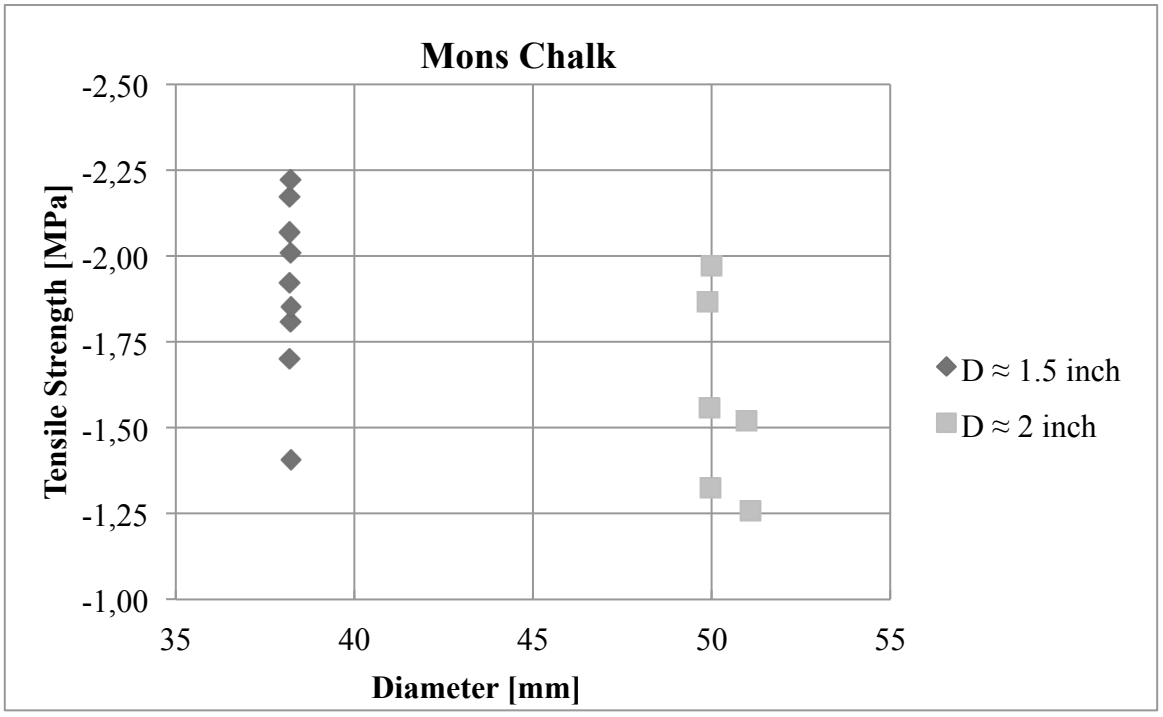

Figure 5-6: Direct tensile strength of Mons chalk in relation to diameter

Looking at the resulting tensile strength for chalk, some kind of size effect was expected, but it seems to be the opposite of the size effect for Castlegate sandstone. The tensile strength for chalk seems to be decreasing with increasing sample size. This will be further discussed in Chapter 6.3.

A typical stress-strain curve for the Mons chalk tested in this thesis is shown in Figure 5-7, where the curve has an exponential shape until the specimen fails. All the tested chalk specimens resulted in approximately the same stress-strain curve, and all curves are found in Appendix C.3 .

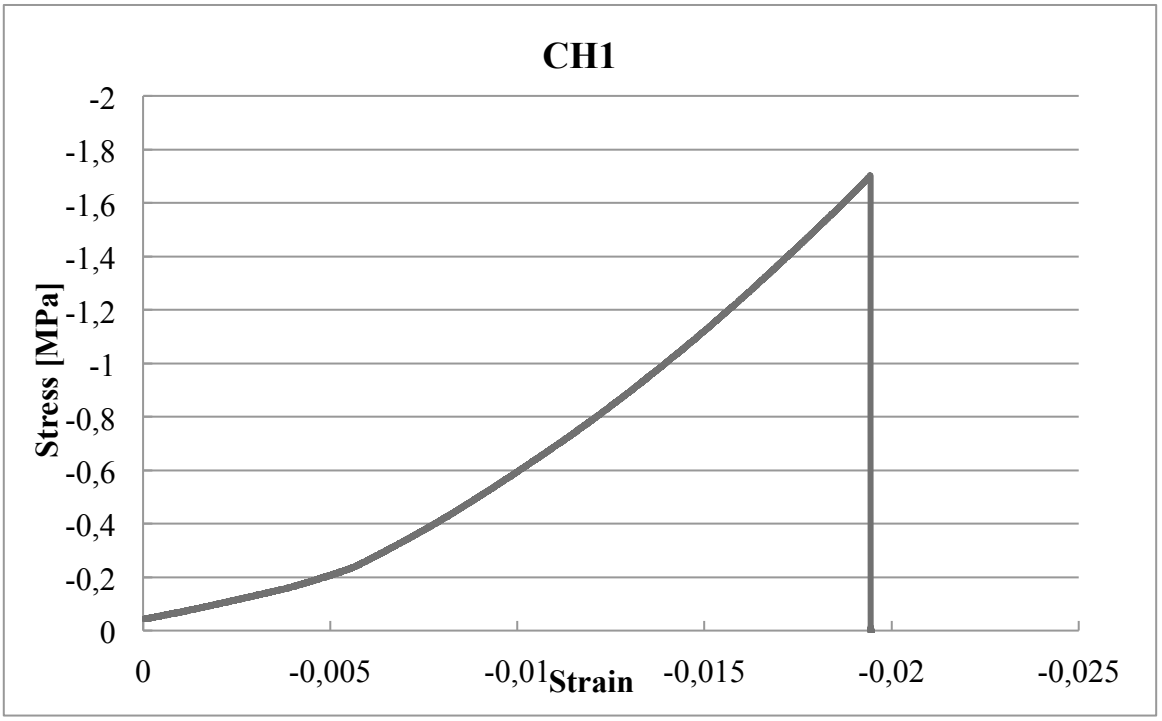

Figure 5-7: Stress-Strain curve for Mons chalk sample 1

5.4 Direct Tensile Strength Compared to Brazilian Strength

An analysis of tensile strength using the Brazilian test(Simpson, 2013) was done on the same rock types as the ones used in this thesis and the results of the two different tests is therefore interesting to compare. In most cases the absolute value of the direct tensile strength is lower than the value from the Brazilian tension test. The Brazilian tensile strengths are positive because the test is performed in compression, so to compare the tensile strengths for the two methods the direct tensile strength results are converted to positive values as well.

The equation found through the literary review, see Chapter 3.2, is not applicable in this case, because the length of the initial crack has not been recorded.

The direct tensile strength methods typically yield lower tensile strengths than the indirect methods when equivalent rock samples are compared. For this reason, direct methods are considered to result in the true tensile strength of the sample (Langford and Perras, 2014).

It seems to be of the common perception in all the literature that the direct tensile strength test yields a lower tensile strength than the Brazilian test. This is can be seen for the tensile strength results of Mancos shale, Figure 5-8, and Castlegate sandstone, Figure 5-9, from the

direct tensile strength tests conducted in this thesis and the Brazilian tests by Simpson (2013). However, for Mons chalk, see Figure 5-10, the Brazilian tensile strengths are actually lower than the direct tensile strengths.

Even though the test specimens used for the different tests have different diameters and therefore a direct comparison is not valid, the direct tensile strength tests for Castlegate sandstone and Mons chalk are done on two different specimen sizes, where one is larger and one is smaller than the diameter of the specimens in the Brazilian tests, and the different strengths can be correlated to some extent.

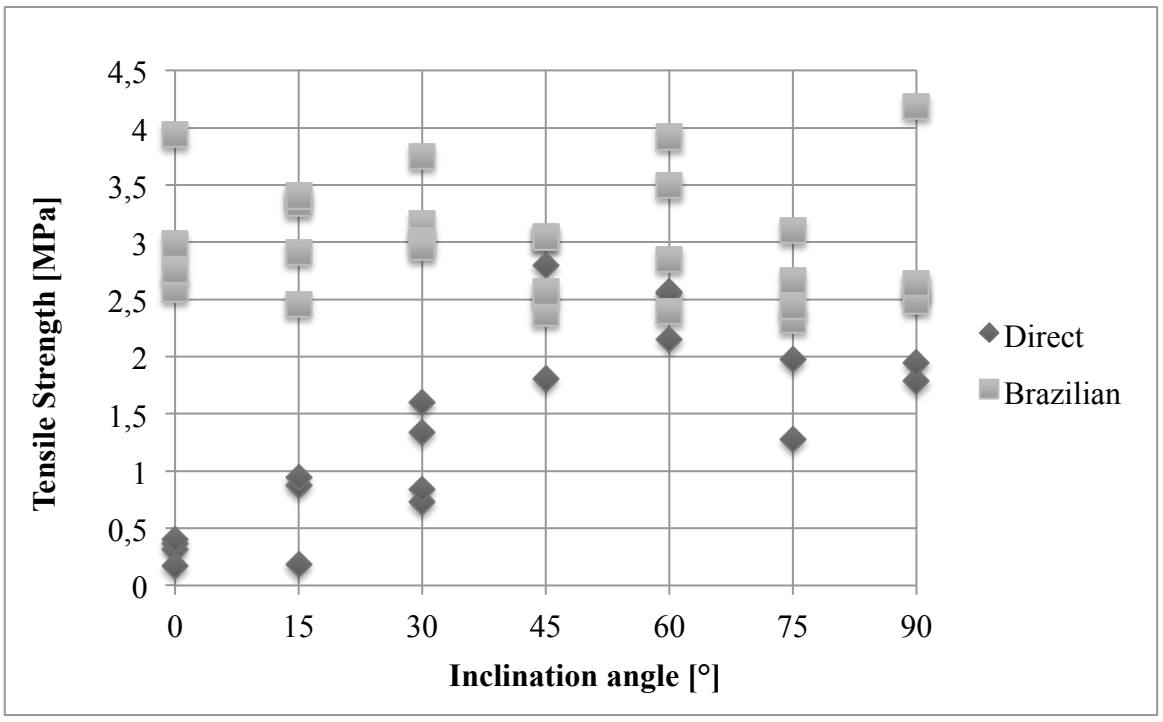

Figure 5-8: Direct tensile strength and Brazilian tensile strength for Mancos shale

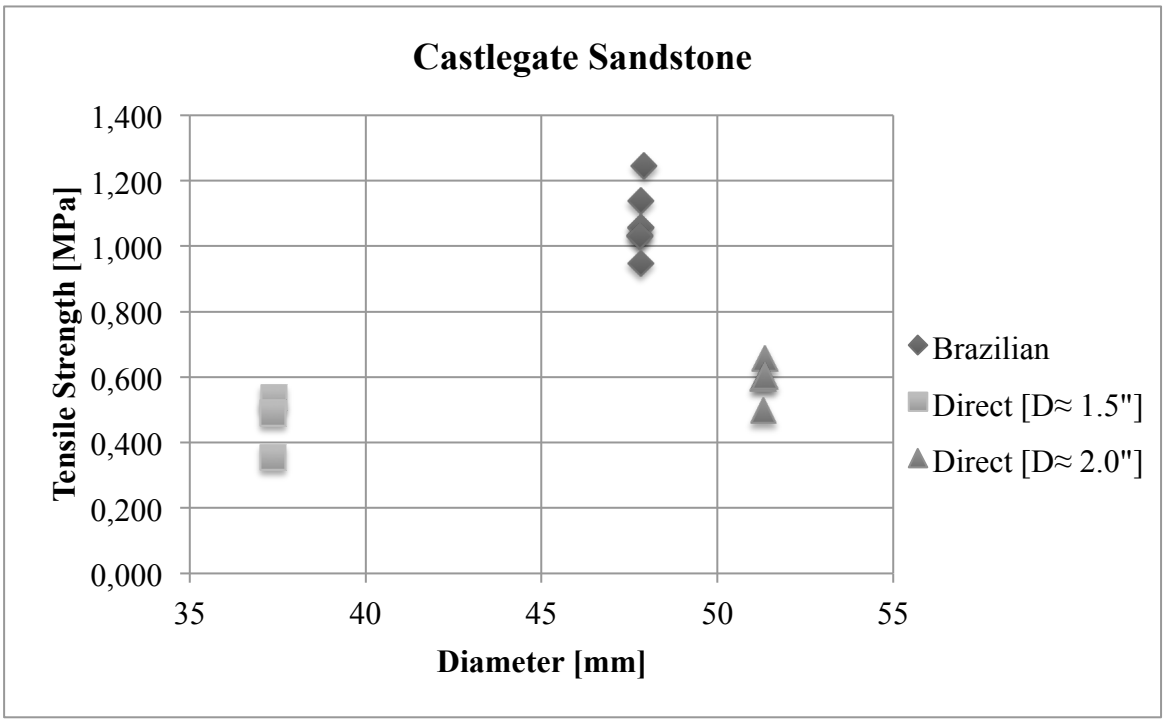

Figure 5-9: Direct tensile strength and Brazilian strength for Castlegate sandstone

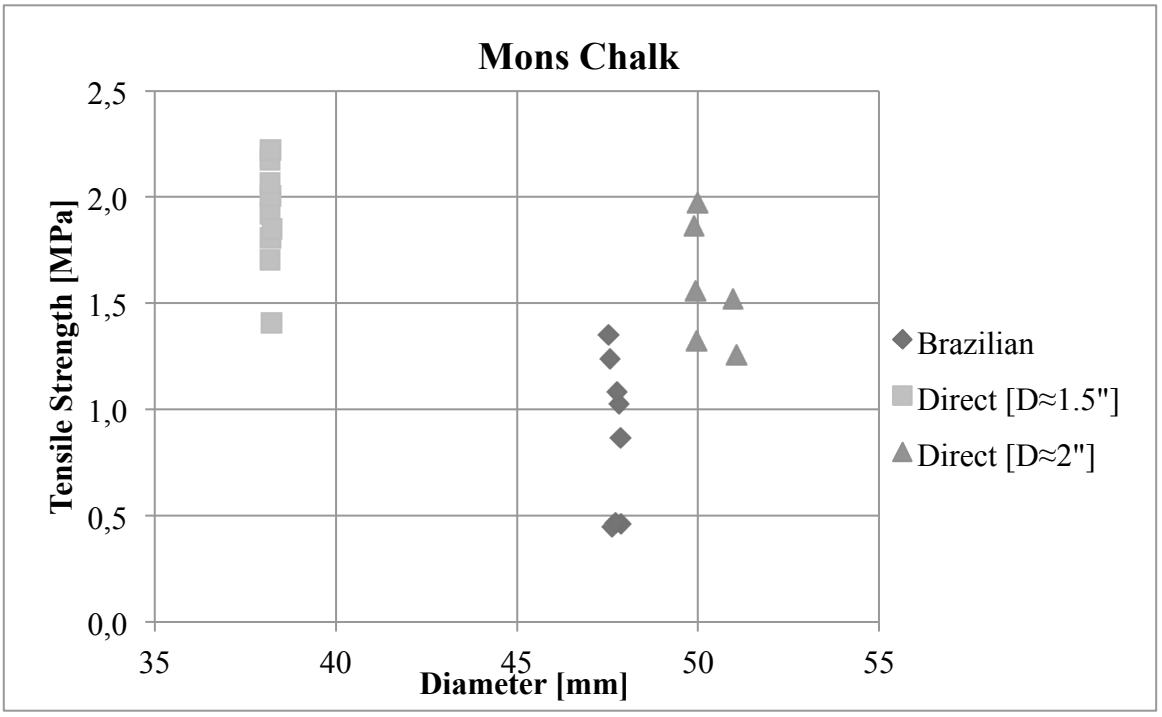

Figure 5-10: Direct tensile strength and Brazilian tensile strength for Mons chalk

5.5 Comparison between Tensile Strength and Fracture Toughness

Concurrently with the work of this thesis, another testing program was conducted in the laboratories at SINTEF by Brevik (2016), measuring the fracture toughness for the same types of rock. Several equations to correlate tensile strength to fracture toughness was found in the literary review, see Chapter 3.3. The four different equations are tested to see which might be a better fit than the others.

In the correlation the mean values and the standard deviation of the tensile strength for the different sizes of chalk and sandstone, along with the different inclination angle of shales, are used to create an upper and lower limit that the fracture toughness needs to fit into. The same is done for the fracture toughness, but for the shale there are only one to two samples tested. Because several of the correlations do not specify if uncorrected or corrected values of the fracture toughness are used, both are used to see which provide better fits. The values for uncorrected and corrected fracture toughness are used as input values to calculate the correlating tensile strength value. Fracture toughness values are calculated from load versus COD data, because these are available for all rock types and also provide a better fit. Figure 5-11 and Figure 5-12 show the results for the corrected fracture toughness from load versus COD in relation to the direct tensile strength and the Brazilian tensile strength respectively. The figures also contain the known correlation to see how well the data from both theses fit with these. The correlation with Brazilian tensile strength was done because the data was available and it provides a better fit with the known correlations.

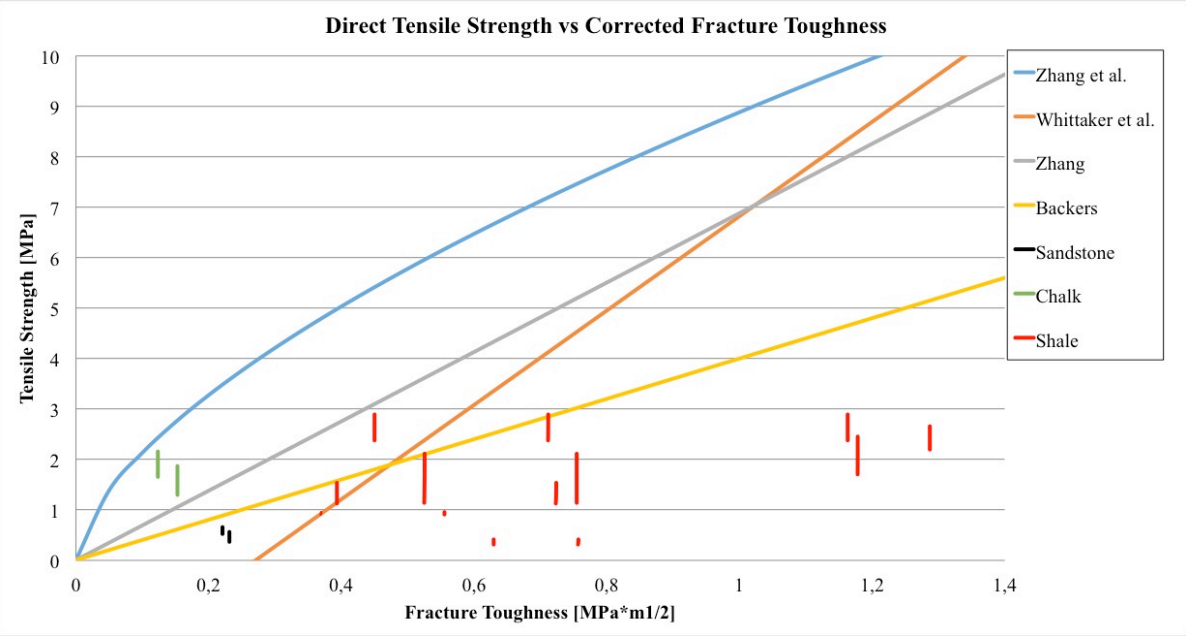

Figure 5-11: Direct tensile strength versus corrected fracture toughness, including known correlations

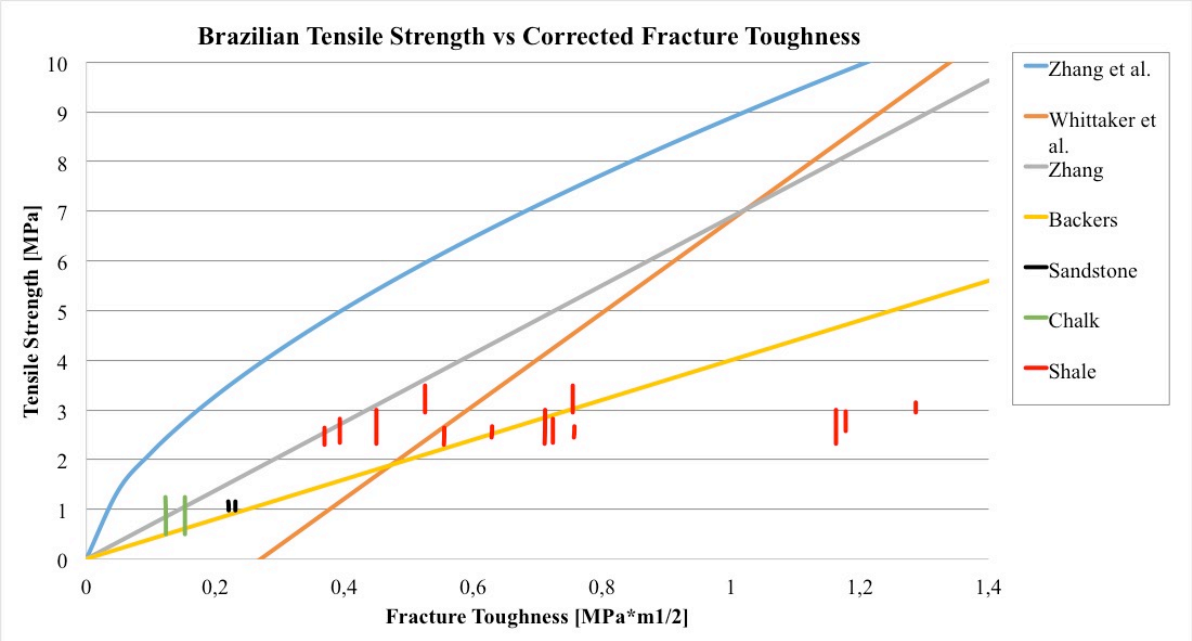

Figure 5-12: Brazilian tensile strength versus corrected fracture toughness, including known correlations

As seen from the figures, the tensile strength and fracture toughness data mainly provide a poor fit with the used correlations. The correlation from Zhang et al. overestimate and does not provide any matches with any of the data, and the correlation from Whittaker et al. only have a few data points that barely matches. The correlations from Backers (2004) and Zhang (2002) provide a better fit with both sets of tensile strength, and the Brazilian tensile strength gives the best fit. Overall Backers correlation is a better match than any of the other correlations regardless of the testing method for tensile strength.

Since all of the four equations identified to compare the tensile strength and the fracture toughness of rocks mainly build on tensile strength results from the Brazilian strength tests, it is not that surprising that the Brazilian tensile strength results from Simpson (2013) shows a better fit with the resulting tensile strength from these equations.

Looking at the results for direct tensile strength in this thesis and fracture toughness, from Brevik (2016), there is no obvious relationship between the values and they are a poor fit to the known correlations. The literature review did not reveal any published relationships between the tensile strengths from direct tensile strength tests and fracture toughness.

6 Discussion

The previous chapter presents the results from the experiments and calculations conducted throughout the work for this thesis. This chapter will take a closer look at the different results and discuss any irregularities or inconsistencies.

6.1 Implementation of the Experiment

The experiments conducted using the direct tensile strength test followed the procedure outlined by ASTM (2008) as closely as possible. The output values of load and time from the software used to conduct the tests can be plotted against each other. For most of the samples, this resulted in an exponential graph, as seen in Figure 6-1 for sample 8 of Castlegate sandstone, and this is the expected result. Some of the samples, however, showed some discrepancies from the expected exponential shape, see Figure 6-2. These discrepancies are also visible in the stress versus strain curves located in Appendix C as the calculated stresses depend on the load. The samples that showed some kind of discrepancy in the shape of the graph includes sample 1, 5 and 7 of Castlegate sandstone, and samples 9, 12, 17, 18 and 19 of Mancos shale. For sample 1 of Castlegate sandstone, the discrepancy is explainable because the test was paused to increase the loading rate to speed up the test. The other two samples of sandstone that showed discrepancies, sample 5 and 7, has no clear explanation, but these two had a lower resulting tensile strength than the two samples that had an exponential time versus load curve, sample 6 and 8. There is therefore a reason to believe that the discrepancies have some sort of effect on the resulting tensile strength, but there is no clear explanation as to why this is.

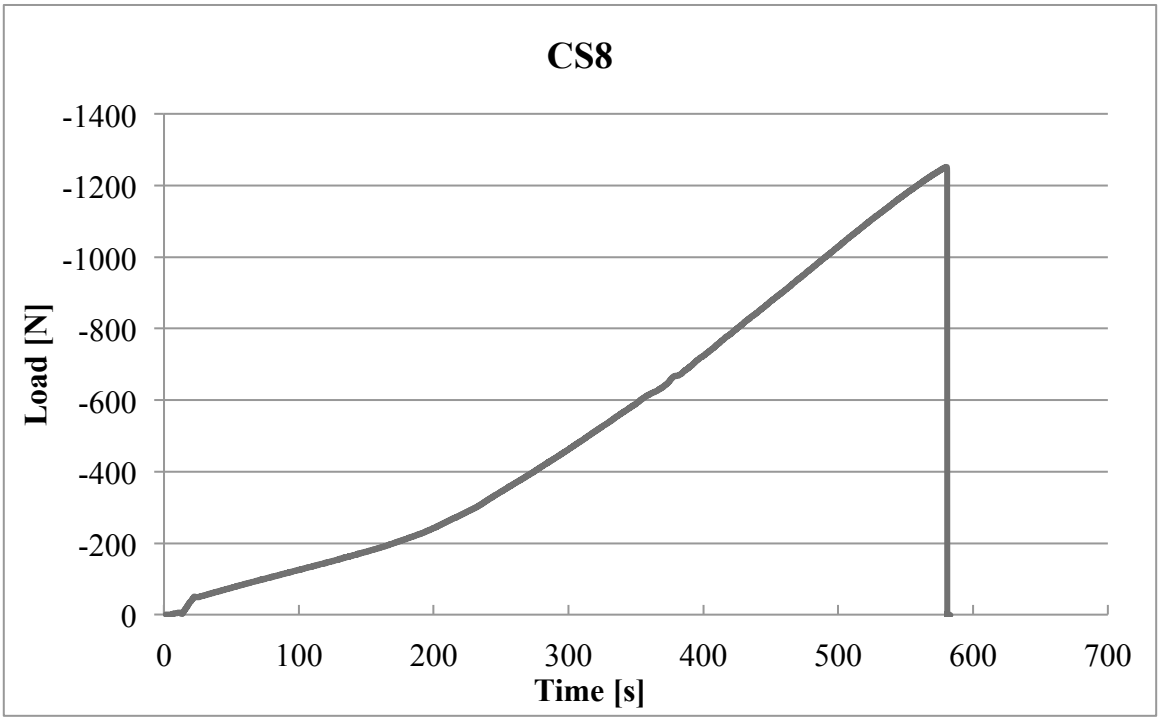

Figure 6-1: Load versus time for Castlegate sandstone sample 8

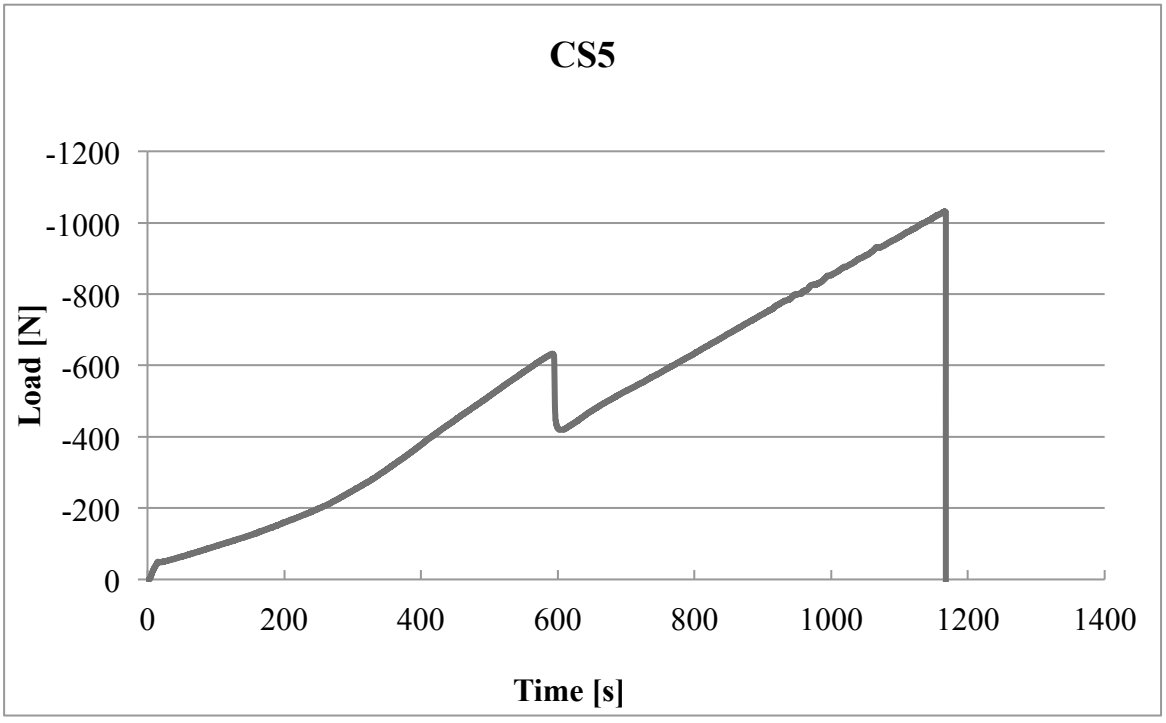

Figure 6-2: Load versus time for Castlegate sandstone sample 5

For Mancos shale, the graphs of the samples with discrepancies have the same kind of shape, where it looks like the load has been constant for a while, until the load goes slightly up and

the sample brakes. One example of the graph shape discrepancies in the shale samples are shown in Figure 6-3.

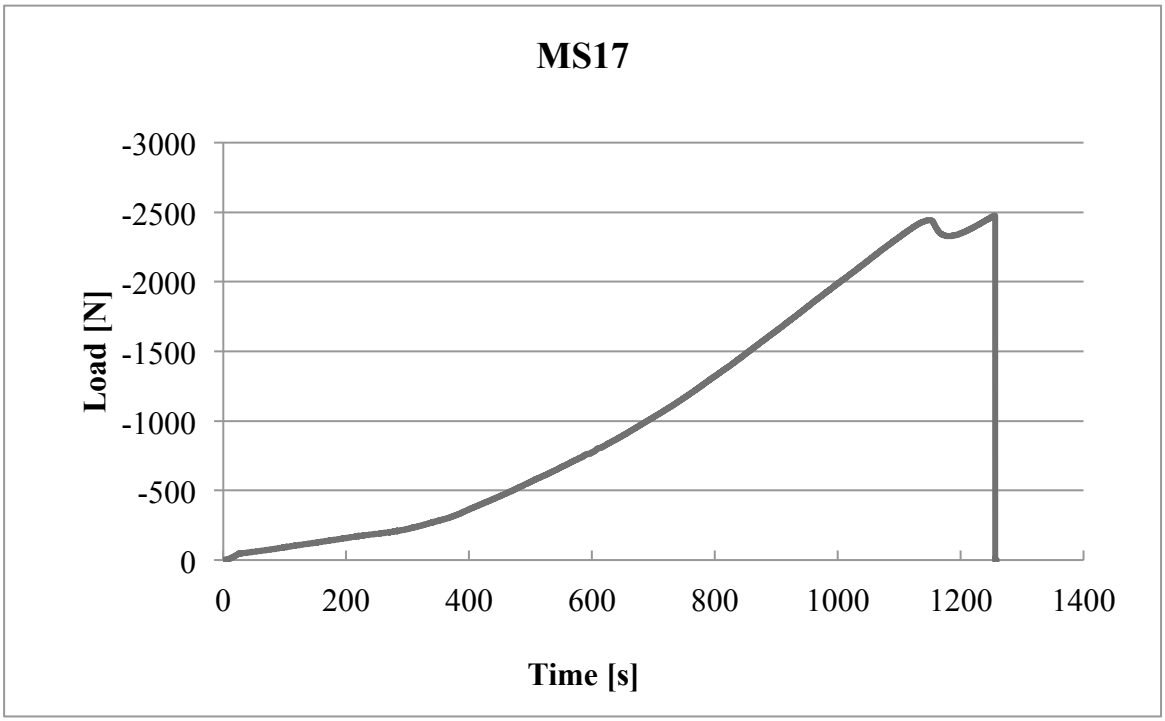

Figure 6-3: Load versus time for Mancos shale sample 17

6.2 Sources of Error

The direct tensile strength tests have been performed as close to the standard method presented by ASTM as possible, and there are several possible sources of error. One of them is the alignment of the specimens, with the longitudinal axis, when gluing them to the end cups. ASTM states that the alignment should be checked by measuring the length between the end cups at three locations 120° apart. The maximum difference between these measurements should be less than 0.10 mm for each 25.0 mm of specimen diameter. This was done, but as the glue used has a short hardening time, it was difficult to do the alignment in the short amount of time. Some of the specimens may therefore not be precisely aligned, and this has an impact on the resulting tensile strength.

The epoxy glue used to glue the specimens to the end cups is assumed to have a higher strength than the specimen itself and therefore it should not interfere with the results. However some of the tested specimens of all three rock types have fractured at the end of the specimen close to the glue, but none of the specimens were pulled out of the end cups during

the end cups, so the assumption that the glue has a higher strength than the specimen seems to hold true.

6.3 Size Effect

The microstructure of many natural materials such as geomaterials and biomaterials and synthetic materials such as steel and concrete is non-uniform. In other words, the characteristics of material show spatial variation in the microscopic scale. For the case of rocks, different minerals, cements, microfissures and voids cause the microstructural heterogeneity (Rafiei and Martin, 2014).

The macroscopic outcome of non-uniform microstructures with weaker and stronger elements distributed within the material is size effect, which implies reduction of overall strength with increasing the size of the sample. While it is still one of the fundamental open problems, the general consensus is that increased number of weaker elements (weaker materials, microfractures, etc.) in a larger sample of material contributes to size effect (Rafiei and Martin, 2014).

Only Castlegate sandstone and Mons chalk were tested at two different specimen sizes to investigate the presence of a size effect on the resulting tensile strength. The literary review showed that the general agreement seems to be that the rock tensile stress decreases as the specimen size increase. This holds true for the chalk tested in this thesis, but not for the sandstone. The direct tensile strength of the largest Mons chalk specimens tested, 36% larger than the smallest, is about 83% of the direct tensile strength of the smallest samples. Reviewing the average values for the direct tensile stress of sandstone, they seem to increase by 27% when the specimen size increase by about 35%. Because the bulk density of the four larger sandstone specimens is about the same as the bulk density for the smaller specimens, the reason for the difference in the direct tensile strength can not be connected to the difference in the amount of pore spaces in the different specimen sizes, as there seems to be about the same amount of pore spaces in all tested specimens of sandstone. The specimens are all cut from the same block, so the mechanic properties should be the same for all specimens. There could have been some undiscovered weakness in some of the samples, but it is not plausible that this is the case for all four specimens of the smallest size. To investigate if the increase in tensile strength with increasing specimen size of Castlegate sandstone is true for all size increases, more specimen sizes needs to be tested.

Even though there is a clear size effect in the tested specimens, the number of specimen sizes tested for this thesis is not enough to make an overall quantification of the size effect.

6.4 Anisotropy Effect on Mancos Shale

Most rocks possess mechanical anisotropy to some extent, including strength anisotropy. This implies that strength varies with the orientation of the principal stresses. (Fjaer and Nes, 2013)

From Figure 5-1 where the direct tensile strengths of Mancos shale, and the average of these, is plotted against the inclination angle to the bedding it is clear that there is an anisotropy effect on the tensile strength. An inclination angle of 45 or 60° yields the highest tensile strength values when looking at the average for each inclination angle. The absolute highest tensile strength was found in sample number 10, at an inclination angle of 45 degrees and is -2.795 MPa. An inclination angle of 0 degrees gives the lowest tensile strengths, and these tensile strengths are about 11% of the highest tensile strength for the tested Mancos shales.

Direct tensile strength tests should be carried out on more specimens of different inclination angle to ensure that the average curve seen in Figure 5-1 is only the result of an anisotropy effect and not existing weaknesses inside the specimens. Then it might also be possible to quantify the anisotropy effect.

6.5 Direct Tensile Strength Versus Brazilian Tensile Strength

For Castlegate sandstone the correlation between the tensile strength for the two methods is in agreement with the literature. The direct tensile strength for Castlegate is about 50% of the Brazilian strength, and the difference here may be partly governed by the amount and distribution of pore spaces and fissures in the rock.

The correlation between the direct tensile strength and the Brazilian tensile strength is according to the tests conducted on Mons chalk for this thesis, the opposite of the correlation found in the literature review. There seems to be no clear reason for this to happen, as the bulk density of the tested specimens for both tests are about the same, the amount of pore spaces in all specimens is assumed to be the same. The direct tensile strength of Mons chalk is about 50% larger than the Brazilian tensile strength. It is interesting to note that the chalk samples are tested for direct tensile strength at both a smaller and a larger diameter than the diameter used in the Brazilian tests.

For Mancos shale it seems like the correlation between the direct tensile strength and the Brazilian tensile strength is affected by the anisotropy effect, because the direct tensile strength at 45 degrees inclination is about 86% of the Brazilian strength, while for 0 degrees inclination it is only about 10% of the Brazilian strength at the same inclination. There seems to be a smaller anisotropy effect on the Brazilian strengths than on the direct tensile strengths.

The specimens used in the Brazilian strength test and the direct tensile strength test do not have the same diameter and can therefore not be directly compared, but overall the values from the direct tensile strength test should be lower than for the Brazilian strength test. Because the test methods operate with different specimen sizes it would have been interesting to measure the initial crack length during the direct tensile strength test so the equation by Rafiei and Martin (2014) identified through the literature review could be used to check if the two different tensile strength results could be linked.

6.6 Tensile Strength versus Fracture Toughness

The relationship between tensile strength exists when it is assumed that tensile failure is the result of coalescence of tensile microcracks. It is also generally agreed that extension of cracks begins in the plane orthogonal to the greatest tension, and hence the tensile strength is one of the controlling factors for fracture toughness, regardless of the mode of fracturing. Different correlations have been established and were discovered through the literary review, and a match was attempted between these known correlations and the tensile strength data in this thesis, Brazilian strength data from Simpson (2013), and the fracture toughness data from Brevik (2016).

Results from the comparison between tensile strengths and fracture toughness is shown in the figures in Chapter 5.5. These results is not surprising, because the rocks tested in this thesis are considered weak to very weak, while none of the used correlations are specifically designed for these types of rocks. The correlations have focused on a broad range of different rock types and testing methods. Since both the tensile strength and the fracture toughness is known to vary with the testing method, it is not very surprising that an overall good match was not found.

The correlation from Backers (2010) achieved the best overall match with the data from Brazilian strength tests and fracture toughness, which is not surprising because this correlation builds on the same testing methods used for these data sets.

Correlations might achieve a higher accuracy if they focus on one specific testing method for each of the parameters; tensile strength and fracture toughness, or if they focus on similar rock types. No new correlation was attempted between the direct tensile strength in this thesis and the fracture toughness from Brevik (2016) due to the low amount of tested specimens and limited time.

7 Conclusion

Tensile strengths have been determined from direct tensile strength tests on Castlegate sandstone, Mancos shale and Mons chalk. For Castlegate sandstone and Mons chalk the size effect has been investigated, and the anisotropy effect has been investigated for Mancos shale. The size effect is clear in both chalk and sandstone, but the chalk specimens have the opposite size effect compared to the sandstone specimens. Only the chalk specimens exhibit the expected size effect where the tensile strength decreases when the specimen size increase. For Mancos shale, different inclination angles relative to the bedding was tested and proved the presence of an anisotropy effect.

Direct tensile strength results showed the expected relationship to Brazilian tensile strength for the Castlegate sandstone and the Mancos shale, where the direct tensile strengths are lower than the Brazilian tensile strength. The direct tensile strength results for Mons chalk showed the opposite relation to the Brazilian tensile strength.

Comparing the tensile strength results to fracture toughness showed some matches with the correlations identified through the literary review.

In this thesis the direct tensile strength tests was carried out at ambient conditions due to limited time, but in the future it would be interesting to conduct the tests at conditions that are closer to the in-situ conditions. In-situ conditions include a confining pressure and elevated temperatures, and these factors are through the literary review linked to the tensile strength of the rock. However, the literary review did not reveal any tensile strength tests done under in-situ conditions, so it is not known if this is at all possible.

Tensile strength is a very important parameter in hydraulic fracturing modeling, as it dictates the minimum borehole pressure required to induce fractures. The use of the tensile strength depends on the software used for simulation of the hydraulic fractures, but for MDEM a tensile failure criterion is used to initiate and propagate fractures. Therefore, the tensile strength results found here is relevant for simulation on the tested rock types. The direct tensile strength also provides a more accurate estimate of the actual tensile strength than other indirect test methods, and is therefore more important than the results from the Brazilian tensile strength tests.

8 Future Work

The work done for this thesis was done with a limited amount of time, knowledge and resources. The completed investigation revealed several interesting relationships and results, but it would be interesting to examine these more closely. Some suggestions for future work are therefore listed below.

- Examine the possibility to perform the direct tensile strength test under in-situ conditions.
- Investigate the relationship between fracture toughness and tensile strength further by testing a broader selection of rocks.
- Perform direct tensile strength test while measuring acoustic emissions and using a high-speed camera to look more closely on fracture initiation and propagation as the rock is exposed to increasing tension.
- Investigate the size effect more closely by testing a broader range of specimen sizes.
- Find a way to record the initial crack length during the direct tensile strength test so the equation by Rafiei and Martin can be verified for the relationship between the BTS and the DTS.

9 Bibliography

ASTM 2008a. Standard Test Method for Direct Tensile Strength of Intact Rock Core Specimens.

ASTM 2008b. Standard Test Method for Splitting Tensile Strength of Intact Rock Core Specimens.

BACKERS, T. 2004. *Fracture Toughness Determination and Micromechanics of Rock Under Mode I and Mode II Loading.* University of Potsdam.

BREVIK, N. Ø. 2016. Experimental Study of Fracture Toughness in Sedimentary Rocks.

FJAER, E. & NES, O. M. 2013. Strength Anisotropy of Mancos Shale. American Rock Mechanics Association.

FJAER, E. H., R.M.; HORSRUD, P.; RAAEN, A.M.; RISNES, R. 2008. Petroleum Related Rock Mechanics.

FUENKAJORN, K. & DAEMEN, J. J. K. 1986. Shape Effect On Ring Test Tensile Strength. American Rock Mechanics Association.

KLANPHUMEESRI, S. 2010. Direct Tension Testing of Rock Specimens.

LANGFORD, J. C. & PERRAS, M. A. 2014. Obtaining Reliable Estimates of Intact Tensile Strength. American Rock Mechanics Association.

RAFIEI, R. H. & MARTIN, C. D. 2014. The Direct and Brazilian Tensile Strength of Rock In the Light of Size Effect and Bimodularity. American Rock Mechanics Association.

SIMPSON, N. D. J. 2013. *An analysis of tensile strength, fracture initiation and propagation in anisotropic rock (gas shale) using Brazilian tests equipped with high speed video and acoustic emission.* Norwegian University of Science and Technology.

YILMAZ, I. Y., Ö. 2014. Use of the core strangle test for determining strenght anisotropy of rocks. *International Journal of Rock Mechanics and Mining Sciences*.

ZHANG, Z. X. 2002. An empirical relation between mode I fracture toughness and the tensile strength of rock.

10 Nomenclature

a	half-length of crack	[mm]
A’	cross-sectional area	[mm^2]
b	half-width of plate	[mm]
C_0	uniaxial compressive strength	[MPa]
D	diameter	[mm]
D_e	equivalent core diameter	[mm]
E	Young’s modulus	[GPa]
F	load	[N]
F_c	failure load	[N]
I_s	point load strength index	[MPa]
K_f	stress concentration factor at center hole boundary	
K_{IC}	mode I fracture toughness (critical stress intensity factor)	[MPa*$m^{1/2}$]
K^C_{IC}	mode I corrected fracture toughness	[MPa*$m^{1/2}$]
P_f	applied load	[N]
r^2	coefficient of determination	
t	thickness	[mm]
T_0	tensile strength	[MPa]
w_s	surface energy	[N/mm]
α	crack radius	[mm]
β	angle between y-axis and bedding plane	[°]
β_c	crack shape factor	
σ_R	ring tensile strength	[MPa]
σ_t	tensile strength	[MPa]
θ	angle between x-axis and bedding plane	[°]

11 Abbreviations

ASTM	American Society of the international association for Testing and Materials
BTS	Brazilian Tensile Strength
CH	Mons Chalk
CID	Consolidated Isotropically Drained test
COD	Clip-gage Opening Displacement
CS	Castlegate Sandstone
DTS	Direct Tensile Strength
HF	Hydraulic Fracturing
MDEM	Modified Discrete Element Method
MS	Mancos Shale
MTS	Material Test Systems Inc.
UCS	Uniaxial Compressive Strength test
XLOT	Extended Leak Off Test

Appendix A Risk Assessment

The work done for this thesis involved work in a laboratory, and therefore some safety precautions needed to be taken. Before gaining access to the laboratory a safety course provided by NTNU and SINTEF was completed. A tour of the laboratory was also completed to locate potential hazards and first aid and safety equipment. Table A-1 shows the potential hazards specifically related to the work done in this thesis as well as the actions taken to limit and avoid these risks.

Table A-1: Risk assessment of potential hazards in the laboratory

Hazards	**Safety measures**
Pinch point hazard due to loading frames present in the laboratory.	Awareness of the hazards related to the equipment. Proper training on the use of the loading frames. The loading frames have a built-in safety barrier and during the experiments hands and feet were kept away from the loading frame.
Harmful chemicals are present in the laboratory.	Chemicals are stored in enclosed cabinets with information related to proper handling and safety precautions.
Spill hazard resulting in slippery floor as a result of using inert oil for Mancos Shale.	Using lids on the buckets when moving the samples inside the laboratory. Avoid spilling when the samples are taken out of the inert oil. Using a rag or cloth specifically made for oil cleanup if inert oil is spilled on the floor and clean up immediately.
Harm to skin, eyes, etc. when using quick hardening glue.	Use safety goggles and gloves at all time when dealing with glue. If contact between glue and skin, apply hot, running water immediately before the glue hardens to avoid skin damage.

Appendix B Data and Resulting Direct Tensile Strength

The tables below include information and test results for all the tested specimens. Note that some numbers are missing, this is due to unsuccessful experiments.

B.1 Mancos Shale

Table B-1: Data and tensile strength for Mancos shale θ = 0°

Sample ID	Diameter [mm]	Length [mm]	Mass [g]	Bulk density [g/cm^3]	Loading Rate [mm/s]	Max Load [N]	Direct tensile strength [MPa]
MS20	37.83	76.91	222.112	2.569	0.10	-353.49	-0.314
MS21	38.27	77.2	229.045	2.579	0.10	-420.47	-0.366
MS22	38.27	76.93	228.245	2.579	0.10	-465.89	-0.405
MS23	38.24	77.12	228.9	2.584	0.10	-196.27	-0.171

Table B-2: Data and tensile strength for Mancos shale θ = 15°

Sample ID	Diameter [mm]	Length [mm]	Mass [g]	Bulk density [g/cm^3]	Loading Rate [mm/s]	Max Load [N]	Direct tensile strength [MPa]
MS5	38.27	76.79	227.977	2.581	0.10	-207.3	-0.180
MS6	38.27	73.18	217.521	2.584	0.05	-1006.08	-0.875
MS7	38.28	76.15	226.741	2.587	0.05	-1084.56	-0.942

Table B-3: Data and tensile strength for Mancos shale θ = 30°

Sample ID	Diameter [mm]	Length [mm]	Mass [g]	Bulk density [g/cm3]	Loading Rate [mm/s]	Max Load [N]	Direct tensile strength [Mpa]
MS1	38.27	77.03	233.13	2.631	0.05	-1543.41	-1.342
MS2	38.29	77.01	228.705	2.579	0.10	-842.17	-0.731
MS3	38.28	77.02	240.374	2.712	0.10	-1835.47	-1.595
MS4	38.28	76.69	227.414	2.577	0.10	-970.18	-0.843

Table B-4: Data and tensile strength for Mancos shale θ = 45°

Sample ID	Diameter [mm]	Length [mm]	Mass [g]	Bulk density [g/cm^3]	Loading Rate [mm/s]	Max Load [N]	Direct tensile strength [MPa]
MS8	38.27	76.73	228.242	2.586	0.08	-2074.07	-1.803
MS9	38.26	77.25	228.918	2.578	0.08	-2915.85	-2.536
MS10	38.28	77.04	228.166	2.573	0.08	-3216.45	-2.795

Table B-5: Data and tensile strength for Mancos shale θ = 60°

Sample ID	Diameter [mm]	Length [mm]	Mass [g]	Bulk density [g/cm^3]	Loading Rate [mm/s]	Max Load [N]	Direct tensile strength [MPa]
MS17	38.27	77.43	229.341	2.575	0.10	-2474.28	-2.151
MS18	38.28	77.5	229.667	2.575	0.10	-2950.25	-2.563
MS19	38.27	77.52	229.4	2.573	0.10	-2937.15	-2.553

Table B-6: Data and tensile strength for Mancos shale θ = 75°

Sample ID	Diameter [mm]	Length [mm]	Mass [g]	Bulk density [g/cm^3]	Loading Rate [mm/s]	Max Load [N]	Direct tensile strength [MPa]
MS14	38.31	72.25	215.422	2.587	0.10	-1474.58	-1.279
MS15	38.28	77.44	230.652	2.588	0.10	-2268.26	-1.971

Table B-7: Data and tensile strength for Mancos shale θ = 90°

Sample ID	Diameter [mm]	Length [mm]	Mass [g]	Bulk density [g/cm^3]	Loading Rate [mm/s]	Max Load [N]	Direct tensile strength [MPa]
MS11	38.28	77.49	230.7	2.587	0.10	-2059.77	-1.790
MS12	38.28	76.82	228.473	2.584	0.10	-2879.35	-2.502
MS13	38.27	76.75	228.206	2.585	0.10	-2237.16	-1.945

B.2 Castlegate Sandstone

Table B-8: Data and tensile strength for Castlegate sandstone

Sample ID	Diameter [mm]	Length [mm]	Mass [g]	Bulk density [g/cm^3]	Loading Rate [mm/s]	Max Load [N]	Direct tensile strength [MPa]
CS1	37.38	76.54	161.61	1.924	0.20	-589.95	-0.538
CS2	37.41	76.55	160.803	1.911	-	-	-
CS3	37.37	76.57	160.881	1.916	0.10	-390.12	-0.356
CS4	37.37	76.65	161.616	1.922	0.08	-536.71	-0.489
CS5	51.31	102.73	408.759	1.924	0.08	-1031.28	-0.499
CS6	51.37	102.69	407.201	1.913	0.10	-1360.38	-0.656
CS7	51.29	102.67	407.998	1.923	0.10	-1231.87	-0.596
CS8	51.37	102.76	406.848	1.910	0.10	-1251.98	-0.604

B.3 Mons Chalk

Table B-9: Data and tensile strength for Mons chalk

Sample ID	Diameter [mm]	Length [mm]	Mass [g]	Bulk density [g/cm^3]	Loading Rate [mm/s]	Max Load [N]	Direct tensile strength [MPa]
CH1	38.19	77.79	141.222	1.585	0.05	-1949.84	-1.702
CH2	38.22	76.56	130.924	1.491	0.10	-1615.29	-1.408
CH3	38.19	77.75	140.683	1.580	0.10	-2201.8	-1.922
CH4	38.21	77.52	140.736	1.583	0.12	-2303.54	-2.009
CH5	38.21	77.61	137.132	1.541	-	-	-
CH6	38.18	77.65	139.805	1.573	0.15	-2368.15	-2.068
CH7	38.18	77.64	139.672	1.571	0.15	-2488.42	-2.174
CH8	38.2	77.68	142.05	1.596	0.15	-2547.01	-2.222
CH9	38.21	77.54	139.452	1.568	0.15	-2074.08	-1.809
CH10	38.23	77.52	141.796	1.593	0.15	-2126.18	-1.852
CH11	38.2	77.54	138.766	1.561	-	-	-
CH12	51.08	101.9	328.952	1.575	0.15	-2576.66	-1.257
CH13	50.96	101.82	331.589	1.597	0.15	-3102.75	-1.521
CH14	49.96	102.04	319.699	1.598	0.15	-2596.69	-1.325
CH15	49.88	101.94	318.412	1.598	0.15	-3648.48	-1.867
CH16	49.93	102.08	319.048	1.596	0.15	-3050.64	-1.558
CH17	49.99	102.11	319.457	1.594	0.15	-3871.04	-1.972

Appendix C Stress-Strain Curves

C.1 Mancos Shale

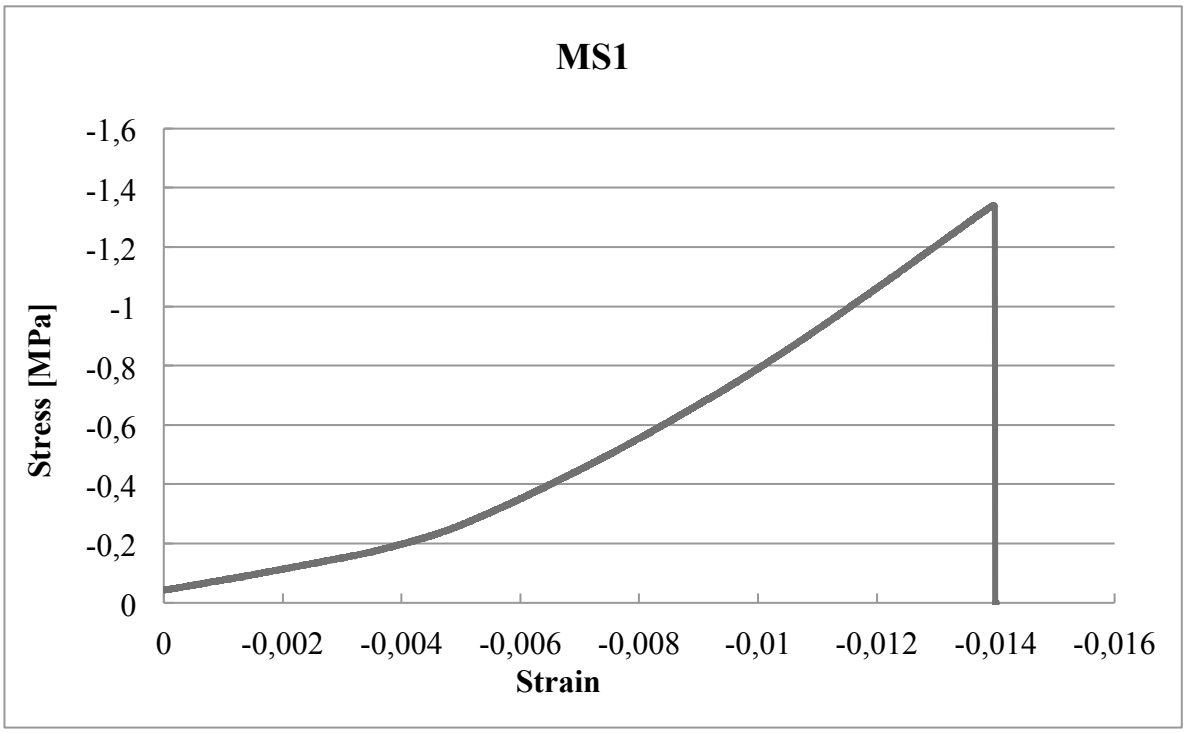

Figure C-1: Stress-Strain curve for Mancos shale sample 1 (θ = 30°)

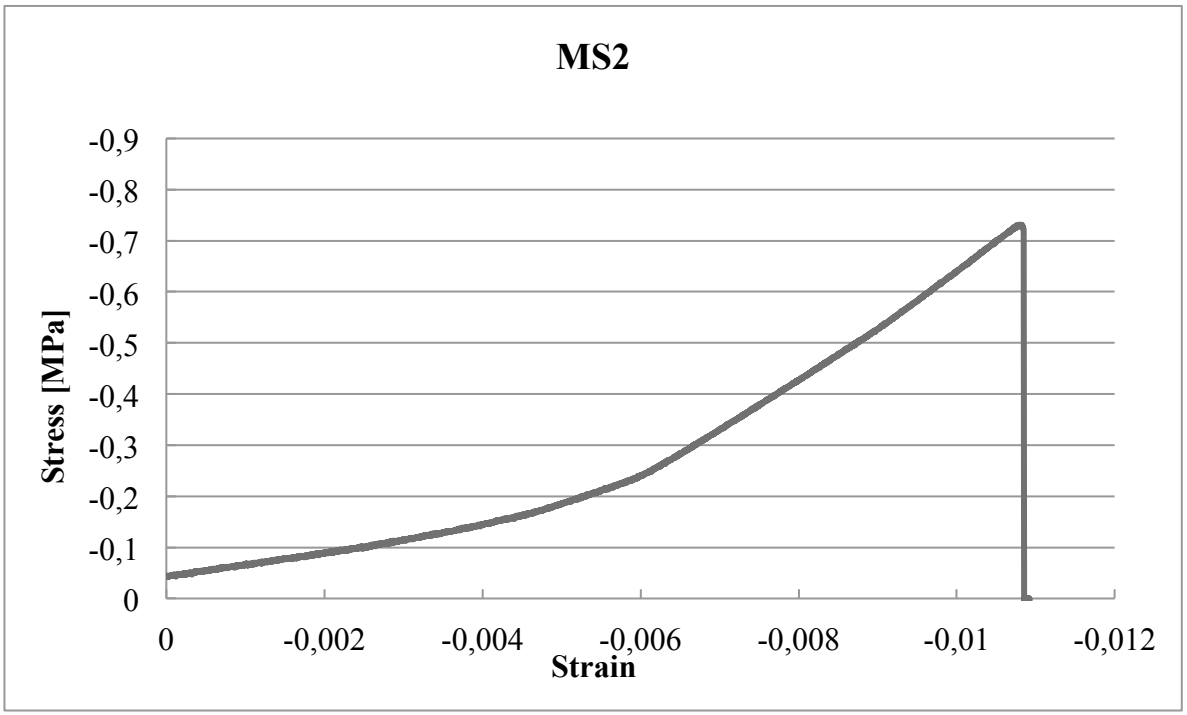

Figure C-2: Stress-Strain curve for Mancos shale sample 2 (θ = 30°)

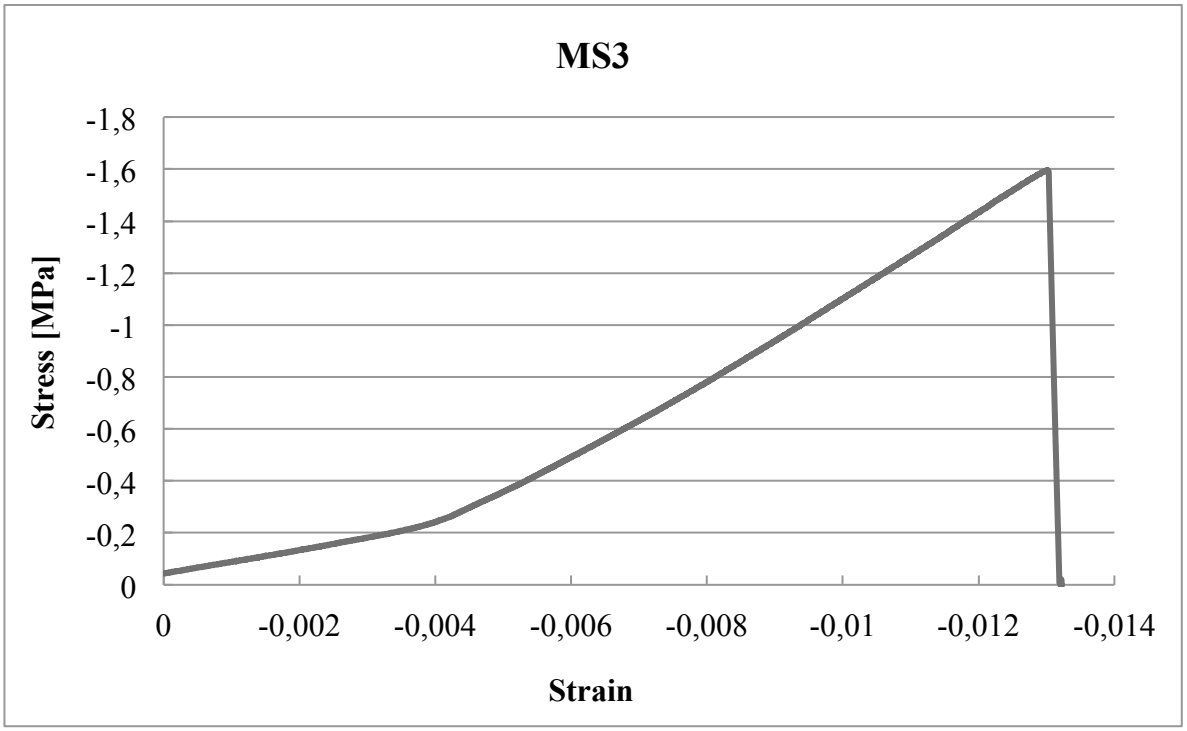

Figure C-3: Stress-Strain curve for Mancos shale sample 3 (θ = 30°)

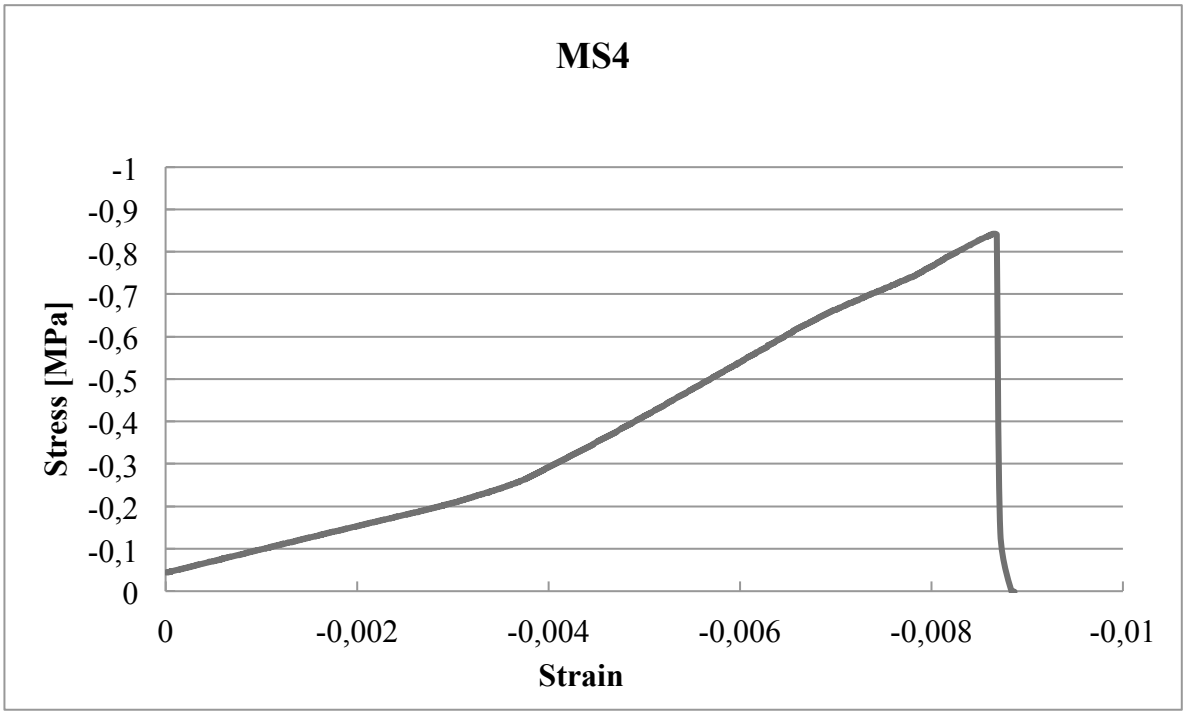

Figure C-4: Stress-Strain curve for Mancos shale sample 4 (θ = 30°)

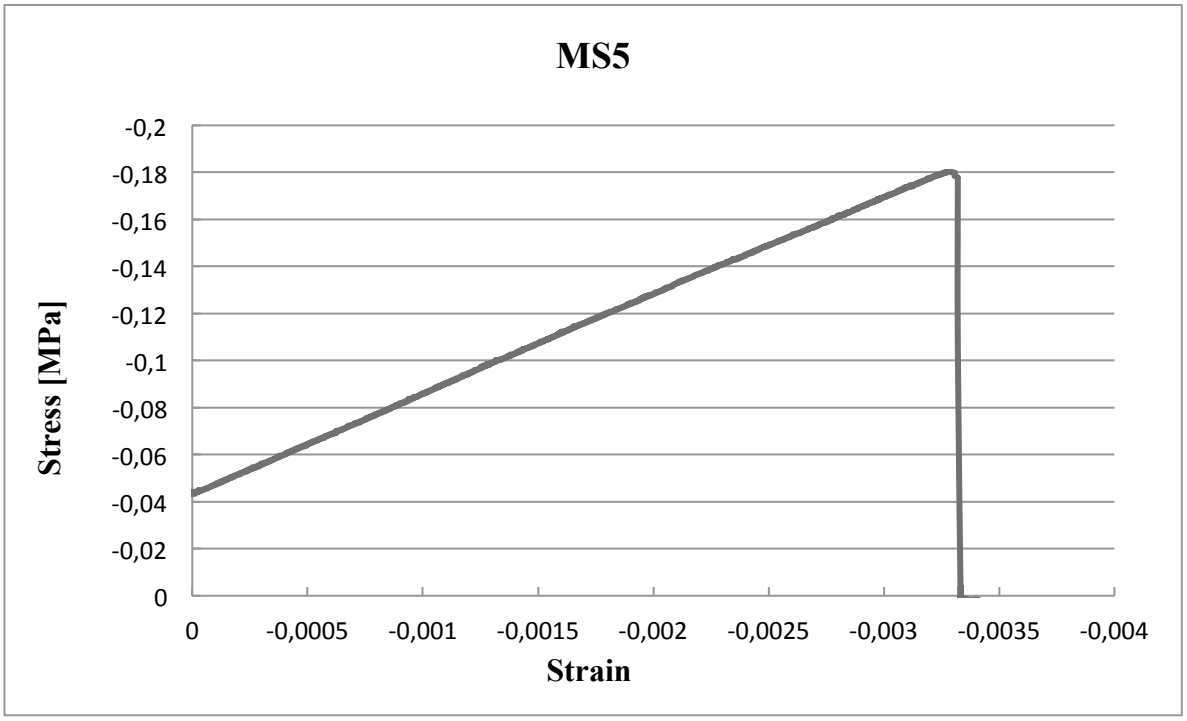

Figure C-5: Stress-Strain curve for Mancos shale sample 5 (θ = 15°)

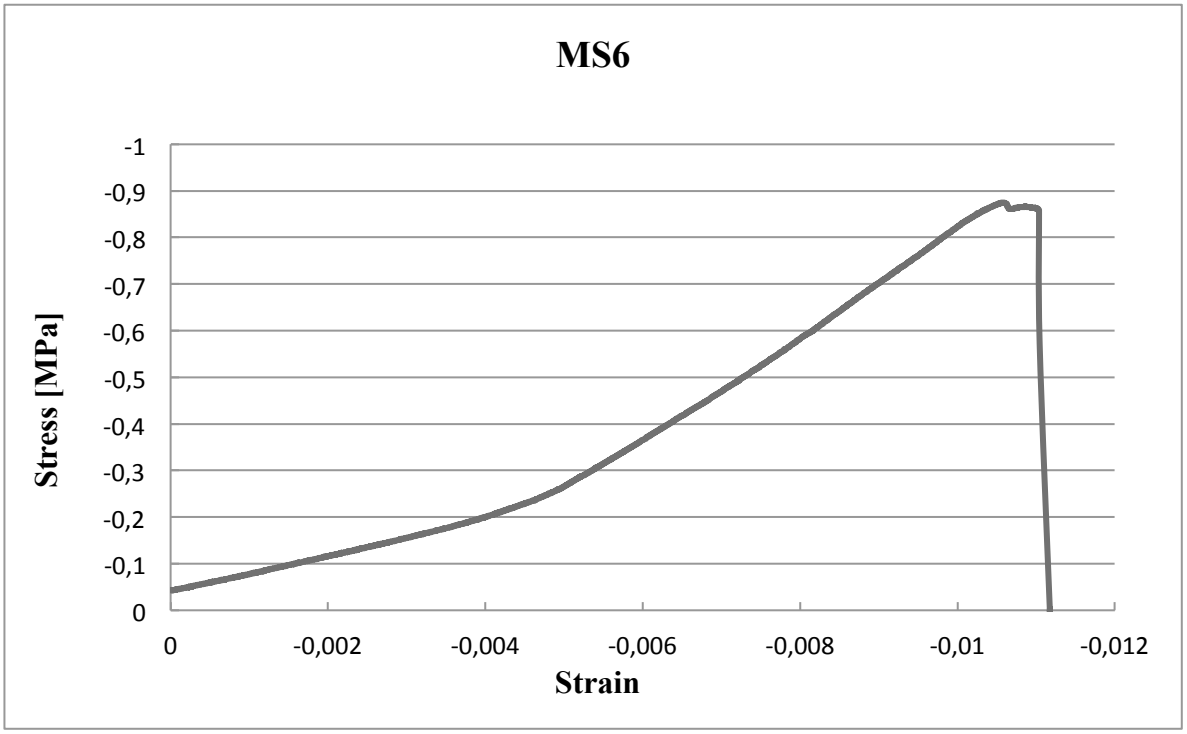

Figure C-6: Stress-Strain curve for Mancos shale sample 6 (θ = 15°)

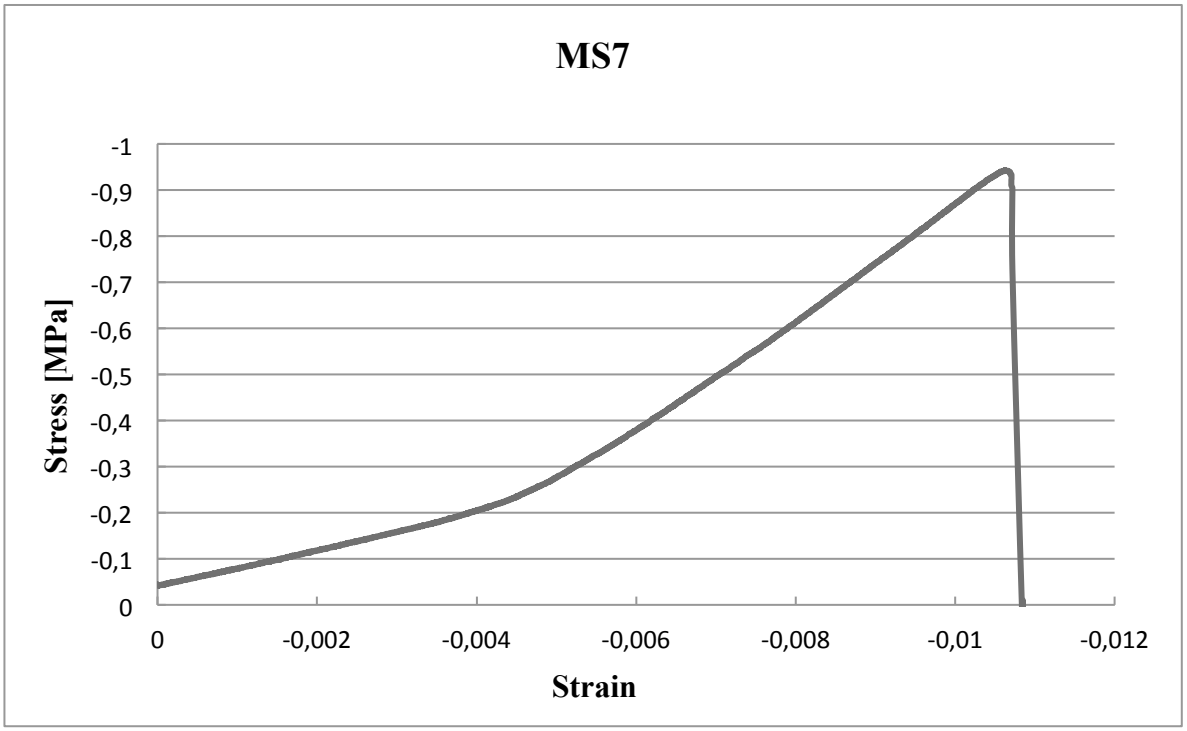

Figure C-7: Stress-Strain curve for Mancos shale sample 7 (θ = 15°)

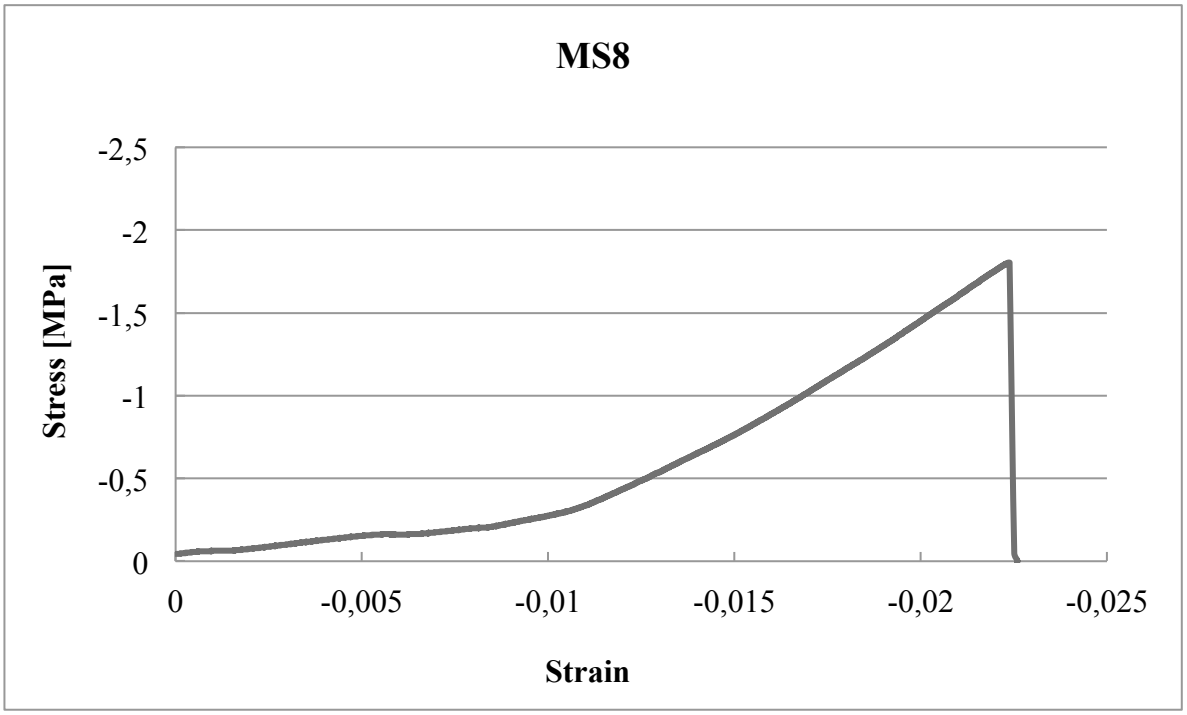

Figure C-8: Stress-Strain curve for Mancos shale sample 8 (θ = 45°)

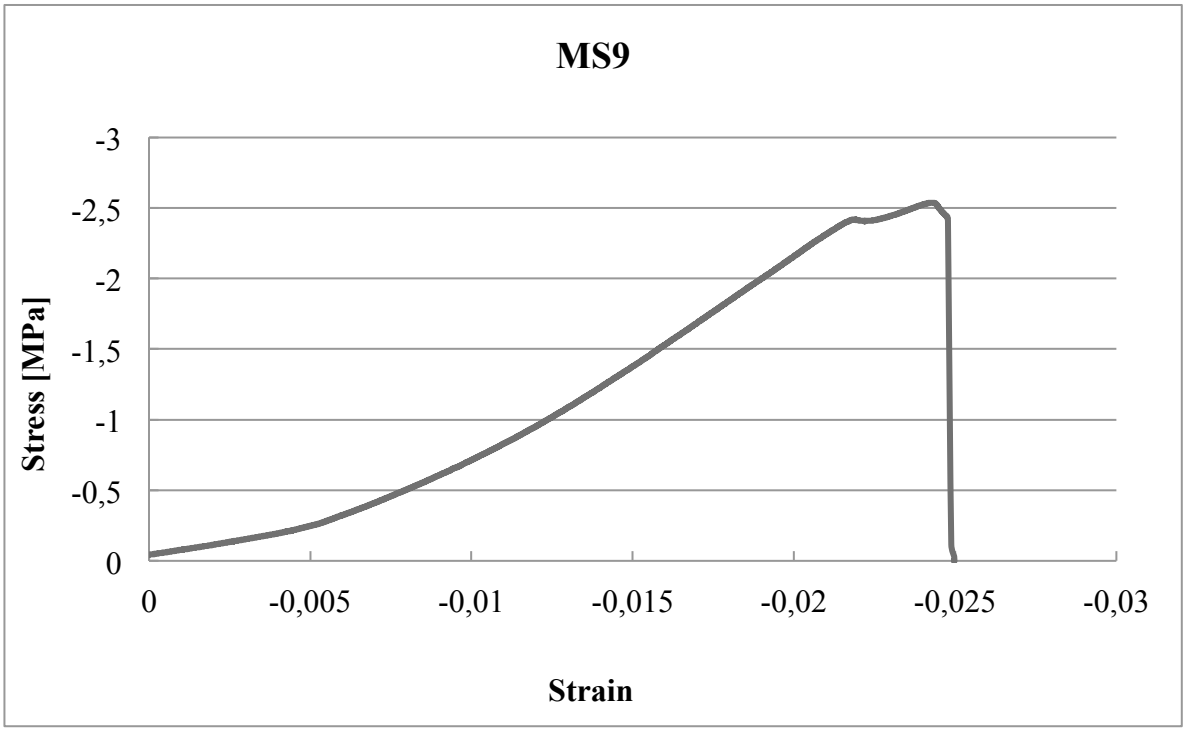

Figure C-9: Stress-Strain curve for Mancos shale sample 9 (θ = 45°)

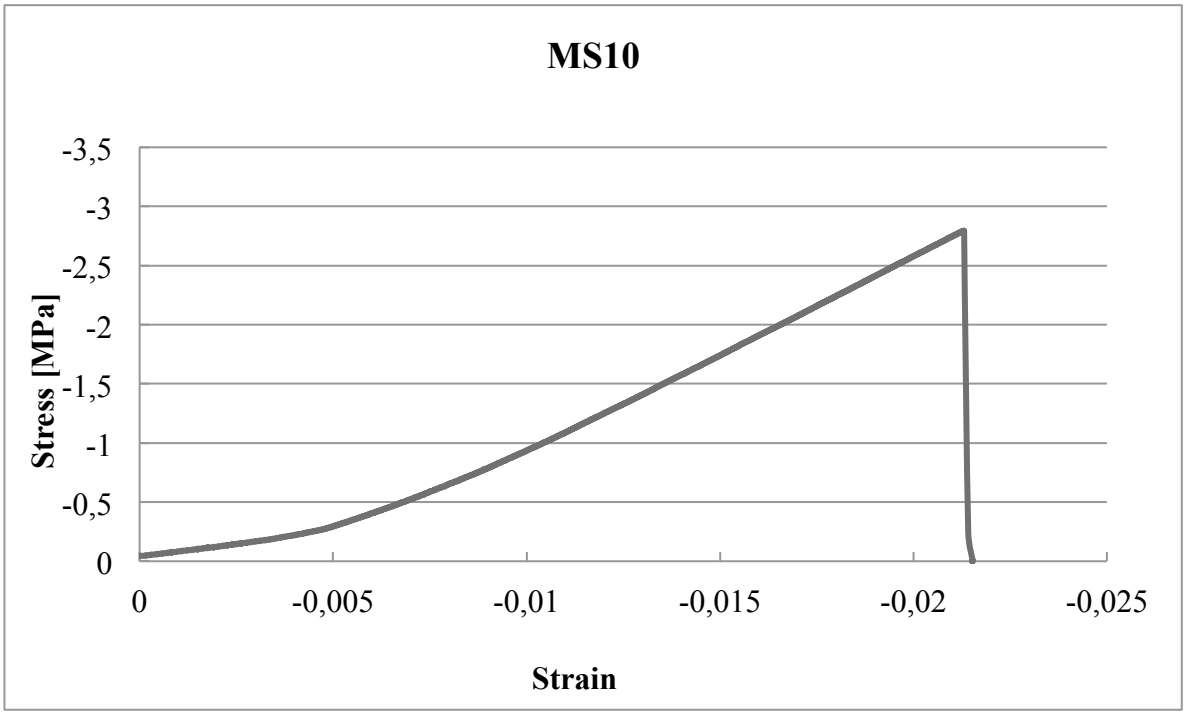

Figure C-10: Stress-Strain curve for Mancos shale sample 10 (θ = 45°)

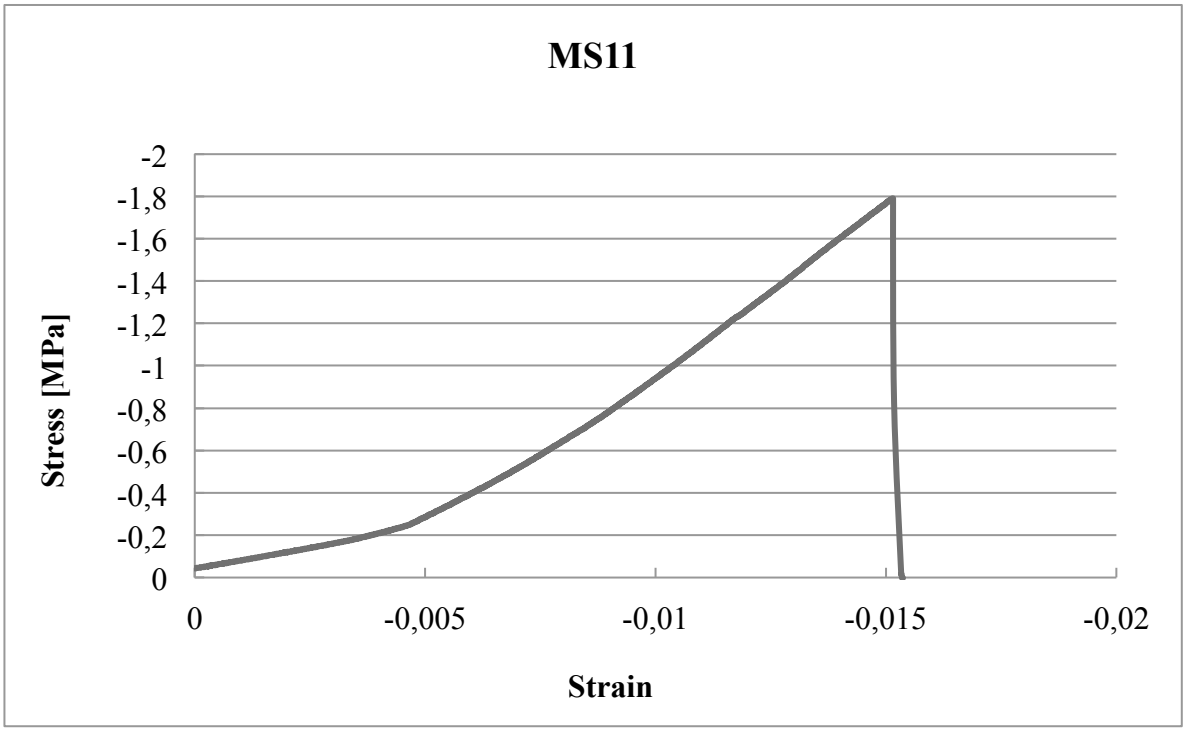

Figure C-11: Stress-Strain curve for Mancos shale sample 11 (θ = 90°)

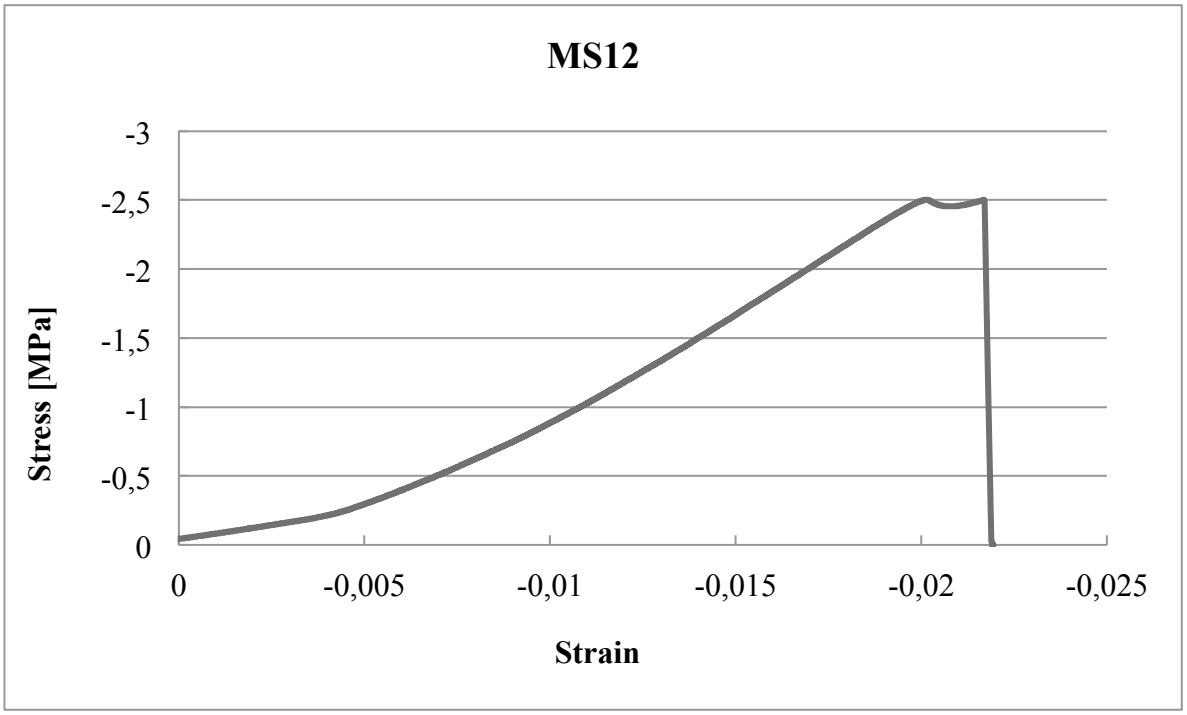

Figure C-12: Stress-Strain curve for Mancos shale sample 12 (θ = 90°)

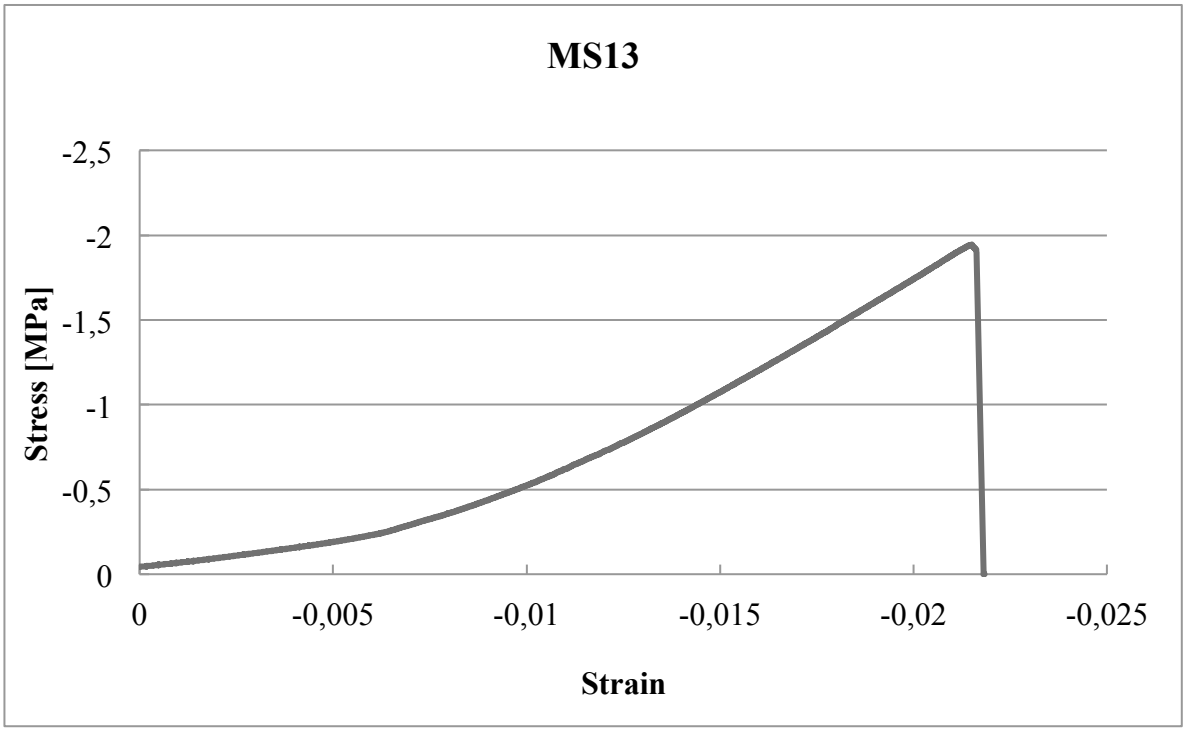

Figure C-13: Stress-Strain curve for Mancos shale sample 13 (θ = 90°)

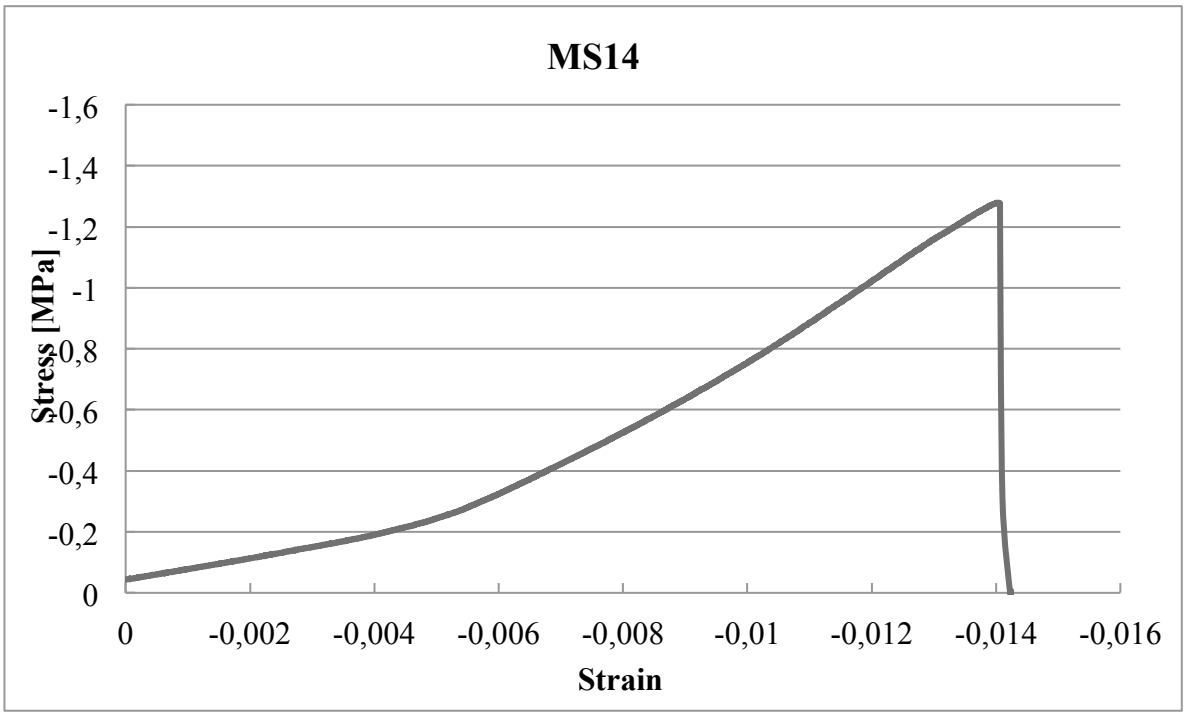

Figure C-14: Stress-Strain curve for Mancos shale sample 14 (θ = 75°)

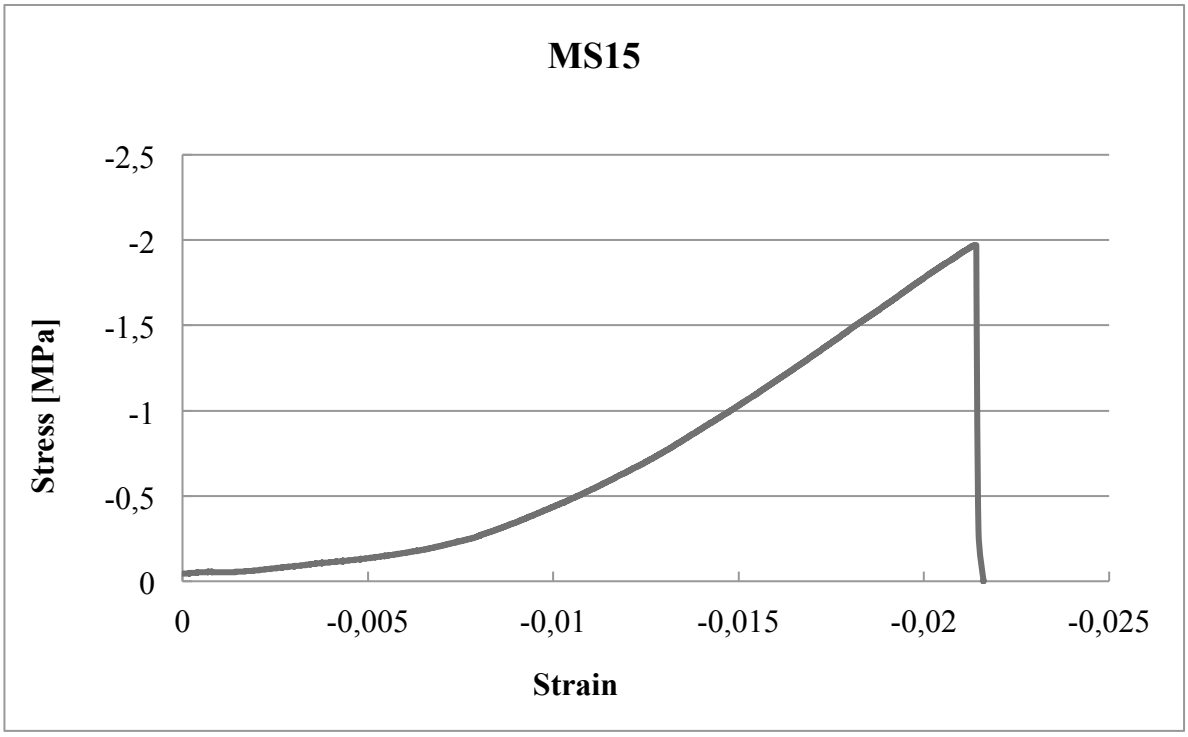

Figure C-15: Stress-Strain curve for Mancos shale sample 15 (θ = 75°)

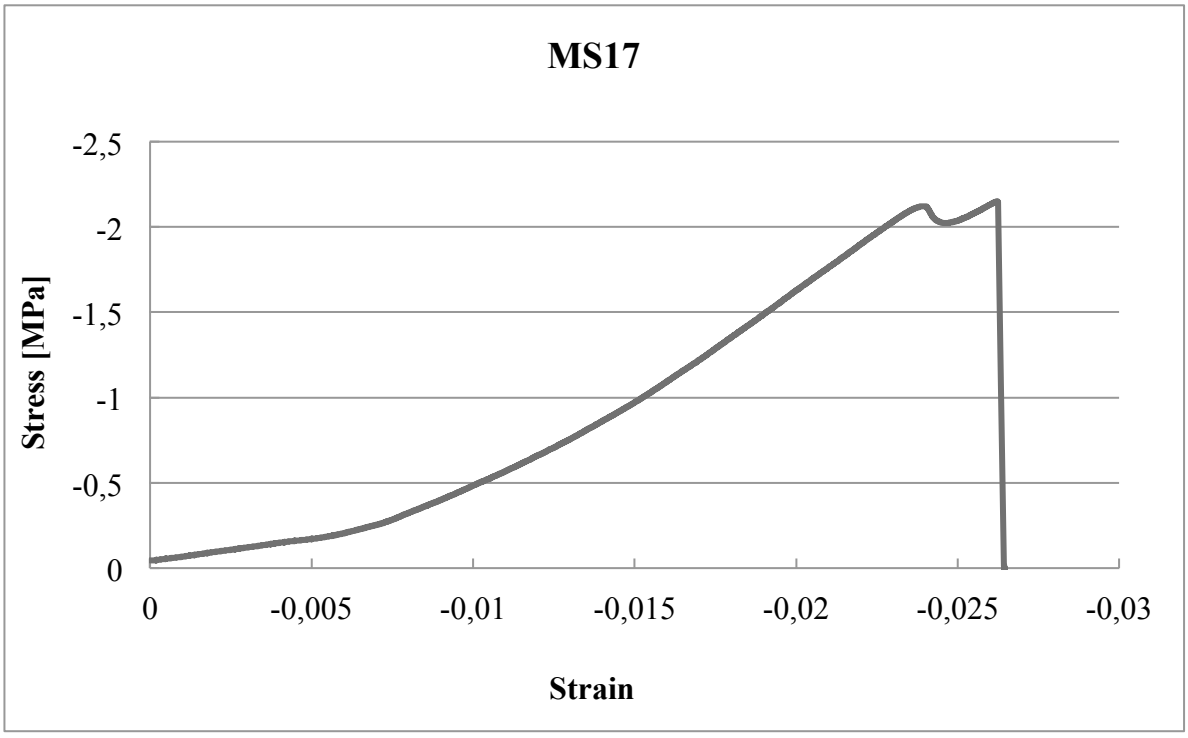

Figure C-16: Stress-Strain curve for Mancos shale sample 17 (θ = 60°)

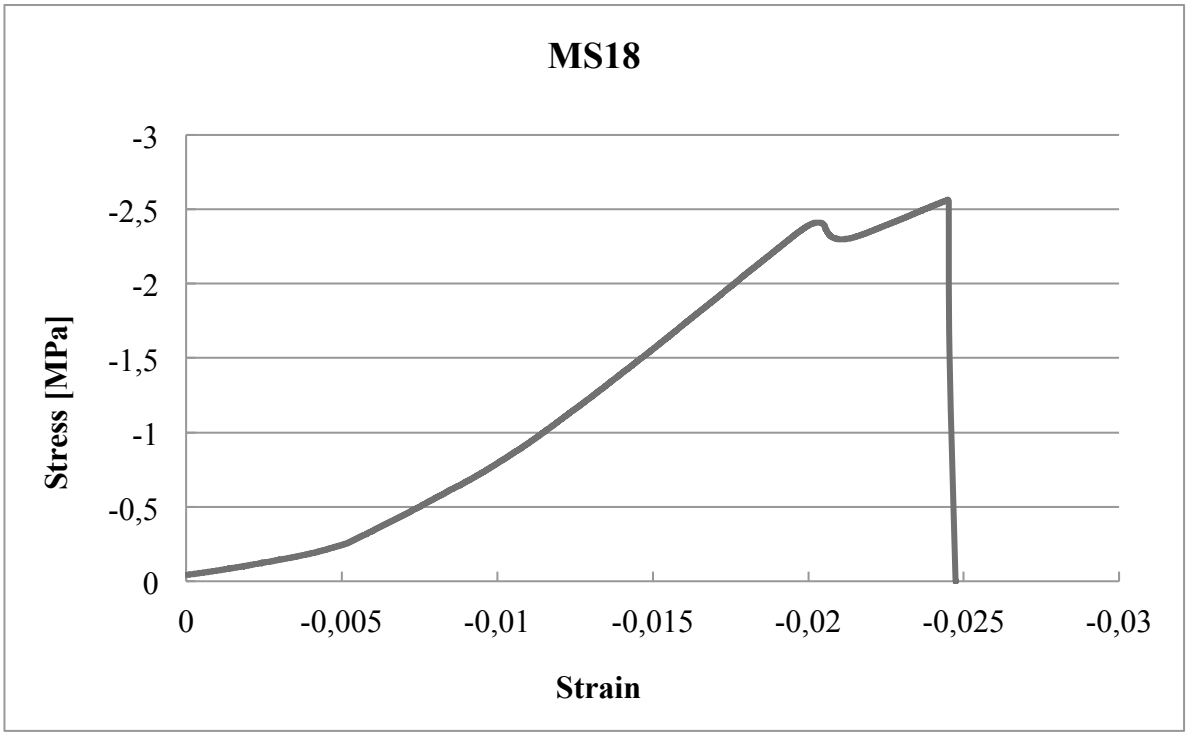

Figure C-17: Stress-Strain curve for Mancos shale sample 18 (θ = 60°)

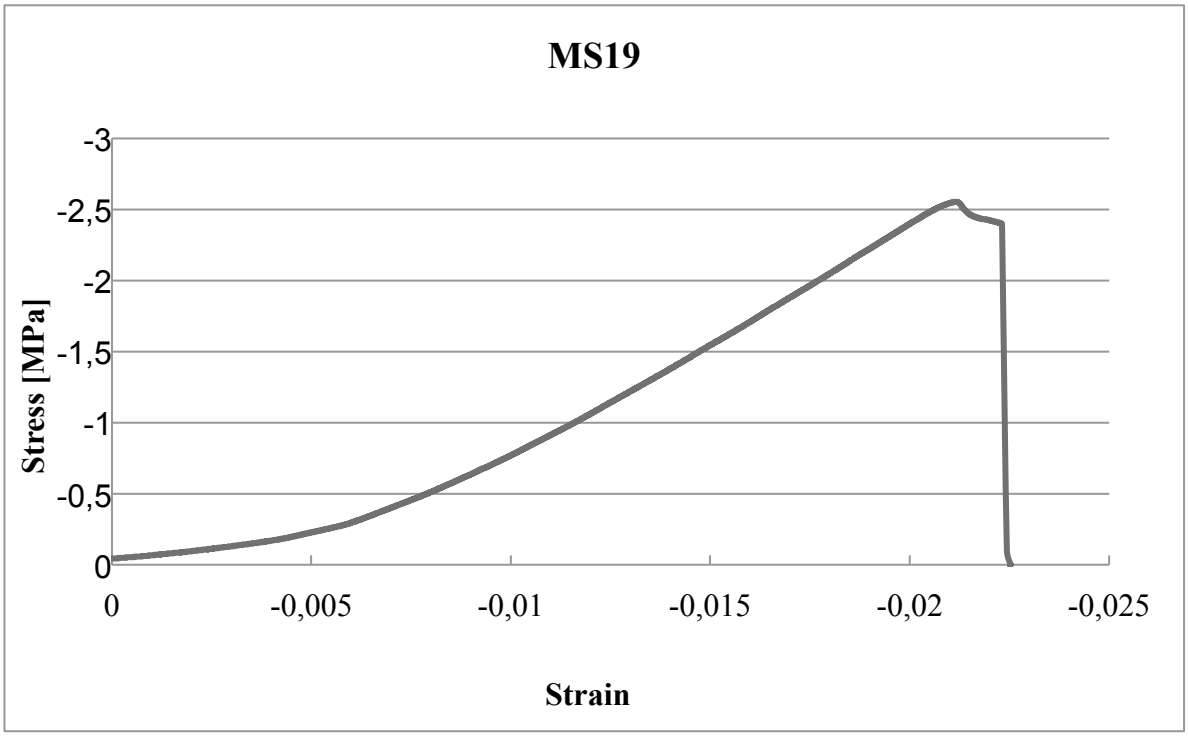

Figure C-18: Stress-Strain curve for Mancos shale sample 19 (θ = 60°)

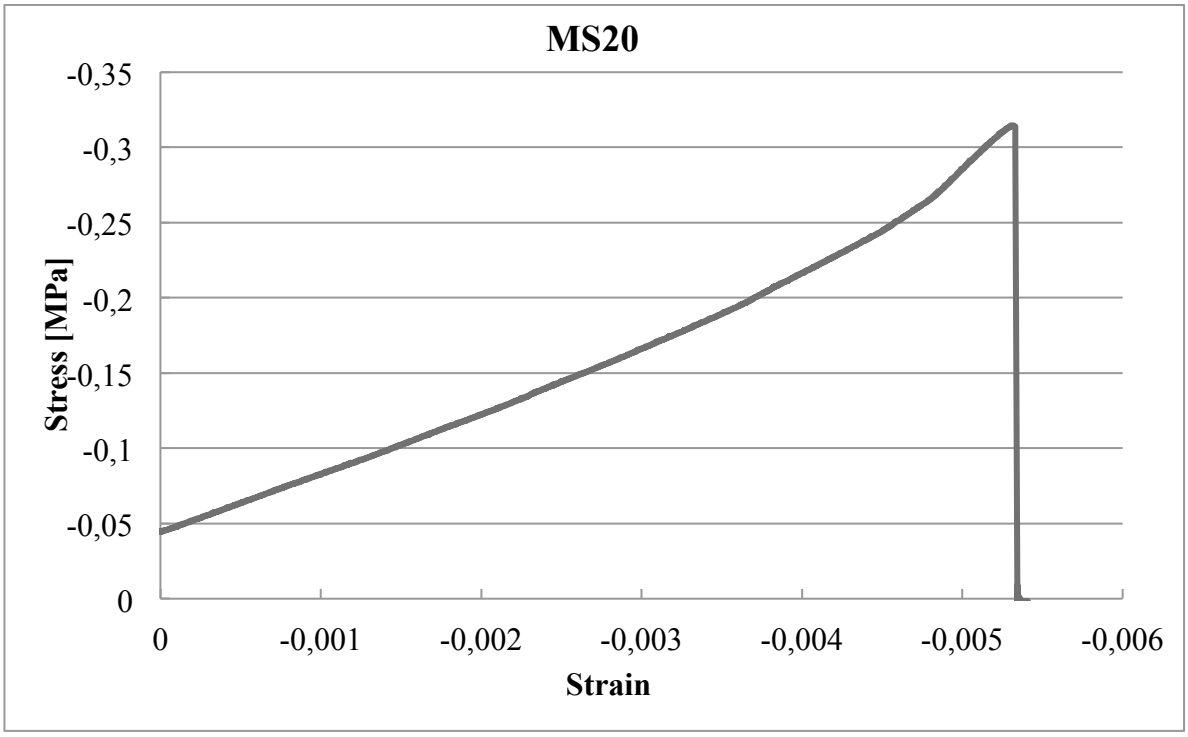

Figure C-19: Stress-Strain curve for Mancos shale sample 20 (θ = 0°)

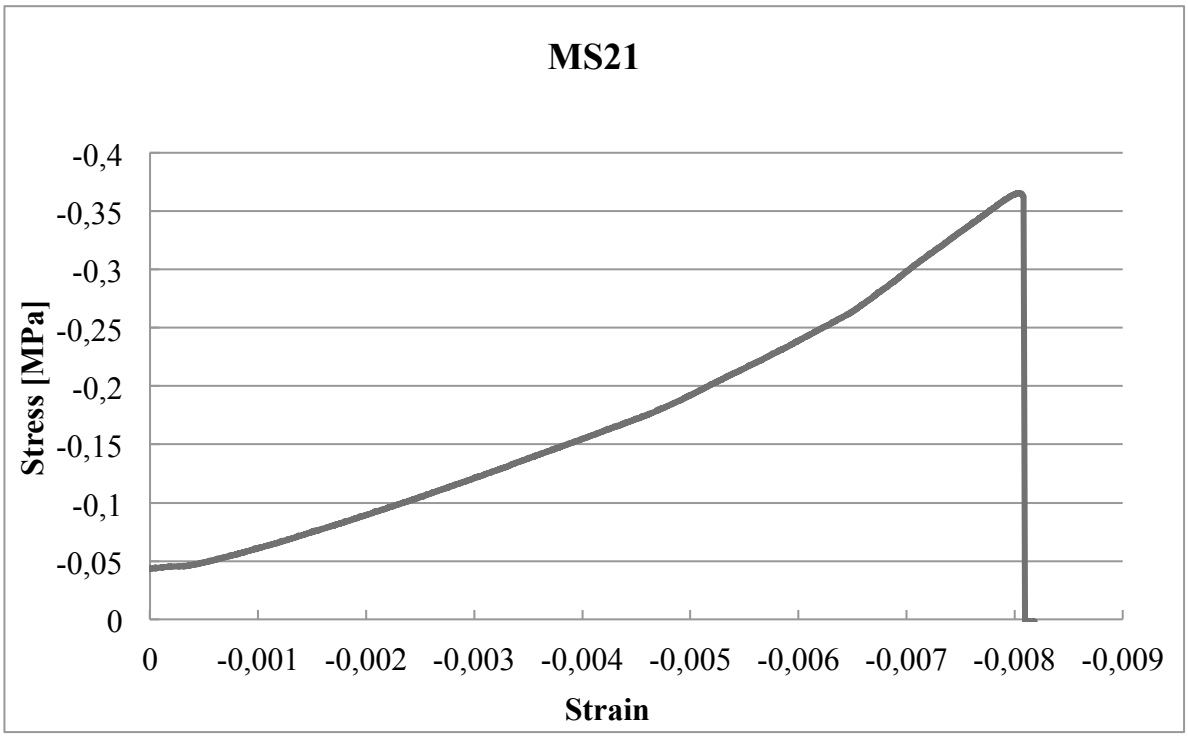

Figure C-20: Stress-Strain curve for Mancos shale sample 21 (θ = 0°)

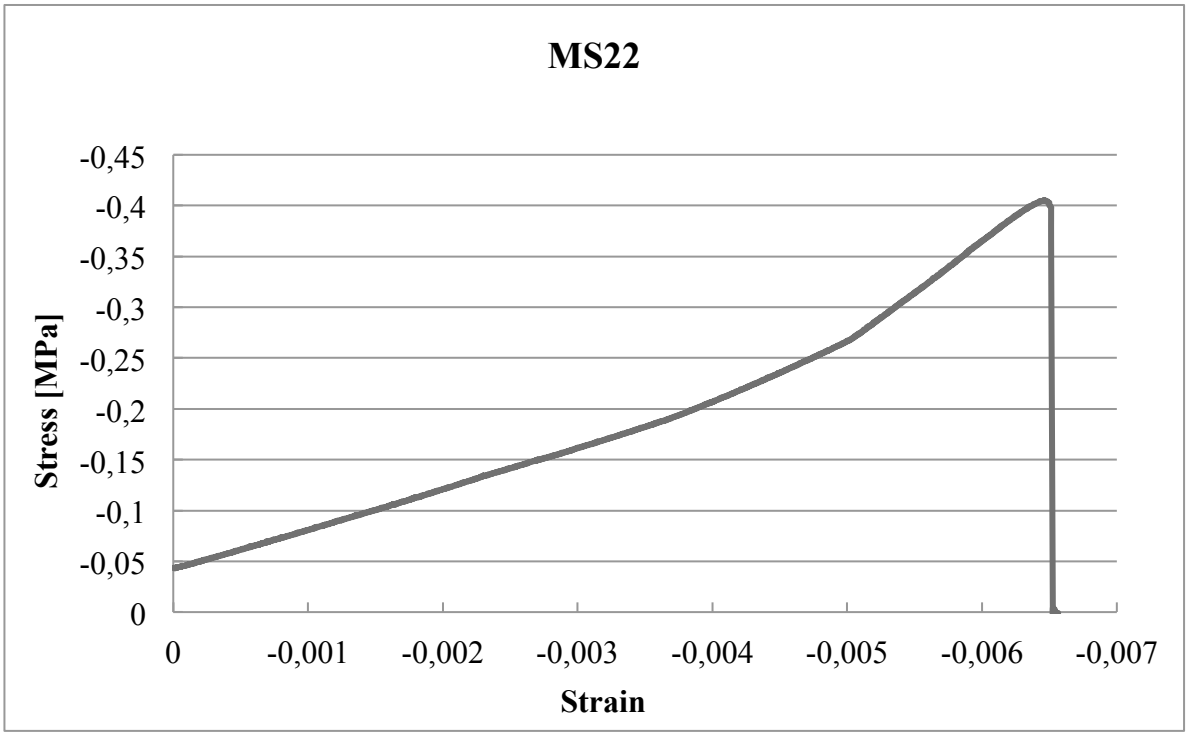

Figure C-21: Stress-Strain curve for Mancos shale sample 22 (θ = 0°)

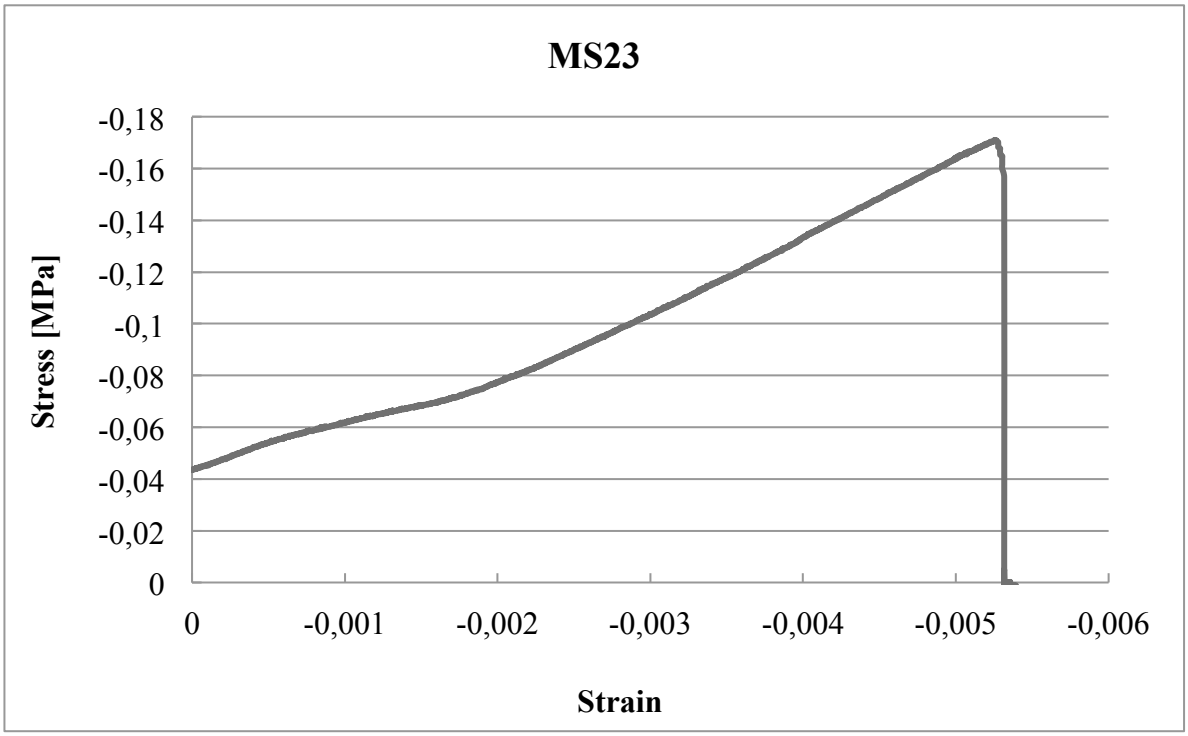

Figure C-22: Stress-Strain curve for Mancos shale sample 23 (θ = 0°)

C.2 Castlegate Sandstone

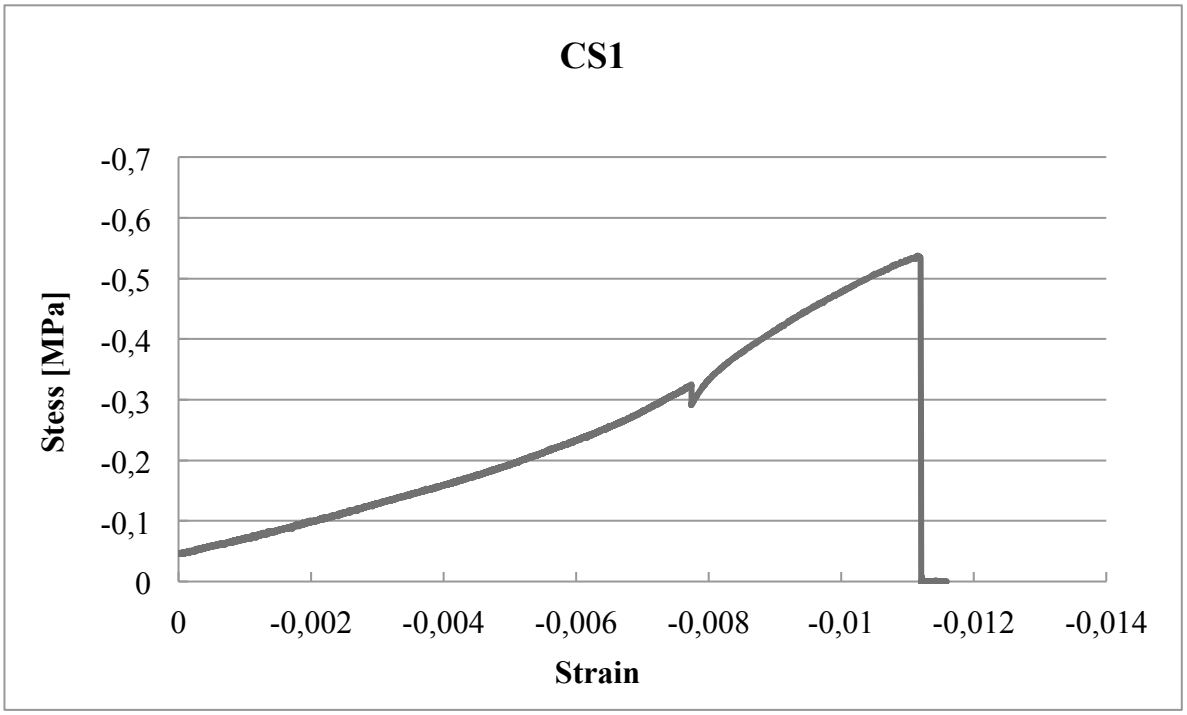

Figure C-23: Stress-Strain curve for Castlegate sandstone sample 1

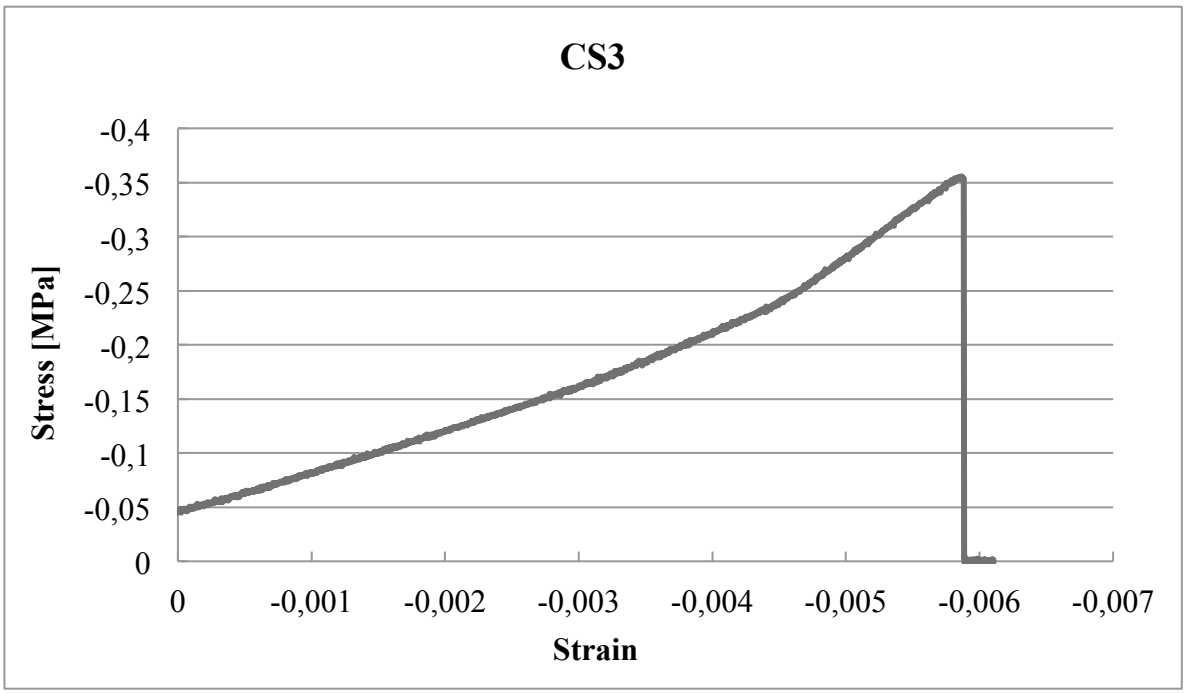

Figure C-24: Stress-Strain curve for Castlegate sandstone sample 3

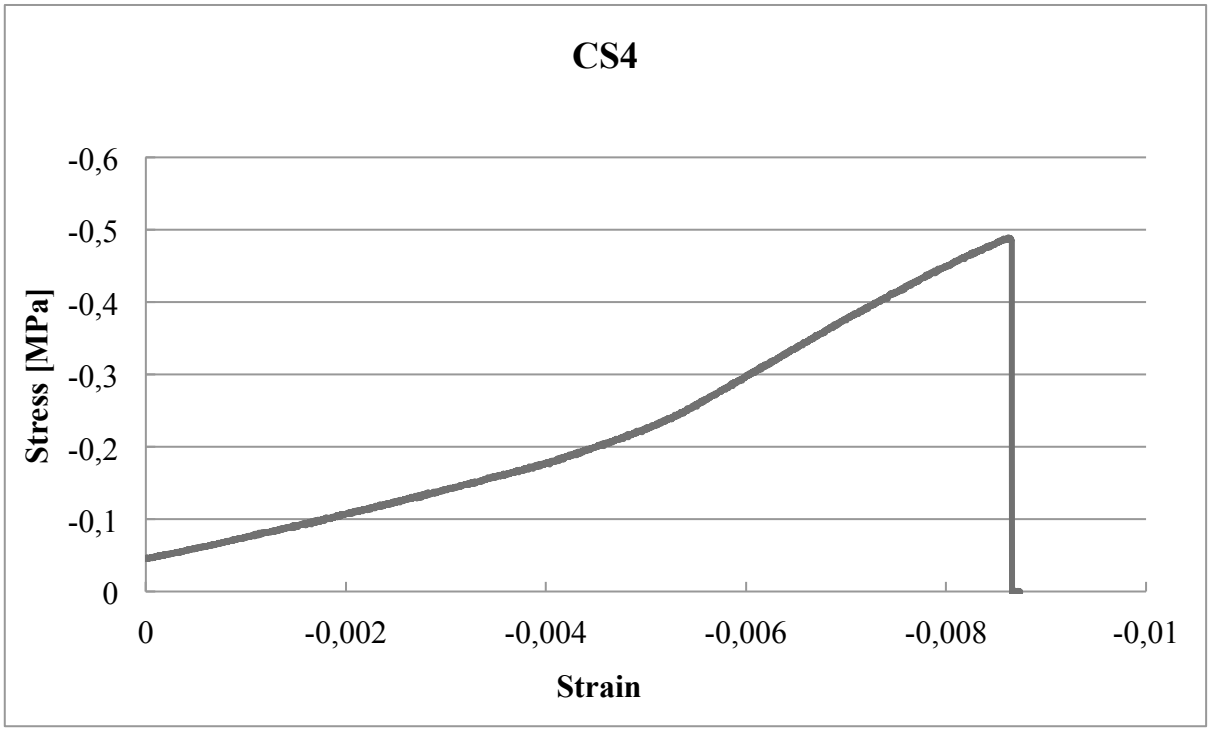

Figure C-25: Stress-Strain curve for Castlegate sandstone sample 4

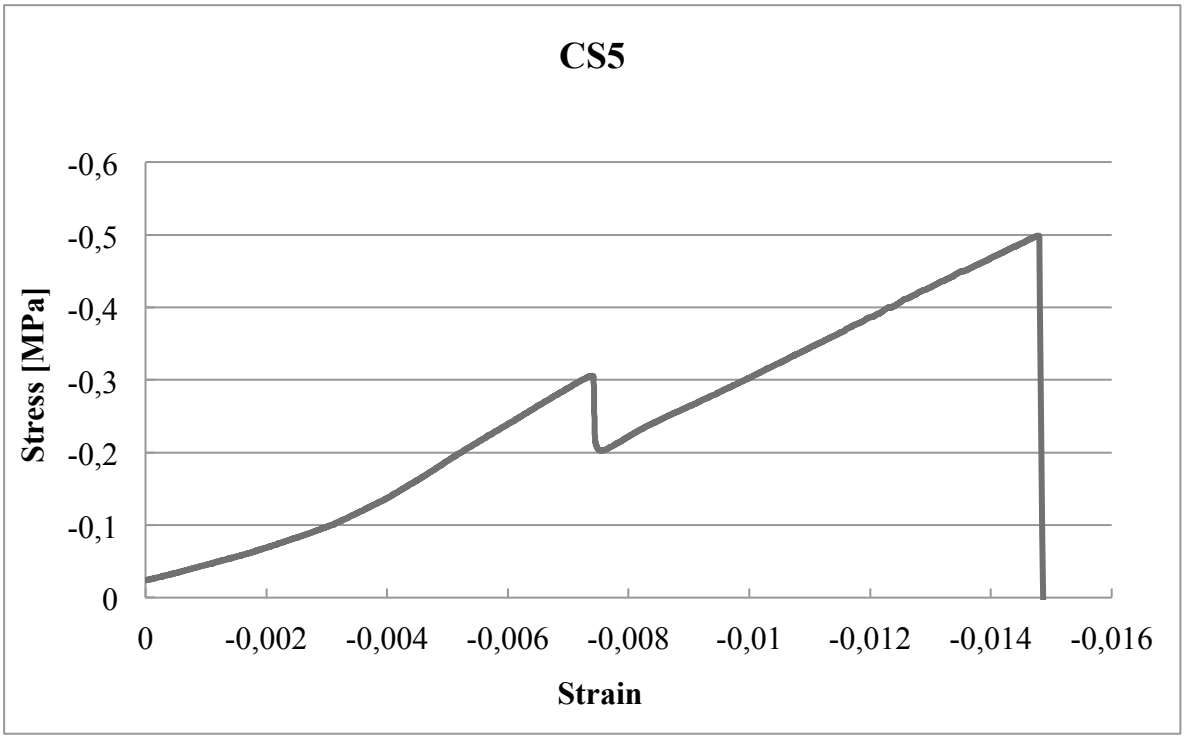

Figure C-26: Stress-Strain curve for Castlegate sandstone sample 5

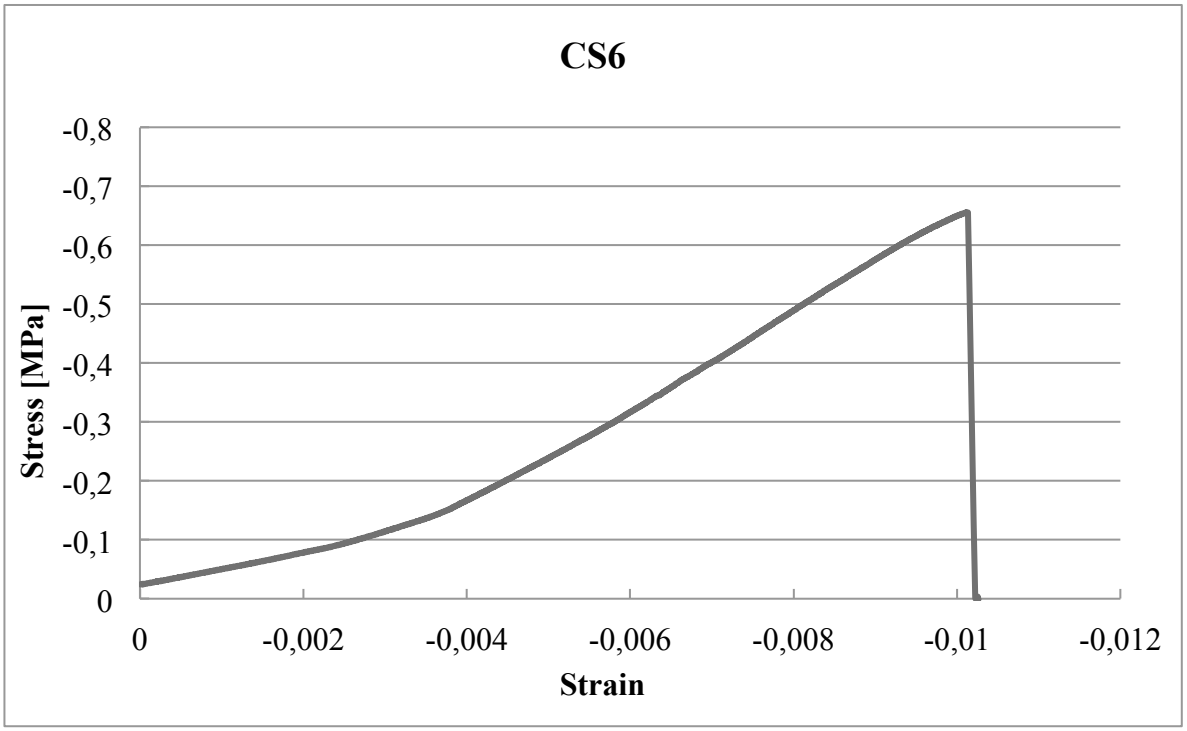

Figure C-27: Stress-Strain curve for Castlegate sandstone sample 6

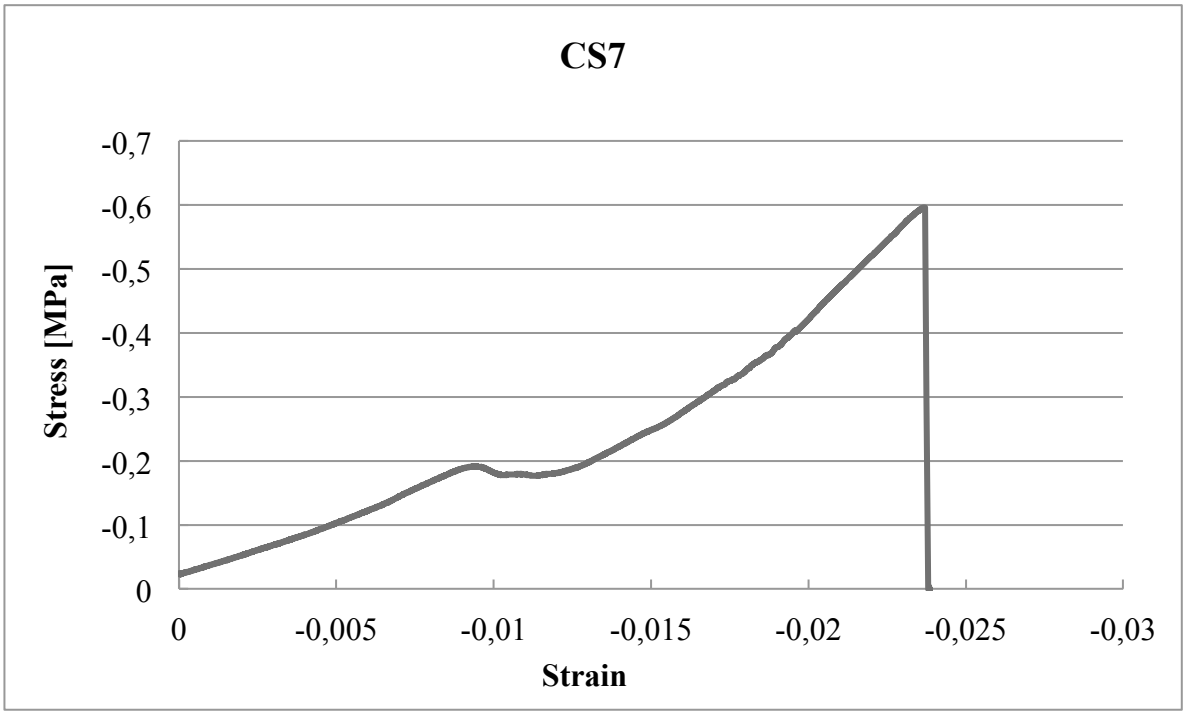

Figure C-28: Stress-Strain curve for Castlegate sandstone sample 7

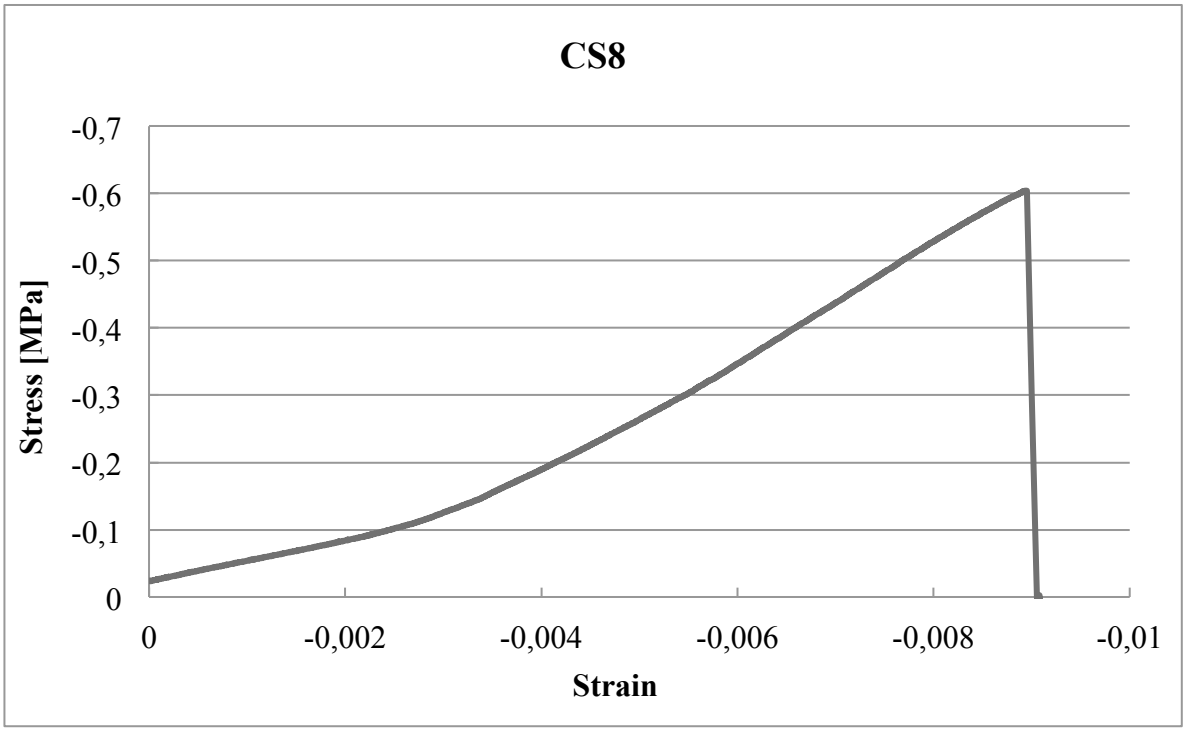

Figure C-29: Stress-Strain curve for Castlegate sandstone sample 8

C.3 Mons Chalk

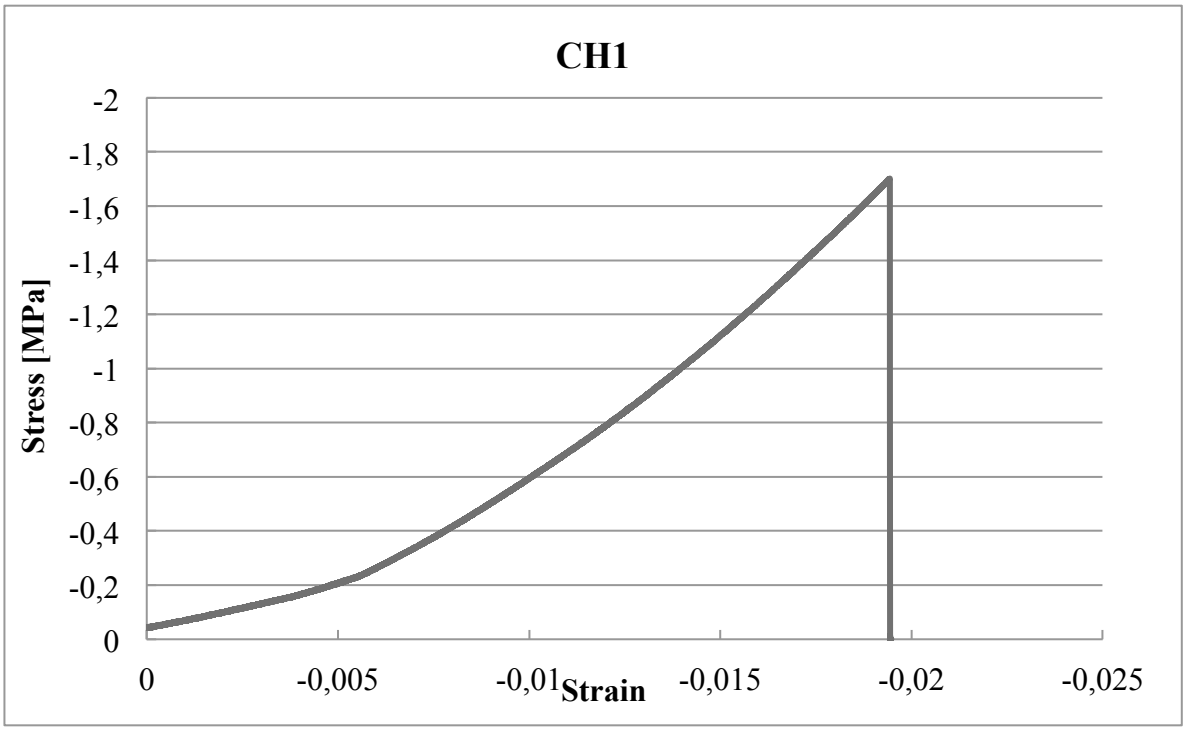

Figure C-30: Stress-Strain curve for Mons chalk sample 1

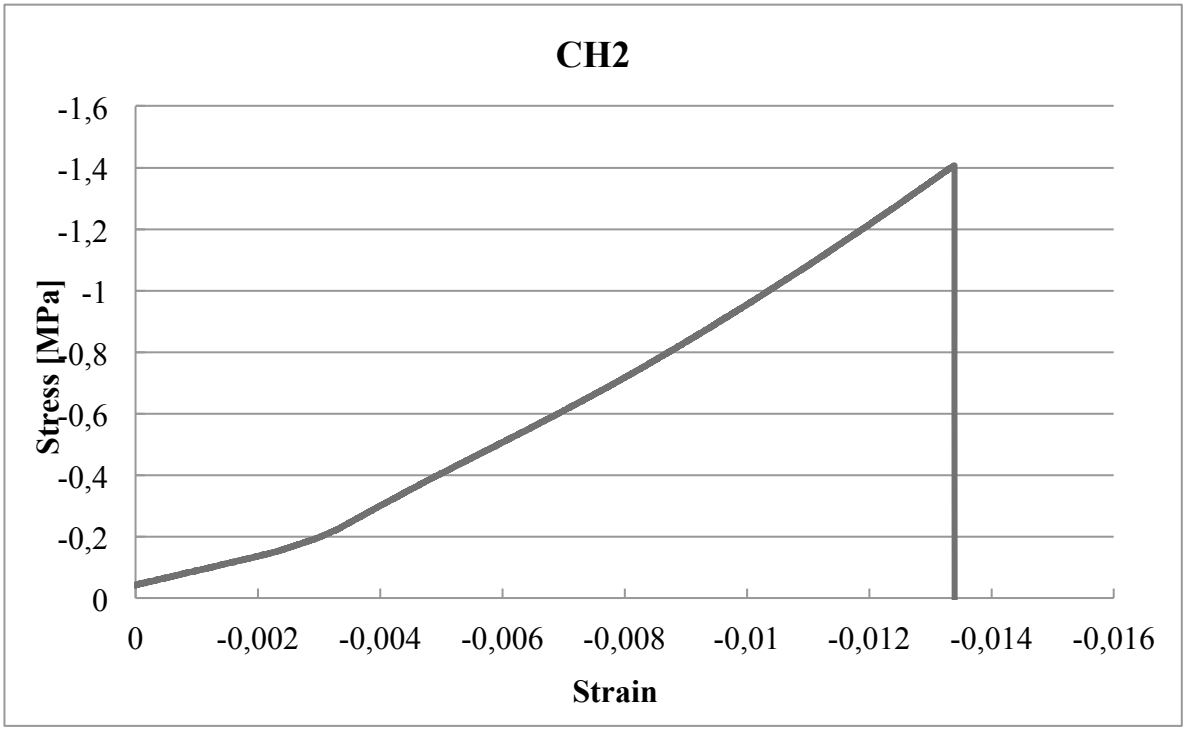

Figure C-31: Stress-Strain curve for Mons chalk sample 2

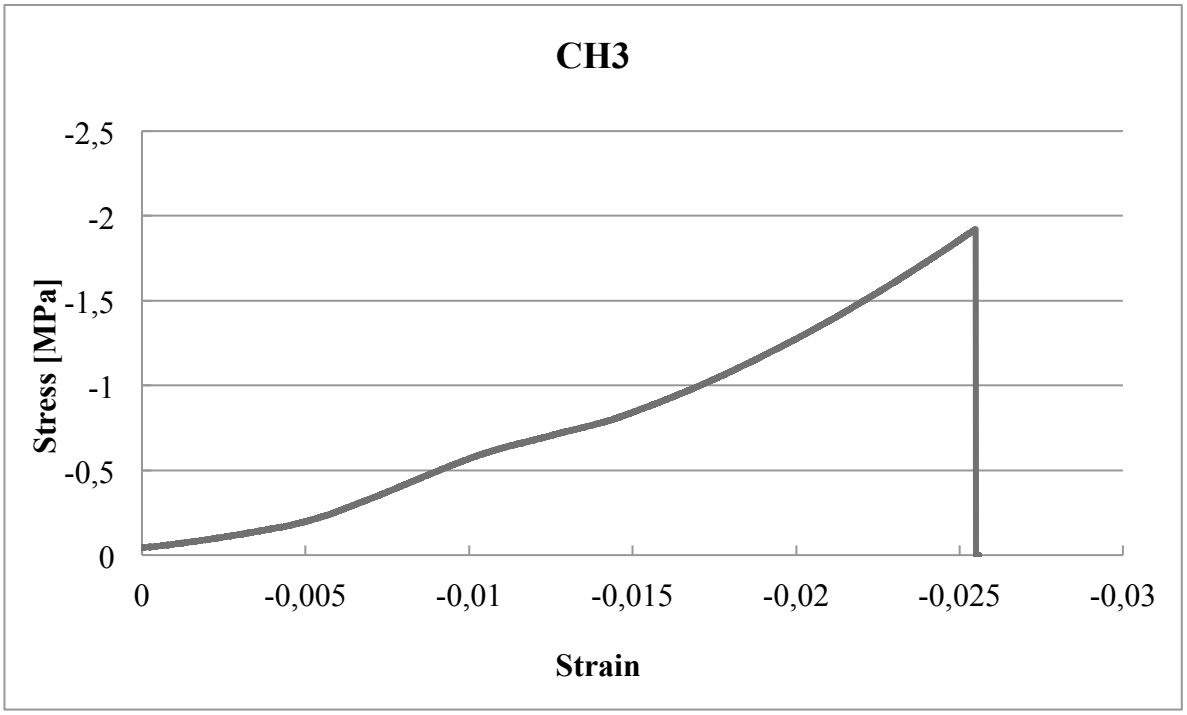

Figure C-32: Stress-Strain curve for Mons chalk sample 3

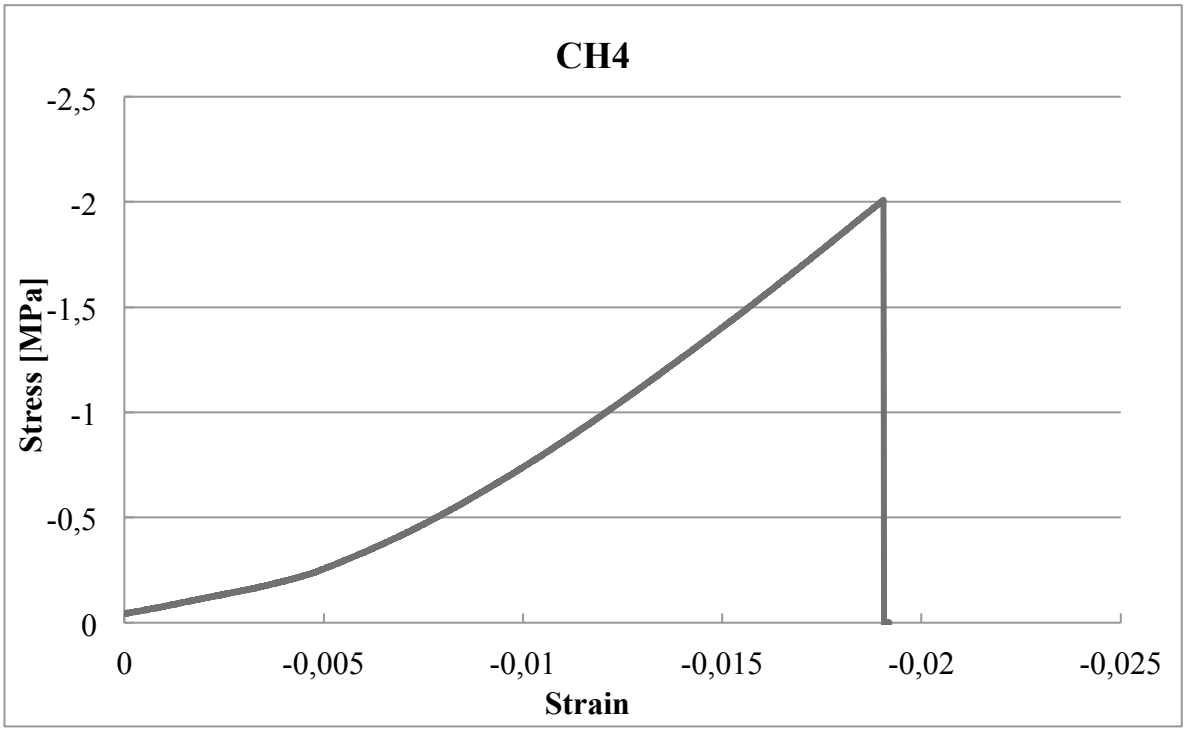

Figure C-33: Stress-Strain curve for Mons chalk sample 4

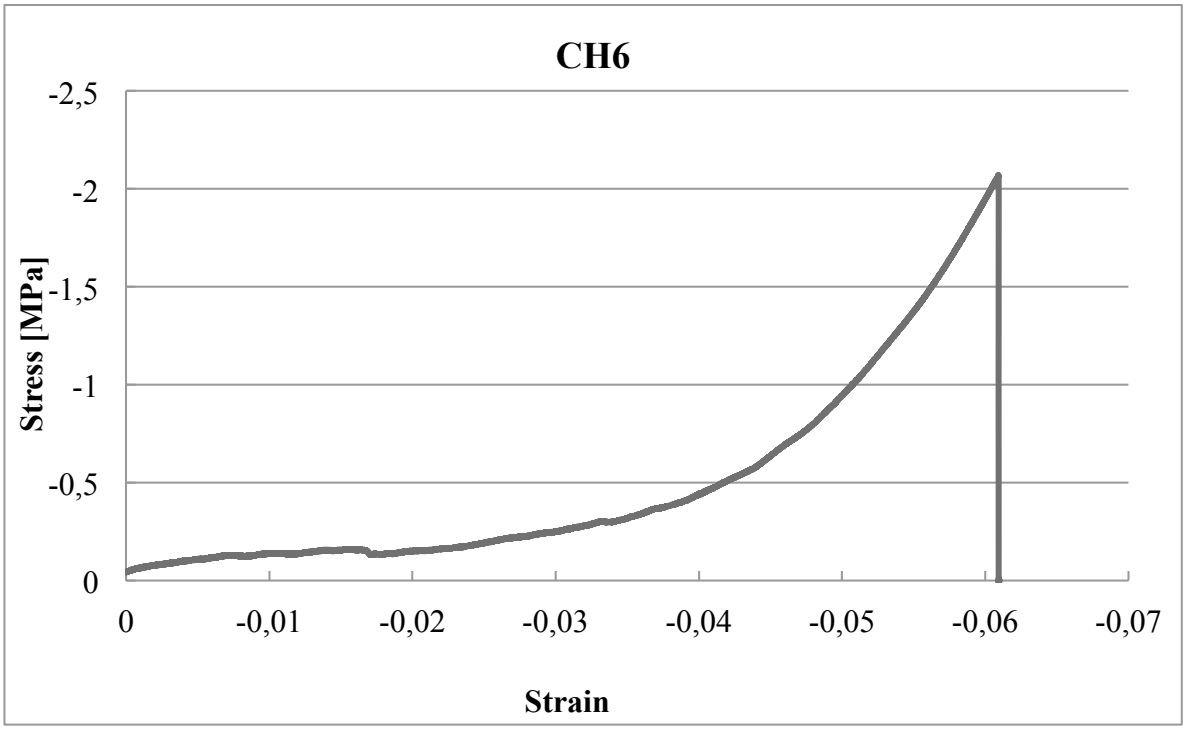

Figure C-34: Stress-Strain curve for Mons chalk sample 6

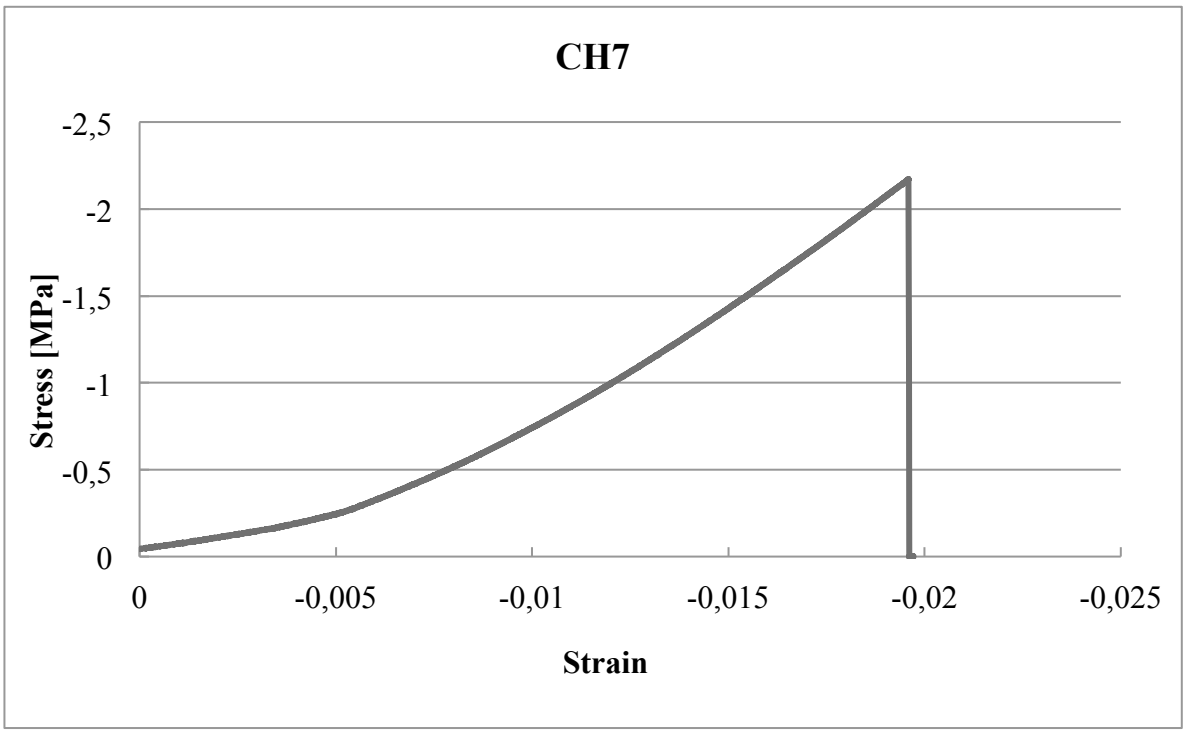

Figure C-35: Stress-Strain curve for Mons chalk sample 7

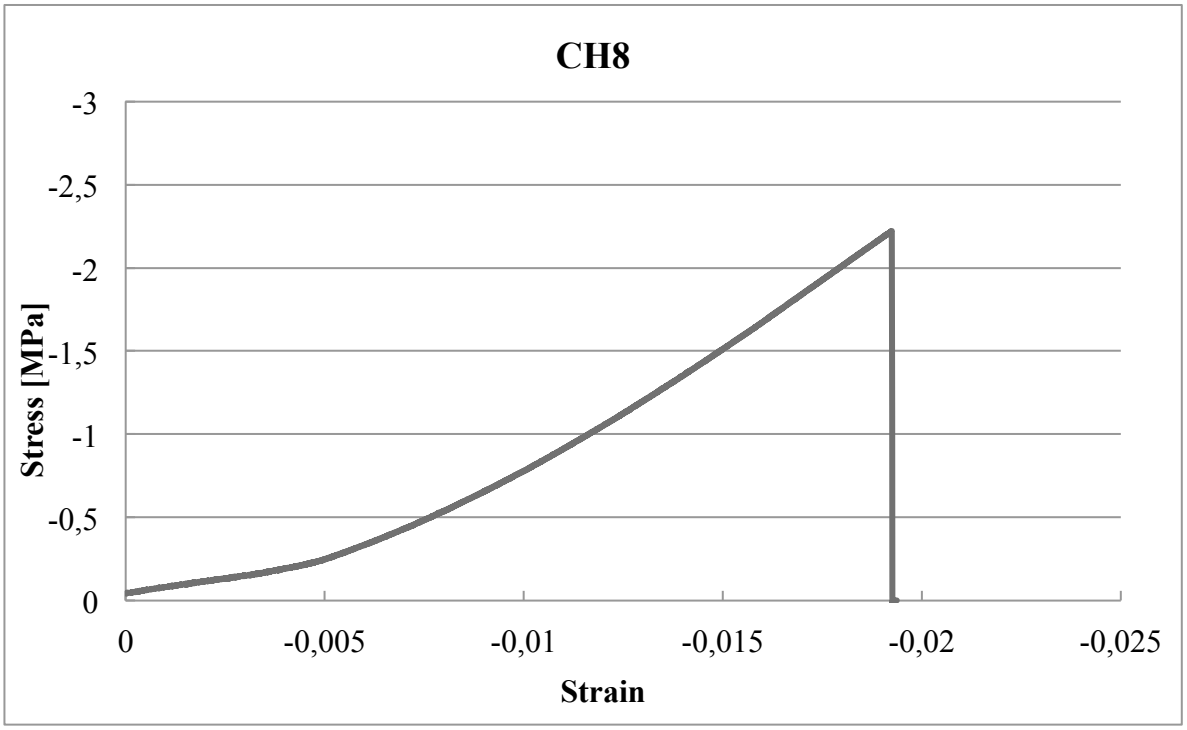

Figure C-36: Stress-Strain curve for Mons chalk sample 8

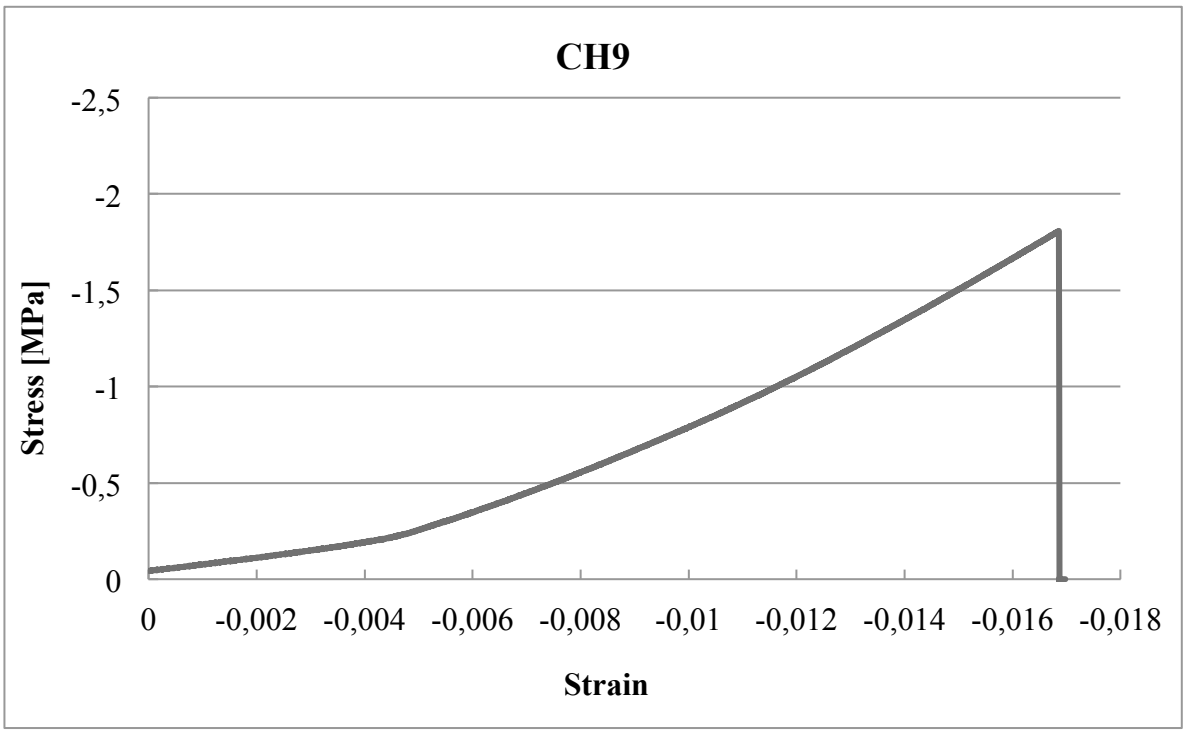

Figure C-37: Stress-Strain curve for Mons chalk sample 9

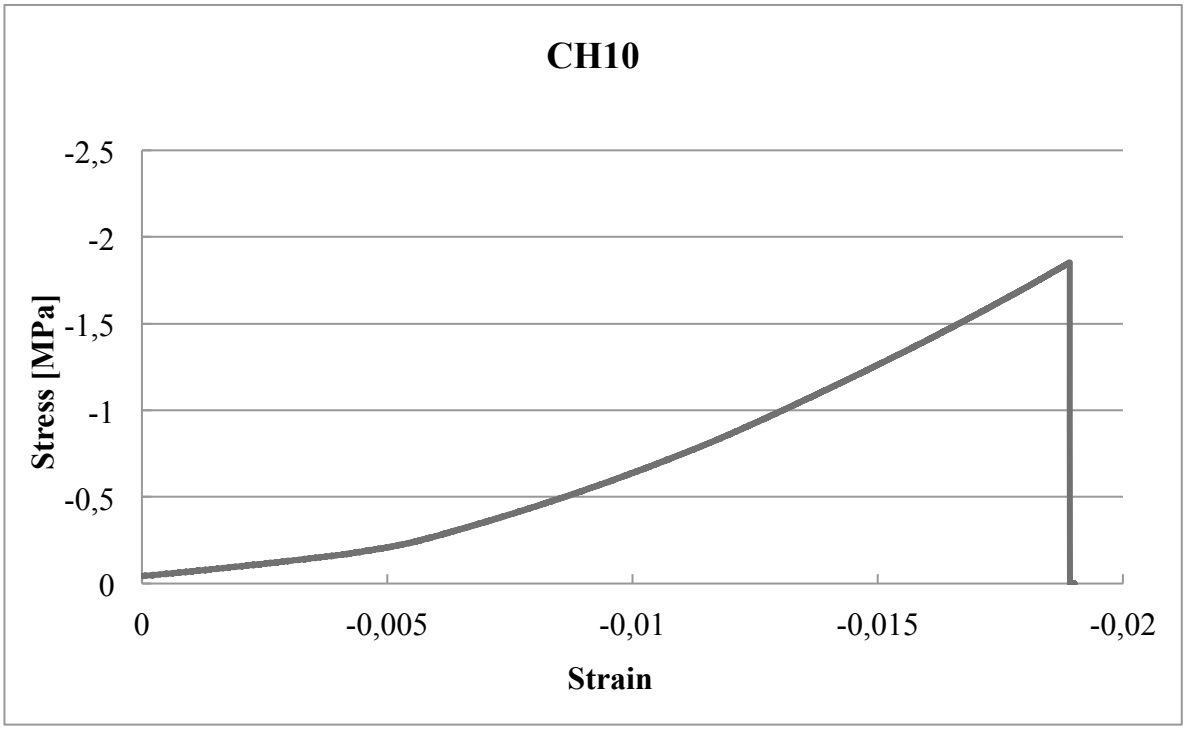

Figure C-38: Stress-Strain curve for Mons chalk sample 10

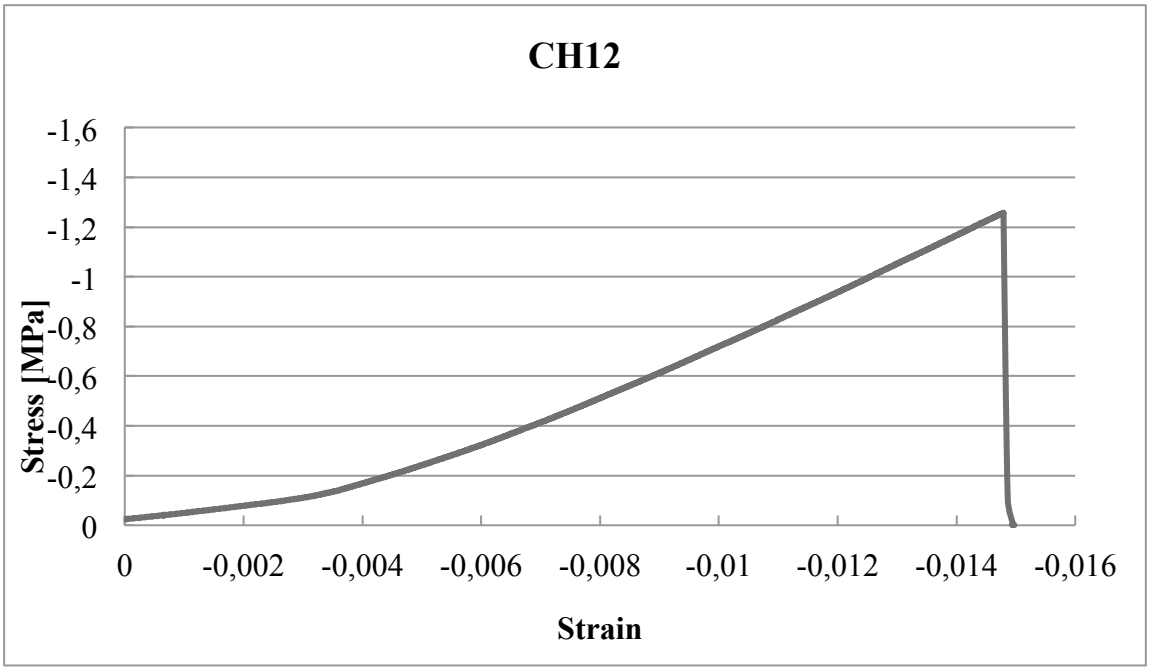

Figure C-39: Stress-Strain curve for Mons chalk sample 12

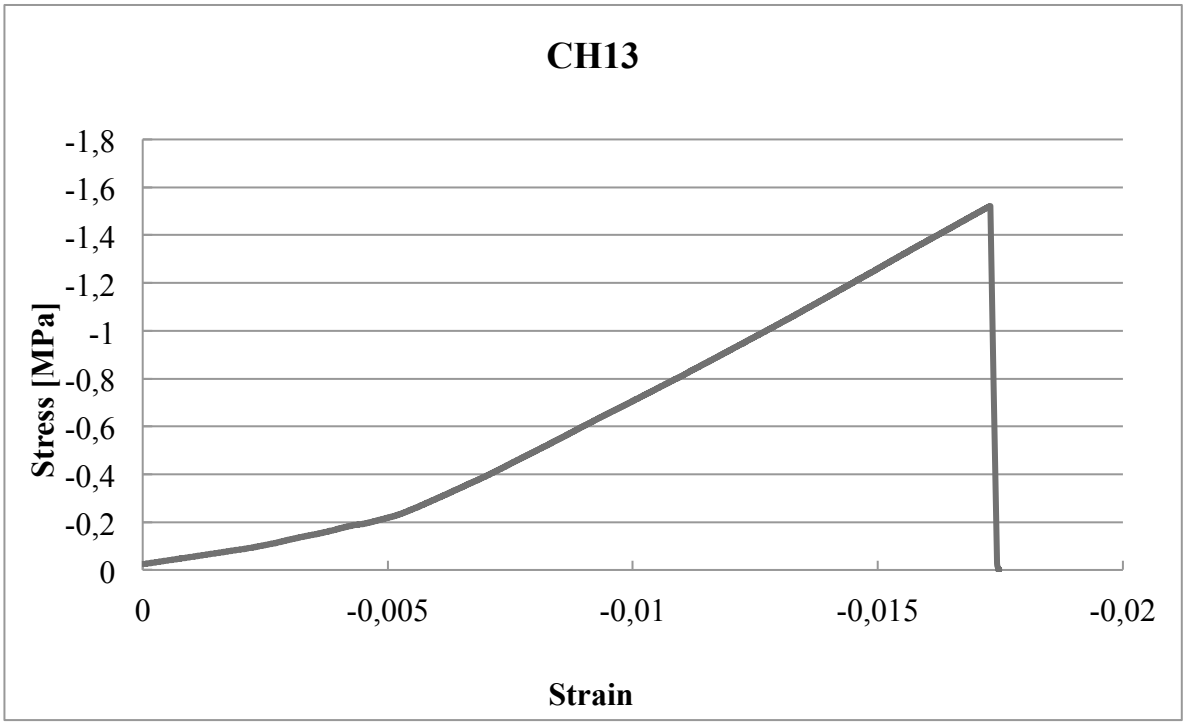

Figure C-40: Stress-Strain curve for Mons chalk sample 13

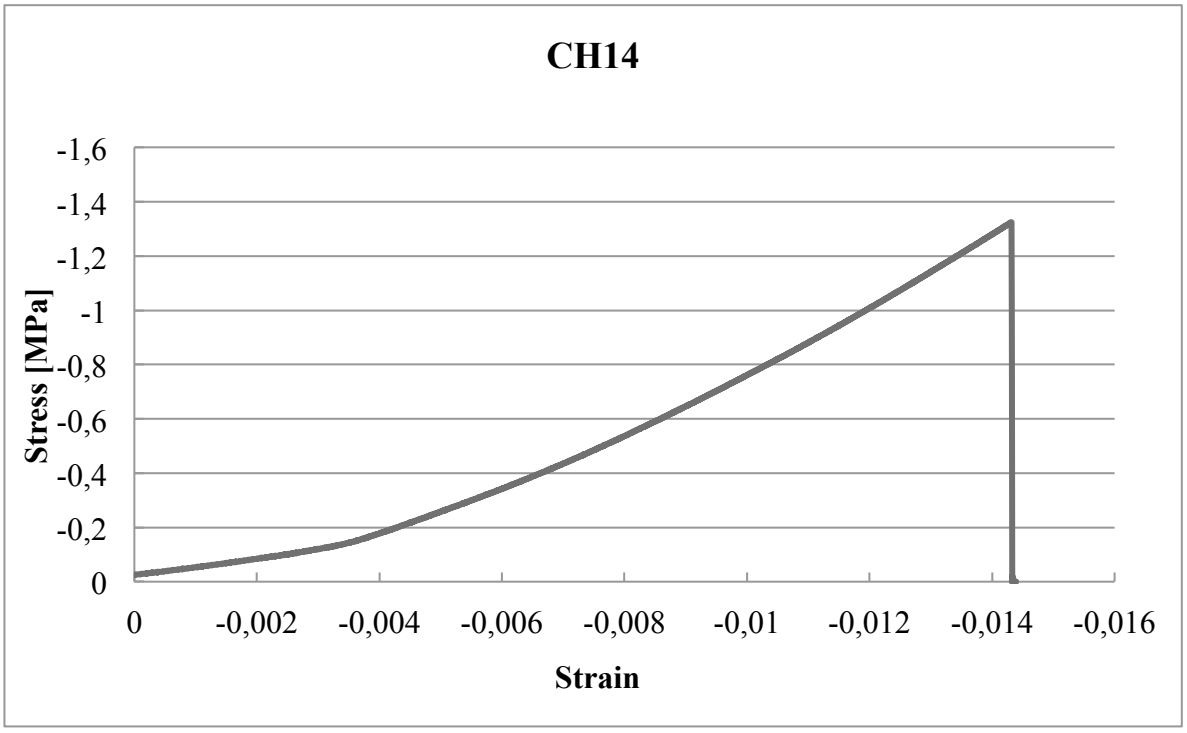

Figure C-41: Stress-Strain curve for Mons chalk sample 14

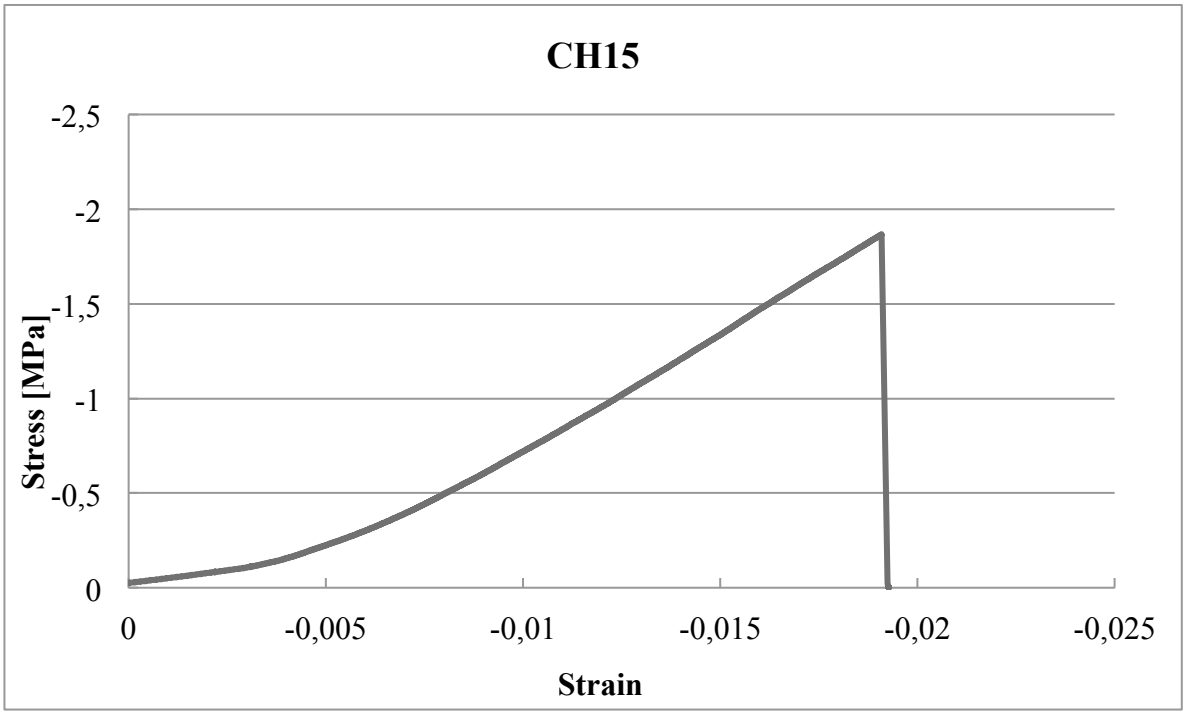

Figure C-42: Stress-Strain curve for Mons chalk sample 15

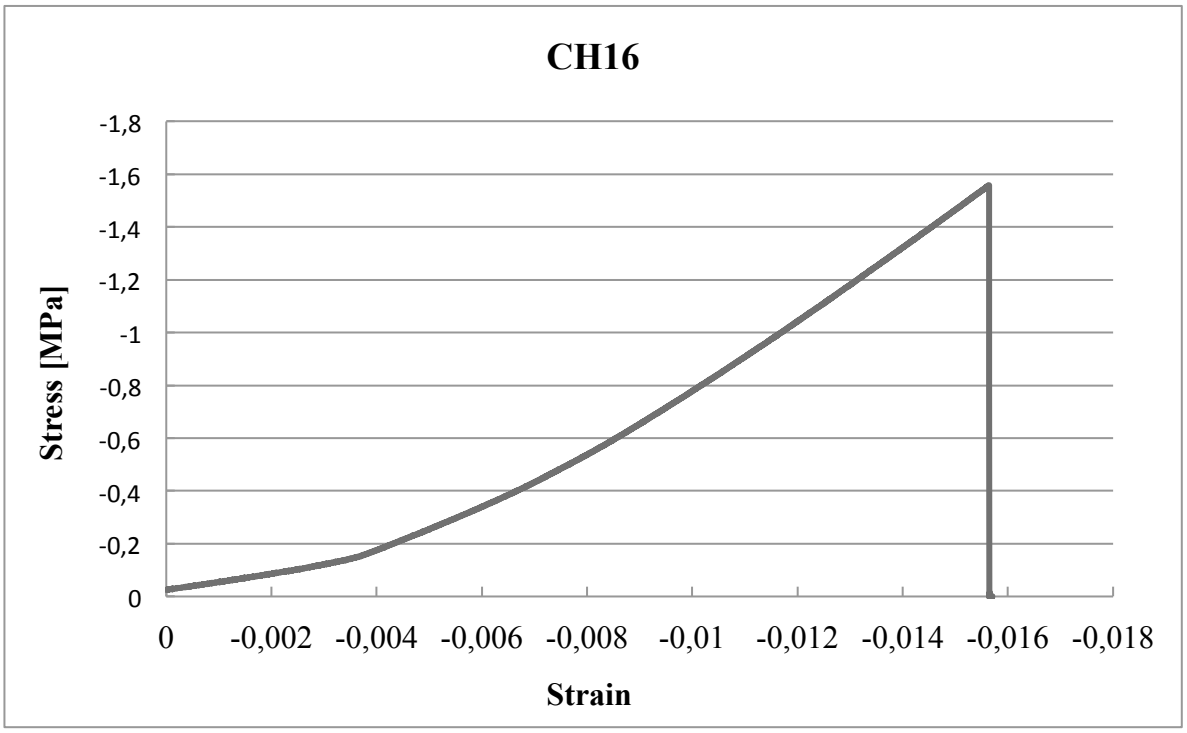

Figure C-43: Stress-Strain curve for Mons chalk sample 16

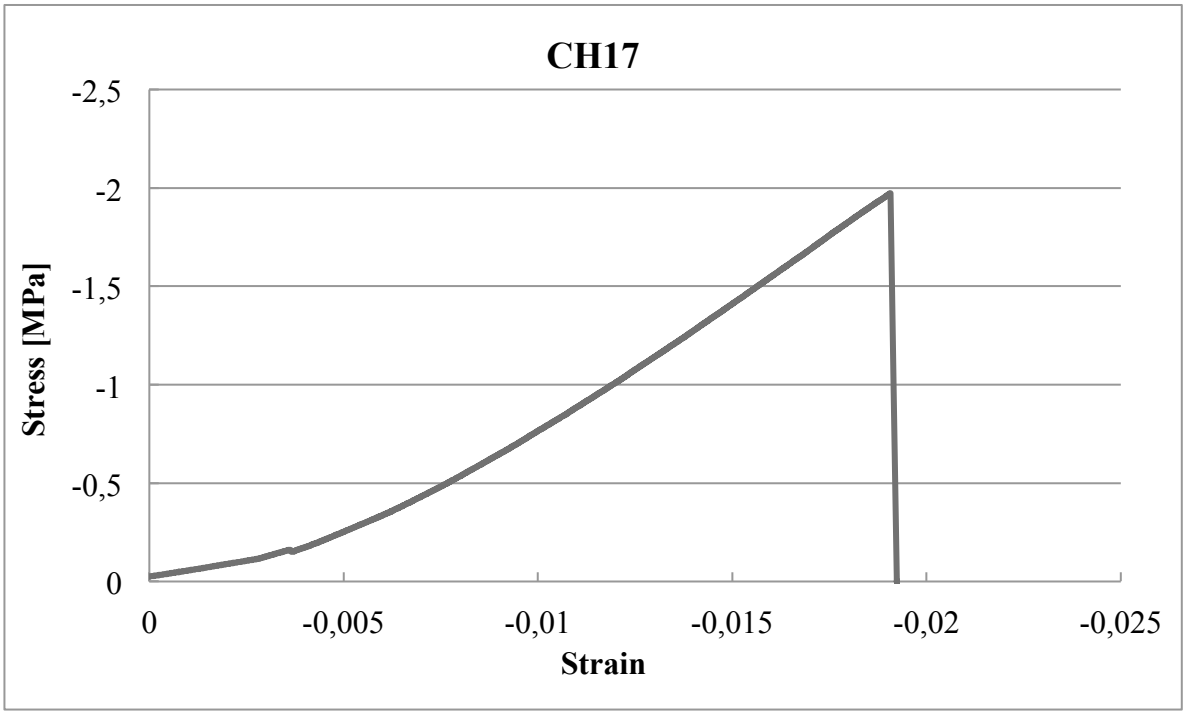

Figure C-44: Stress-Strain curve for Mons chalk sample 17

Appendix D Pictures of Samples After Testing

D.1 Mancos Shale

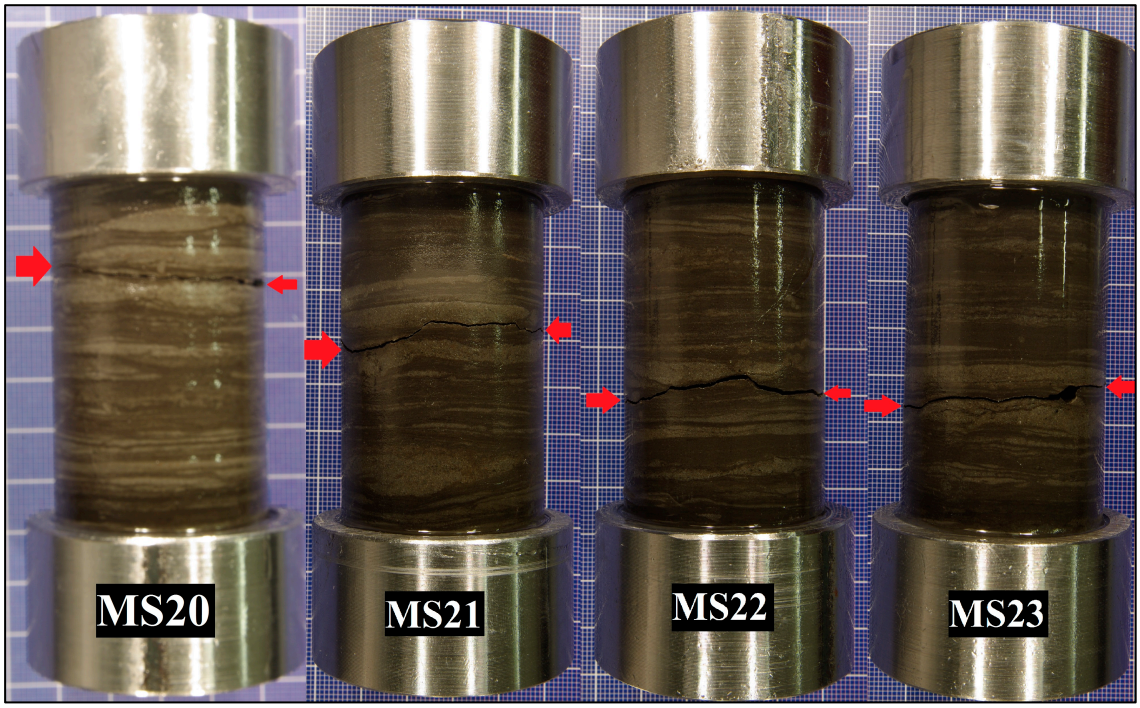

Figure D-1: Mancos shale (0 degrees inclination) after testing

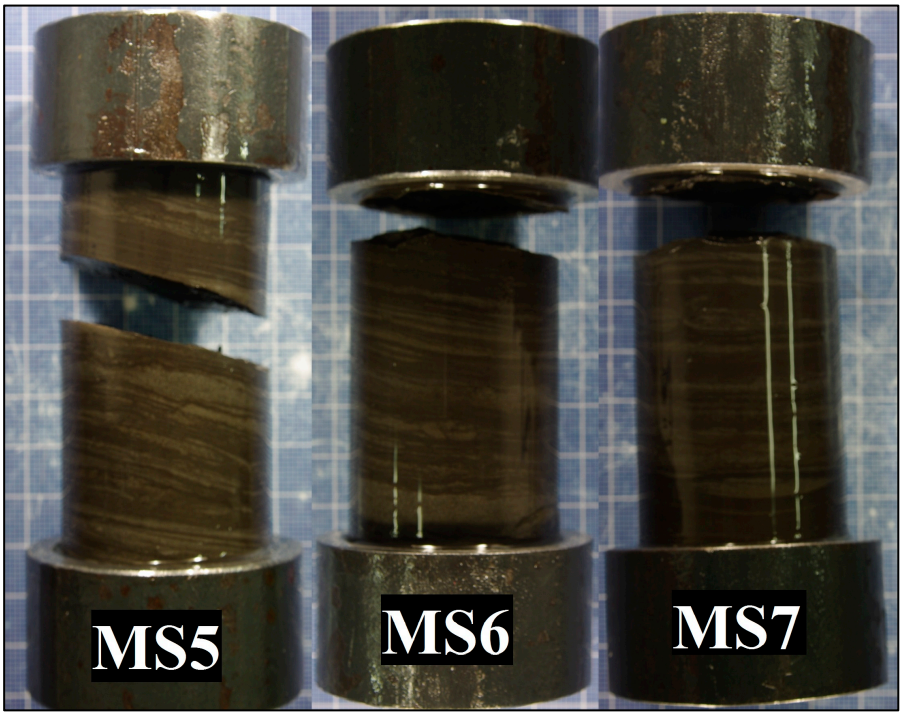

Figure D-2: Mancos shale (15 degrees inclination) after testing

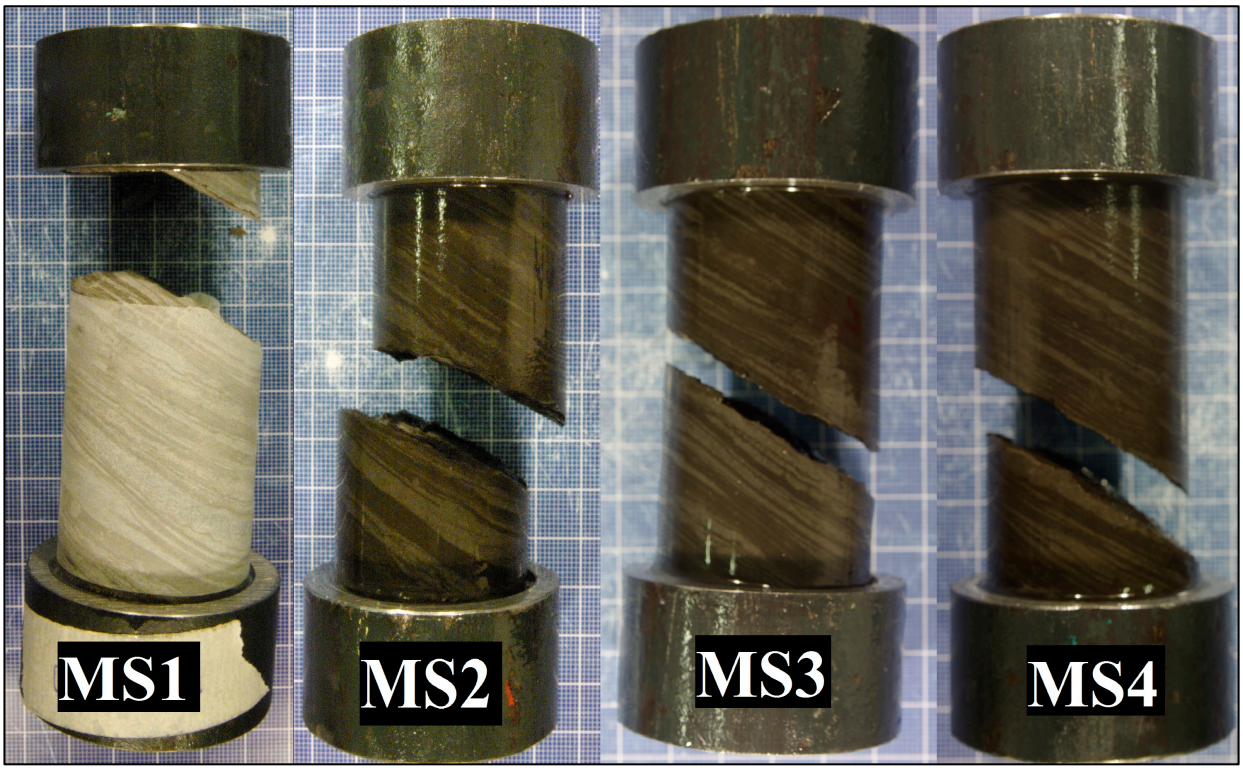

Figure D-3: Mancos shale (30 degrees inclination) after testing

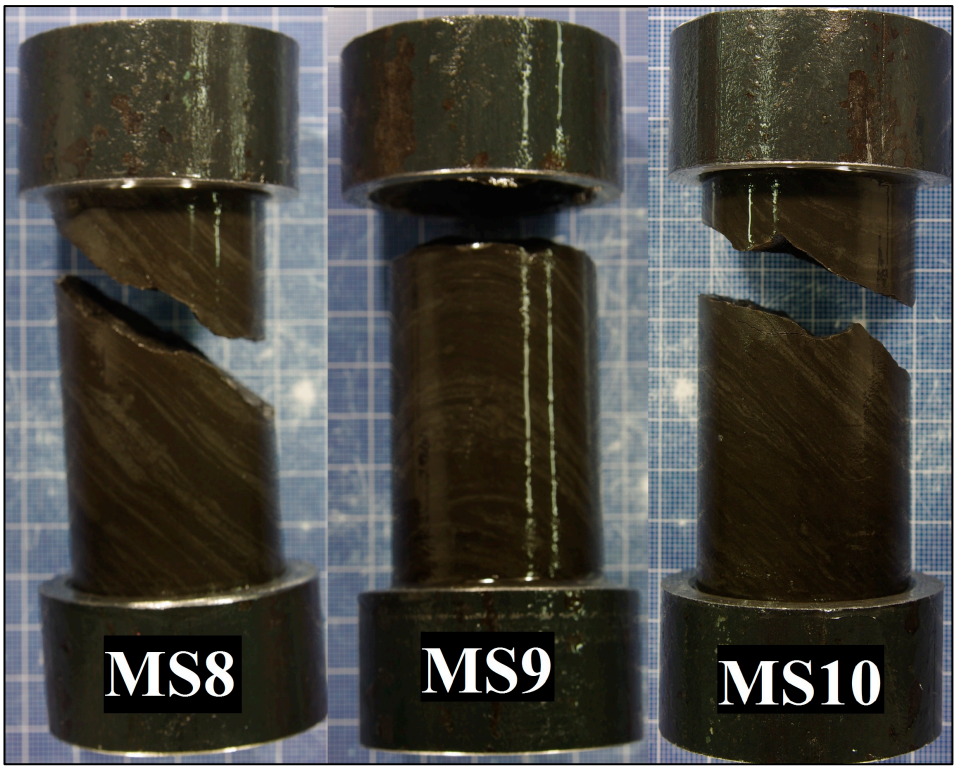

Figure D-4: Mancos shale (45 degrees inclination) after testing

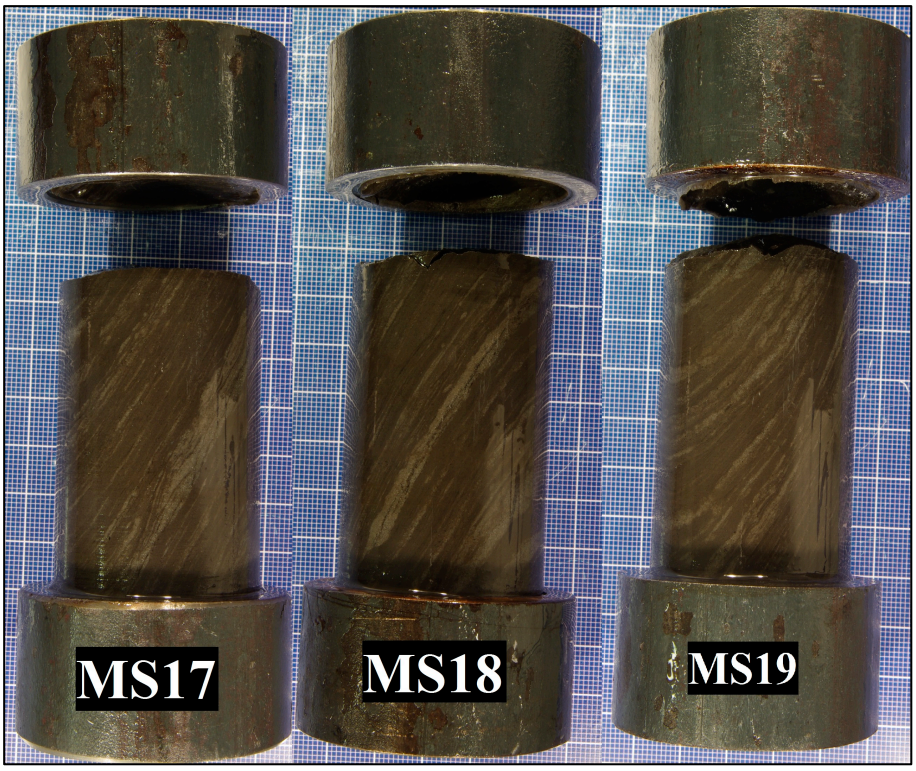

Figure D-5: Mancos shale (60 degrees inclination) after testing

Figure D-6: Mancos shale (75 degrees inclination) after testing

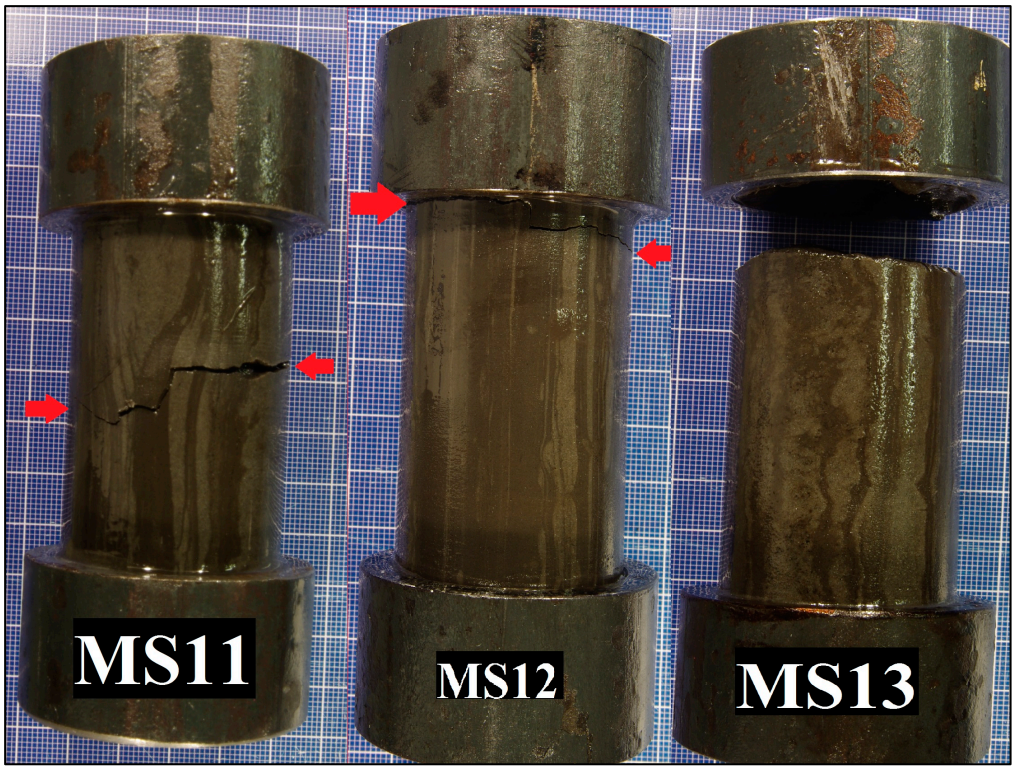

Figure D-7: Mancos shale (90 degrees inclination) after testing

D.2 Castlegate Sandstone

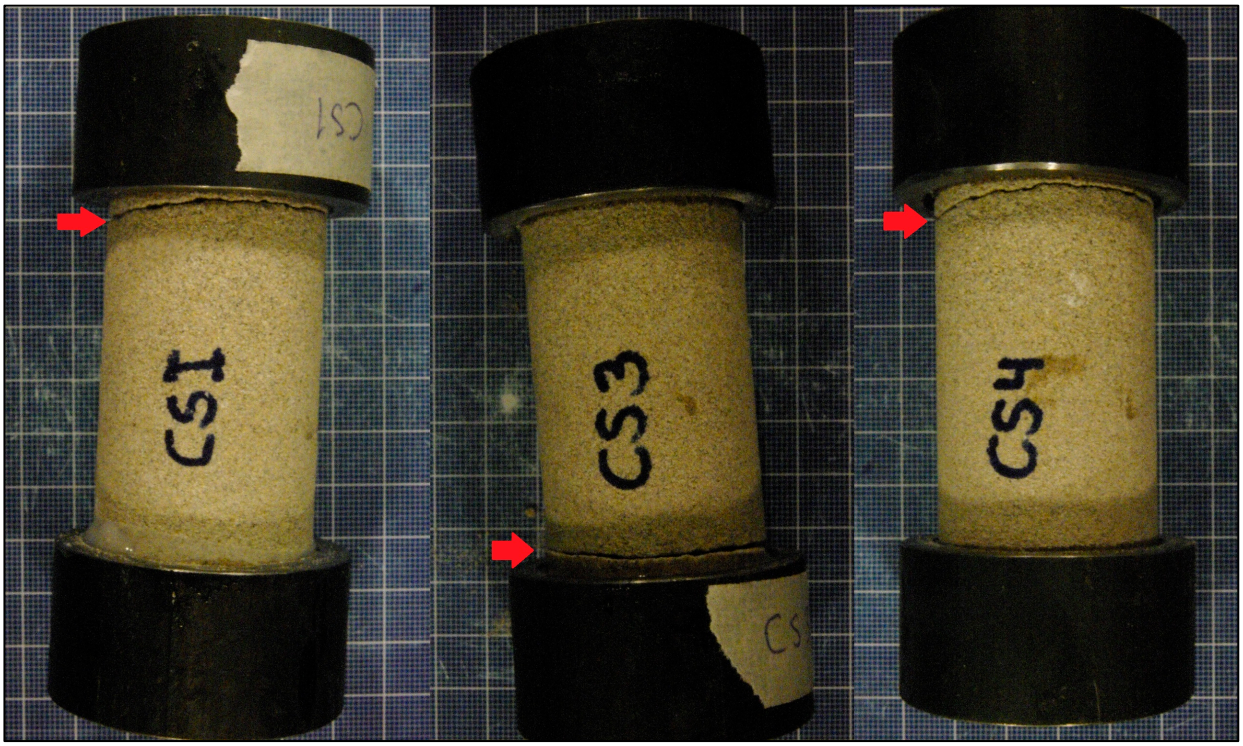

Figure D-8: Castlegate sandstone (diameter approximately 1.5") after testing

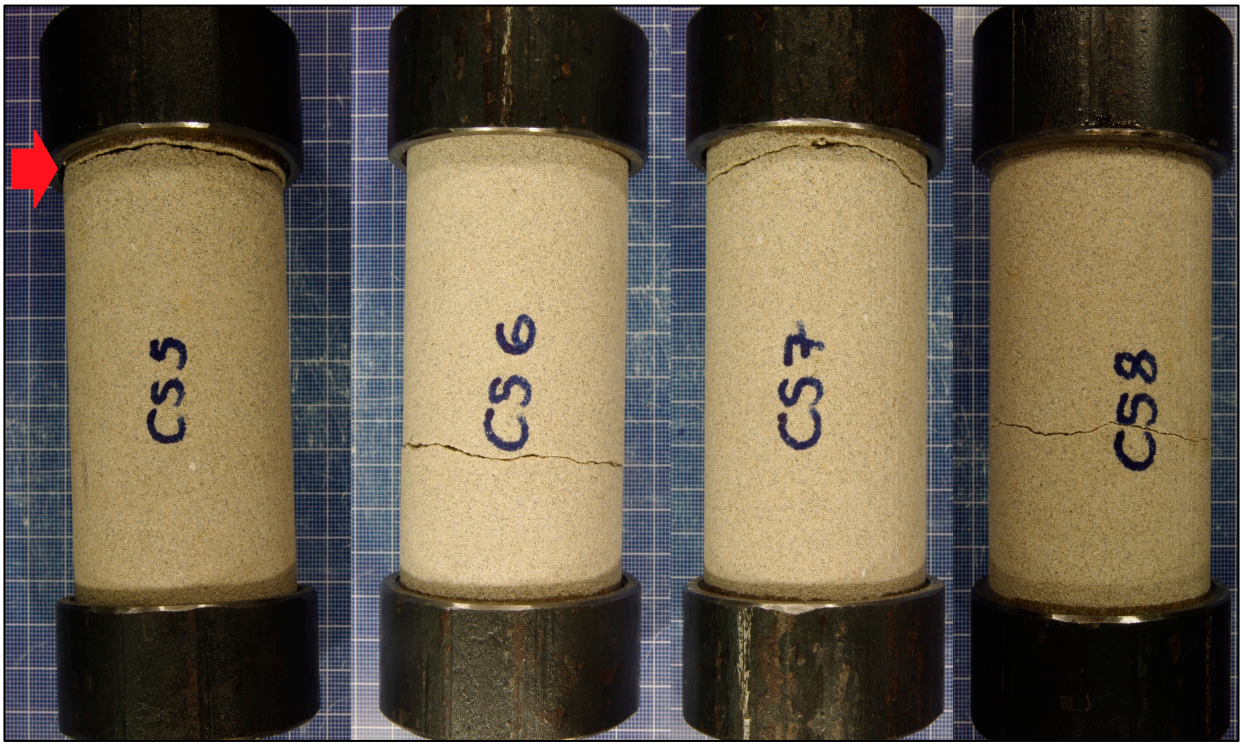

Figure D-9: Castlegate sandstone (diameter approximately 2") after testing

D.3 Mons Chalk

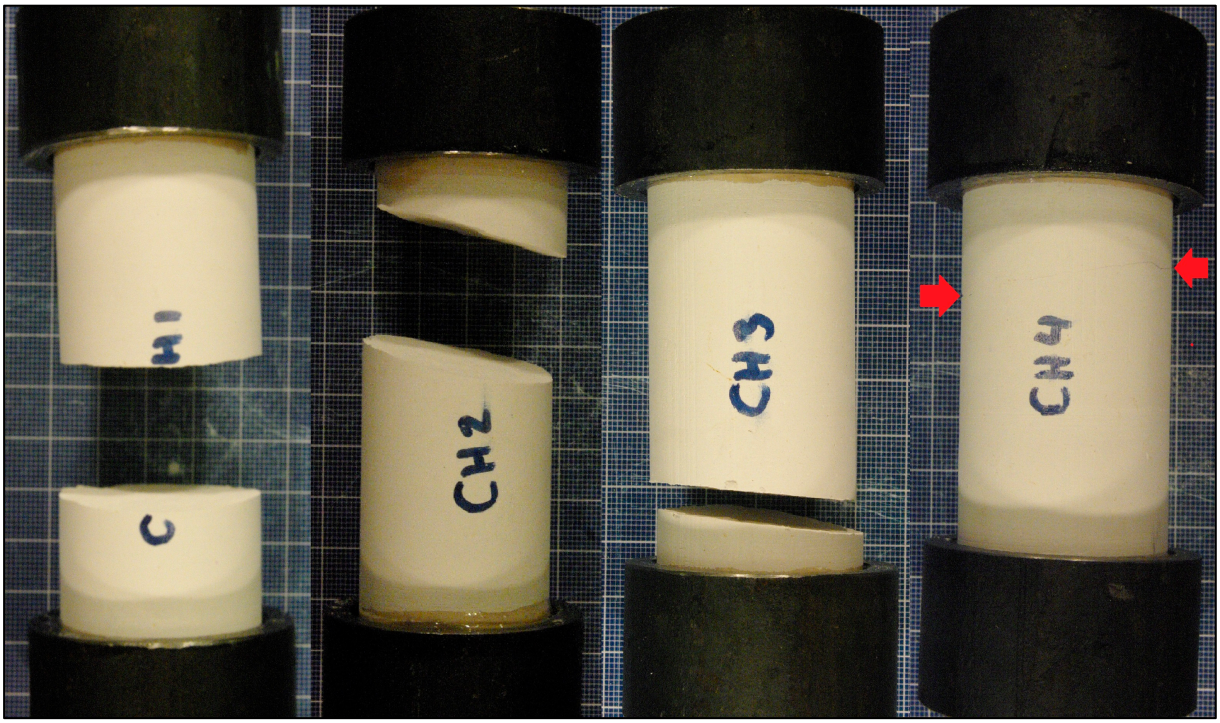

Figure D-10: Mons chalk samples 1 - 4 (diameter approximately 1.5") after testing

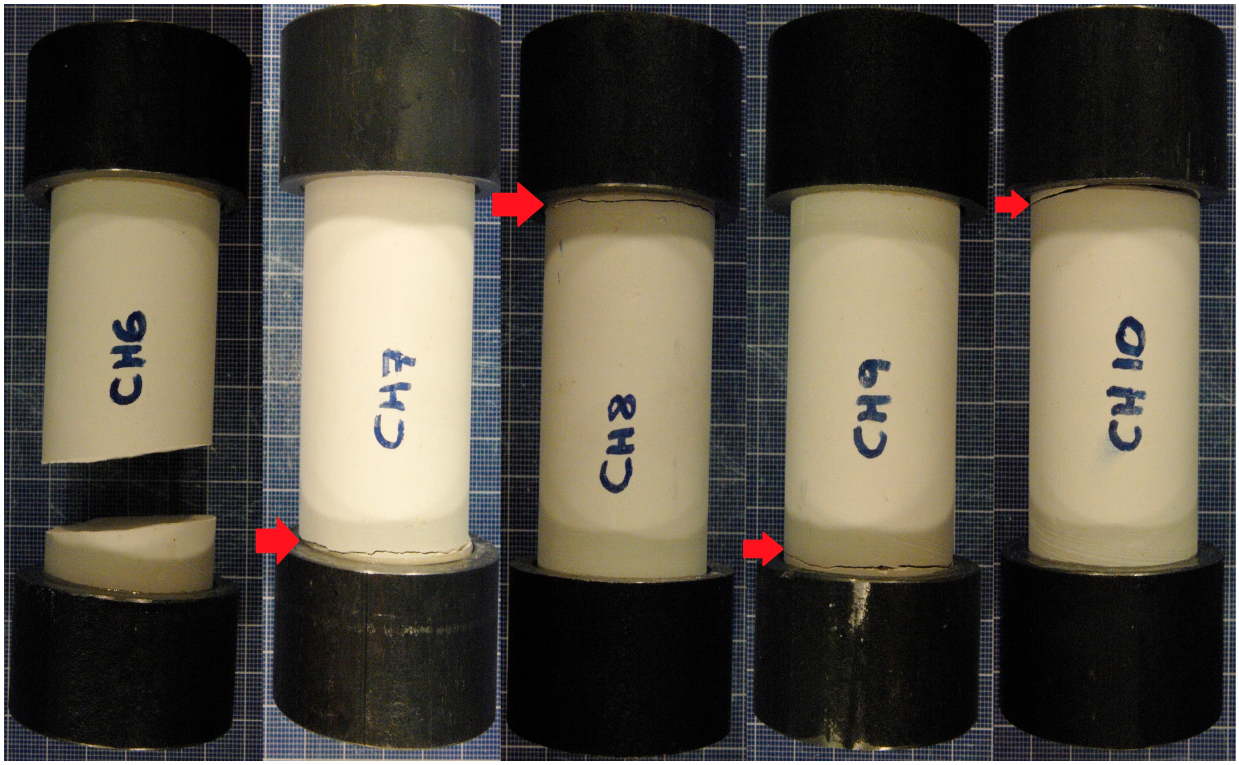

Figure D-11: Mons chalk samples 6 - 10 (diameter approximately 1.5") after testing

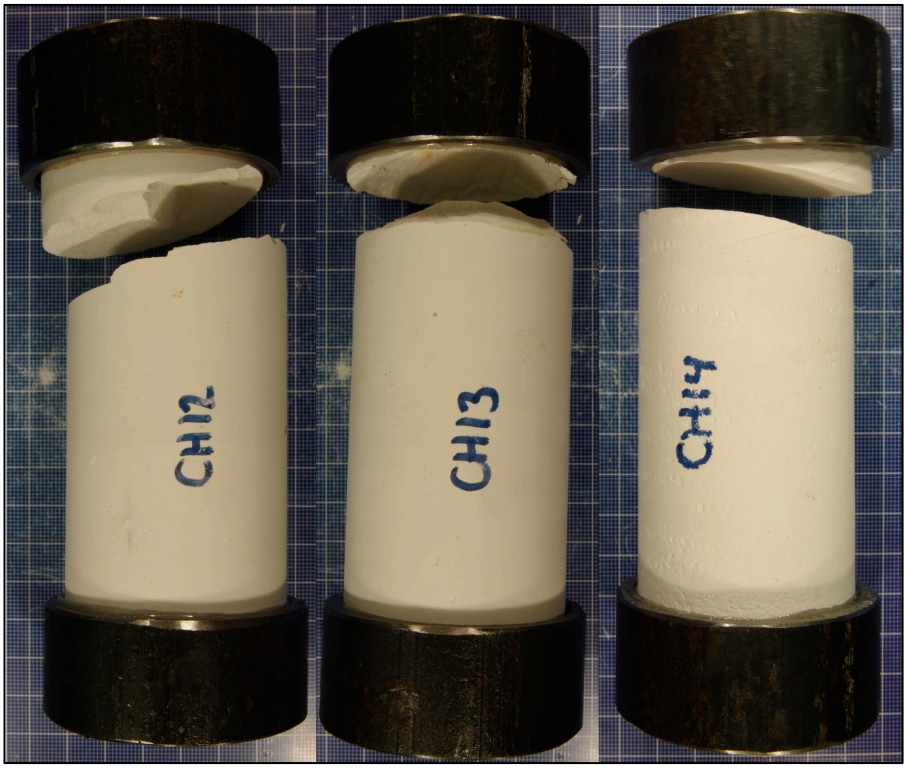

Figure D-12: Mons chalk samples 12 - 14 (diameter approximately 2") after testing

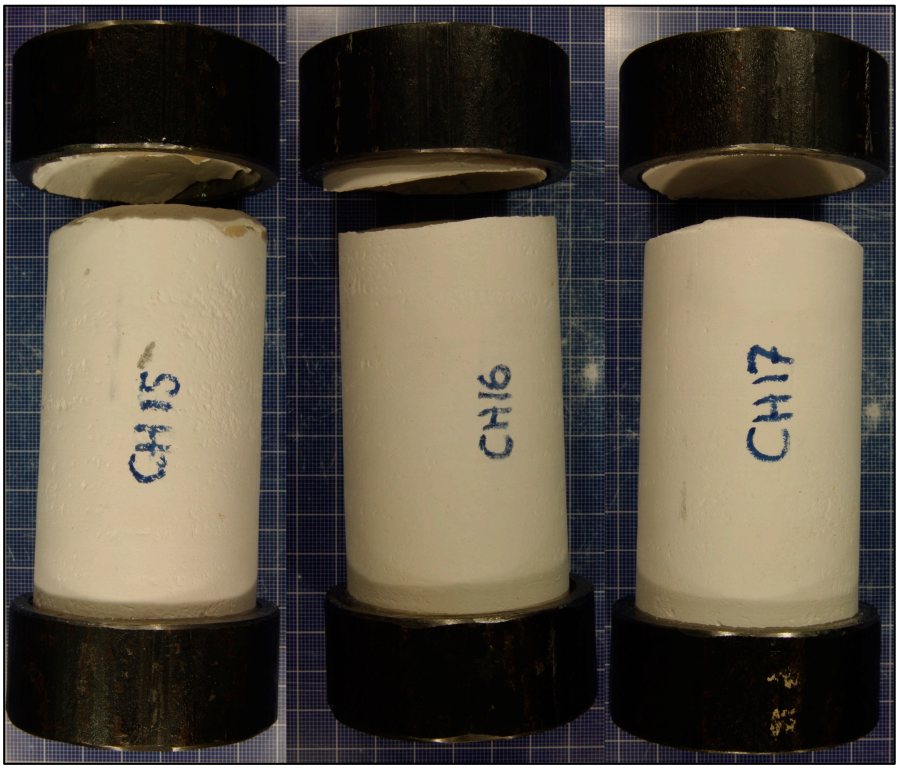

Figure D-13: Mons chalk samples 15 - 17 (diameter approximately 2") after testing

Appendix E Fracture Toughness Data

Table E-1: Mode I fracture toughness data for Mons chalk and Castlegate sandstone (Load versus COD data) (Brevik, 2016)

Rock Type and Specimen Size	Fracture Toughness K_{IC} [MPa*m$^{1/2}$]	Corrected Fracture Toughness K^{C}_{IC} [MPa*m$^{1/2}$]
Mons chalk [D≈1.5"]	0.091 ± 0.022	0.124 ± 0.025
Mons chalk [D≈2.0"]	0.134 ± 0.027	0.153 ± 0.020
Castlegate sandstone [D≈1.5"]	0.097 ± 0.003	0.231 ± 0.016
Castlegate sandstone [D≈2.0"]	0.114 ± 0.007	0.221 ± 0.017

Table E-2: Mode I fracture toughness data for Mancos shale (Load versus COD data) (Brevik, 2016)

Inclination Angle [°]	Notch Placement	Fracture Toughness K_{IC} [MPa*m$^{1/2}$]	Corrected Fracture Toughness K^{C}_{IC} [MPa*m$^{1/2}$]
0	-	0.414	0.757
0	-	0.427	0.630
15	Parallel	0.369	0.370
15	Perpendicular	0.415	0.555
30	Parallel	0.457	0.724
30	Perpendicular	0.326	0.393
45	Parallel	0.626	1.163
45	Perpendicular	0.208	0.450
45	Perpendicular	0.326	0.712
60	Perpendicular	0.573	1.287
75	Perpendicular	0.472	0.526
75	Parallel	0.420	0.755
90	Parallel	0.722	1.178